The differential regulation of podosome formation by Cytohesin-2 is mediated via α5β1 integrin and the small GTPase RhoA

– **Dissertation** –

Zur

Erlangung des Doktorgrades (Dr. rer. nat.)

der

Mathematisch-Naturwissenschaftlichen Fakultät

der

Rheinischen Friedrich-Wilhelms-Universität Bonn

vorgelegt von

Angrit Mareike Namislo

aus Bonn

Bonn, Juni 2019

Angefertigt mit Genehmigung der Mathematisch-Naturwissenschaftlichen Fakultät der
Rheinischen Friedrich-Wilhelms-Universität Bonn

1. Gutachter: Prof. Dr.Waldemar Kolanus

2. Gutachter: PD Dr. Heike Weighardt

Tag der Promotion: 06.09.2019

Erscheinungsjahr: 2019

Contents

Preliminary remarks

According to the common practice in English scientific writing, this dissertation is written using the first-person plural narrator. I have written this thesis without help from third parties and used only the indicated sources.

All experiments described in this thesis have been performed by me except for

- the processing of RNA samples, as well as the subsequent sequencing and analysis of RNA transcriptome data, which was conducted by the laboratory of Prof. Joachim Schultze (Department for Genomics & Immunoregulation, LIMES Institute, Bonn University).

- the µCT scanning procedure, which was performed by the laboratory of Prof. Christoph Bourauel from the Dental Clinic of Bonn University. Sample preparation as well as analysis of the µCT scans was conducted by me.

Abbreviations

µCT	micro computer tomography
APS	ammonium persulfate
Arf	ADP ribosylation factor
BCA	bicinchoninic acid
BMD	bone mineral density
BMDCs	bone marrow-derived dendritic cells
BrefA	Brefeldin A
BSA	bovine serum albumine
cDC	conventional DCs
CR3	complement receptor 3
CR4	complement receptor 4
Cyth	cytohesin
DABCO	diazabicyclooctane
DAPI	diamidinophenylindole
DC	dendritic cell
DNA	deoxyribonucleid acid
dNTPs	deoxynucleotides
DTT	dithiothreitol
E. coli	Escherichia coli
ECL	enhanced chemiluminescence
ECM	extracellular matrix
EDTA	Ethylenediaminetetraacetic acid
EGTA	ethyleneglycotetraacetic acid
ER	endoplasmic reticulum
ERK	extracellular signal–regulated kinases
EtOH	ethanol
FA	focal adhesion
F-actin	fibrillar actin
FAK	focal adhesion kinase
FCS	fetal calf serum
FGF	fibroblast growth factor
FN	fibronectin
FRET	fluorescence resonance energy transfer
GAP	GTPase activating protein
GDI	Guanine nucleotide dissociation inhibitors
GEF	guanine nucleotide exchange factor
GM-CSF	granulocyte/monocyte colony stimulating factor
HBSS	Hank's balanced salt solution
hpt	hours post transfection
HRP	horse-radish peroxidase
ICAM	intercellular adhesion molecule
iDCs	immature bone marrow-derived dendritic cells
IF	immunofluorescence
ILK	integrin linked kinase

JNK	c-Jun N-terminal kinase
kd	knock-down
KO	knock-out
LB	lysogeny broth
LIMK	LIM kinase
MFI	median fluorescence intensity
MLC	myosin light chain
MLCK	myosin light chain kinase
MMP	matrix metalloprotease
mRNA	messenger RNA
NCAM	Neural cell adhesion molecule
NHS	N-hydroxysuccinimide
N-WASP	neuronal Wiscott-Aldrich protein
o.n.	overnight
PBS	phosphate buffered saline
PCR	polymerase chain reaction
PDMS	polydimethyl-siloxane
PECAM	platelet endothelial cell adhesion molecule
Pen/Strep	Penicillin and Streptomycin
PFA	paraformaldehyde
PIP_3	Phosphatidylinositol (3,4,5)-trisphosphate
PIP_2	Phosphatidylinositol (4,5)-bisphosphate
PI3K	phosphatidylinositol 3-kinases
PIP5K	phosphatidylinositol-4-phosphate 5-kinase
PKC	protein kinase C
PKD	protein kinase D
PLL	poly-L-lysine
PMSF	Phenylmethylsulfonyl fluoride
Pyk2	protein tyrosine kinase 2
RNA	ribonucleic acid
ROCK	Rho-associated coiled-coil-containing kinase
rpm	rounds per minute
RT	room temperature
SD	standard deviation
SDS	sodium dodecyl sulfate
SEM	standard error of the mean
siRNA	small interfering RNA
TBST	tris-buffered saline with Tween
TEMED	Tetramethylethylendiamine
VCAM	vascular cell adhesion molecule
vWF	von Willebrand factor
WASP	Wiscott-Aldrich syndrome protein
WAVE	WASP-family verprolin homologous proteins
WRC	WAVE regulatory complex
wt	wildtype

1. Introduction

The human body consists of roughly 3.72 x 10^{13} cells[1], which are organized into different organs and tissues with very specific functions. This strict organization and localization of every single cell - not only in terms of the whole body but also within a specific organ structure - is key to a normally functioning body. The correct localization and interaction of a cell with its surroundings within every organ is crucial both for tissue integrity and stability, as well as for tissue function.[2] Therefore, it is important to understand how cells interact physically with their environment and how the environment influences cellular behavior in turn.

1.1. The extracellular matrix

The local environment that a cell encounters differs very much depending on the specific tissue. It does not only consist of other cells but also of the extracellular matrix (ECM), which is made up of roughly 300 proteins that are produced, secreted, and modified by the surrounding cells, especially fibroblasts. Typical ECM components are collagens, proteoglycans and glycoproteins, but the exact composition differs from tissue to tissue.[3]

ECM occurs in two major subtypes: Interstitial matrix on one hand forms a three-dimensional network that surrounds cells within tissue and contains especially collagens, fibronectin and elastic fibers. Basement membranes on the other hand separate different tissues from each other, for example endothelia or epithelia from the underlying stroma, and are mainly made up of the non-fibrillar collagen IV and laminin.[4]

Fibrillar collagens, especially collagen I, provide stability and stiffness, while elasticity is generated by elastic fibers consisting of elastin and the glycoproteins fibrillin or fibulin. In addition, proteoglycans, including aggrecan, versican, perlecan, and decorin, contain negatively charged glycosaminoglycan chains, which are important for hydration of the ECM. Moreover, proteoglycans also bind and retain growth factors, like fibroblast growth factor (FGF). The group of glycoproteins (e.g. fibronectin (FN) or laminin) interconnects different components of the ECM and often links the ECM to cellular adhesion receptors.[3,5] A special case of ECM-like protein aggregates are hemostatic plugs, which are formed during coagulation of blood and contain not only von Willebrand factor (vWF) and fibrin, which is cleaved from fibrinogen during the coagulation cascade, but also plasma FN. Plasma FN is either derived from the circulation or secreted directly by platelets and further stabilizes the fibrin clot.[6]

Many components of the ECM can be recognized by cell surface receptors and help to anchor cells within the tissue and even provide signaling input to alter cellular responses.

1.2. Integrins are central adhesion receptors

The contact between cells and their environment is mediated through specialized receptors on the cells' surface. There are several different classes of adhesion receptors, including cadherins, selectins, the Ig superfamily, and integrins. Cadherins and selectins both mediate direct contact between cells. Cadherins interact with other cadherins on neighboring cells forming, for example, adherens junctions or desmosomes.[7] Selectins recognize sialylated sugar structures on the surface of other cells and are found, for instance, on endothelia or leukocytes.[8] The Ig superfamily of cell adhesion receptors also mediates mostly adhesion between different cells. Members of this family include ICAM (intercellular adhesion molecule) or VCAM (vascular cell adhesion molecule), which serve as ligands for integrins on other cells, or NCAM (neural cell adhesion molecule) and PECAM (platelet endothelial cell adhesion molecule), which prefer homophilic interactions.[9] Integrins, however, are not only able to bind structures on other cells but they are also the main class of cell-matrix adhesion receptors.[10]

1.2.1. Diversity of integrins and their specificity

Integrins are type I transmembrane proteins with an extracellular domain that is responsible for ligand binding, a transmembrane domain and a cytoplasmic domain, which mediates intracellular signaling. They always occur as dimers consisting of an α- and a β-chain, and the 8 different β-chains and 18 α-chains in mammals can form 24 different integrins (see figure **1.1**). These 24 integrin dimers differ especially in their affinity for different ligands, although several integrins can bind the same ligand and one integrin dimer might be able to recognize several ligands. β1-integrins in general can bind a variety of collagens, but also laminin, FN, osteopontin or VCAM. β2-integrins are exclusively expressed by cells of hematopoietic origin and recognize ICAM or fibrinogen.[11]

With this diversity of integrin combinations every cell (type) can express a unique repertoire of integrin receptors, which is tailored to the specific needs and functions of the cell. The expression of β2 integrins, for example, enables immune cells to bind to ICAM expressed on activated endothelia and is crucial for the extravasation process from the blood into tissue.[12,13] Moreover,

integrins recognizing vWF are found in platelets, whose function in coagulation depends on being able to bind this protein.[14]

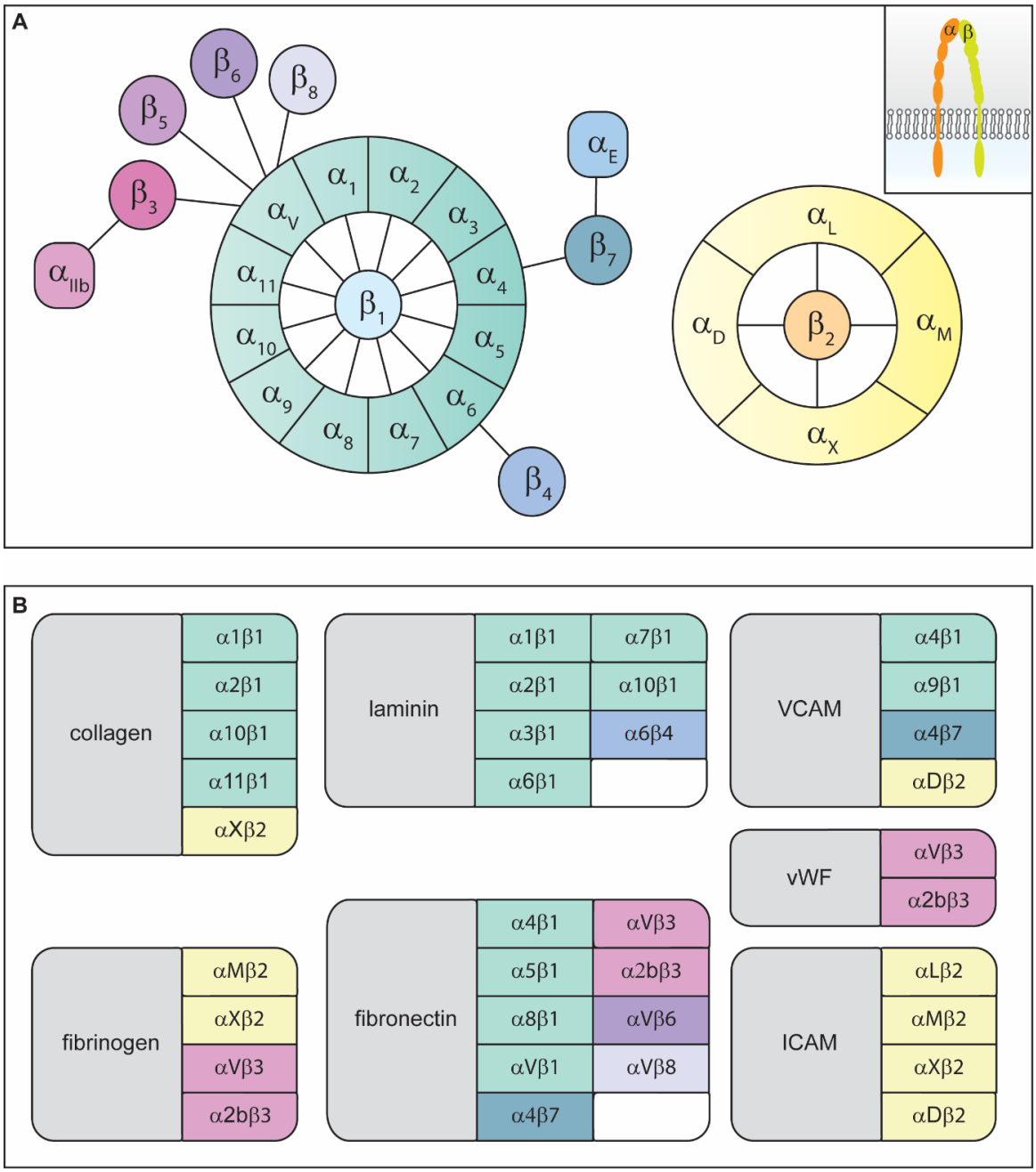

Figure 1.1 – Integrin diversity

Different β integrin chains can pair with several α integrins to form a huge variety of 24 different integrin dimers (**A**). Each dimer binds a certain panel of ligands and several components of ECM can be recognized by more than one integrin dimer. Selected integrin ligands are listed with the respective binding integrins[11] (**B**).

1.2.2. Integrin function

The main functions of integrins are cell adhesion and subsequent signal transduction into the cell. Several knock-out (KO) mice for different integrins illustrate the importance of this process. Many integrins are crucial players during development and mice deficient for β1, α4, or α5 integrins die during embryogenesis[15–17], while KO of integrin αv, α3, α6 or α8 is perinatally lethal due to developmental defects in the kidneys, muscle tissue or blood vessels[18–21].

Other integrins are relevant in a more restricted context and the respective KO mice are viable, but have phenotypes corresponding to the specific integrin function. β2 integrins and their alpha chains, for example, are important for leukocyte adhesion and loss of these integrins results in immunodeficiencies.[22–25] Others, like integrin α2b, are important for hemostasis[14] or for muscle fiber integrity, as shown for integrin α7[26].

Apart from their classical roles in adhesion, several integrins are also involved in phagocytosis. These include two β2 integrins, namely αMβ2 (also known as complement receptor 3, CR3) and αXβ2 (complement receptor 4, CR4), which mediate uptake of complement-opsonized pathogens. But other integrin classes, e.g. β1 or β3 integrins, have also been reported to mediate engulfment of apoptotic cells or ECM components and these roles are not restricted to professional phagocytes.[27]

1.2.3. Integrin activation (inside-out)

Considering the striking phenotypes of integrin KO mice, it becomes apparent that integrin activation has to be tightly controlled. This is especially the case in immune cells, where integrin activity is often specifically required during an immune reaction and has to be turned on and off at specific time points.

The activation of integrins is accompanied by a series of well characterized conformational changes that control the affinity of an integrin for its ligand. In its inactive state the extracellular domain of the integrin is bent towards the cell membrane, thereby preventing binding of the ligand. Upon stimulation, however, the conformation enters an intermediate state, where the extracellular domain extends but the head piece, which is ultimately responsible for ligand binding, is still closed. For full integrin activation, also the integrin headpiece opens completely to allow optimal ligand binding (figure **1.2**).[28]

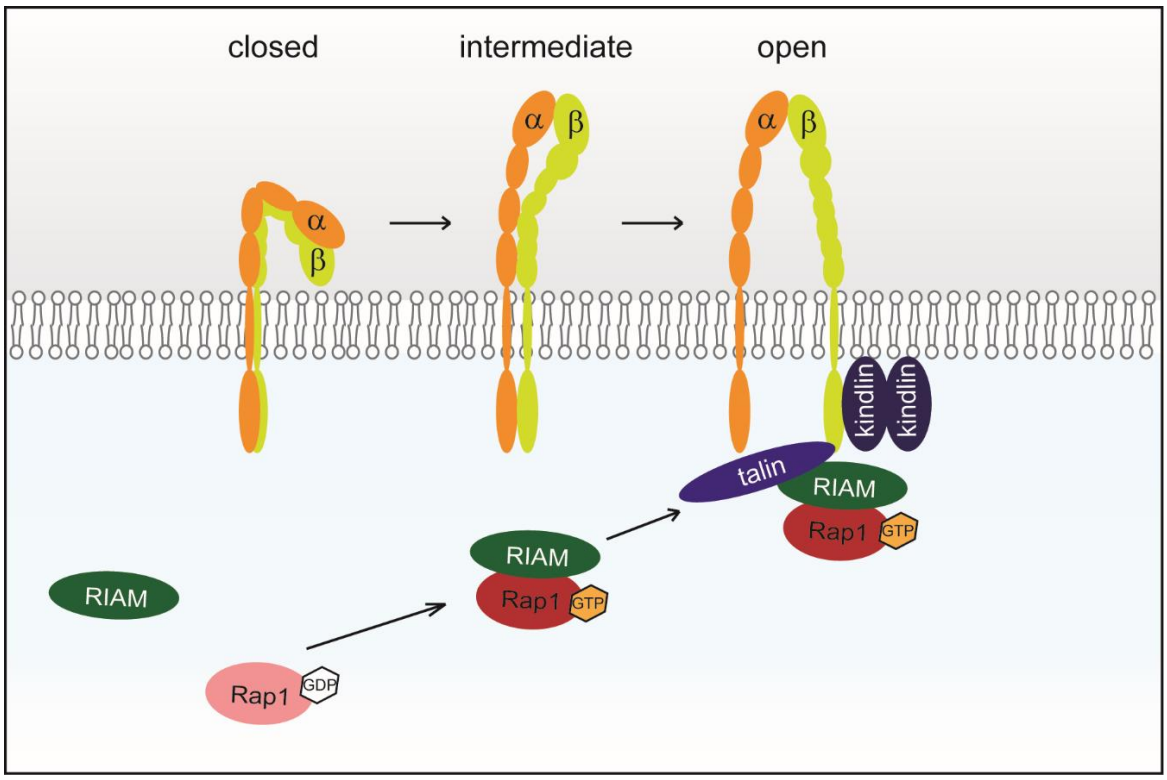

Figure 1.2 – Integrin Activation
Integrin activation from closed (inactive) via intermediate to open (fully active) conformation is induced by activators like talin or kindlin. Rap1 can mediate recruitment of talin via its effector RIAM.

The induction of integrin activation from within the cell (also termed inside-out signaling) is majorly controlled by talin and talin KO in mice is embryonically lethal[29]. Binding of this protein to the cytoplasmic tail of β integrins induces the conformational activation described above.[30]
The recruitment and concomitant binding of talin to the integrin is typically induced via the Rap1-RIAM axis. Stimulation of a cell by cytokines leads to activation of the small GTPase Rap1, possibly via protein kinase C (PKC), which then activates talin via its effector RIAM.[28] Moreover, there are other known Rap1 effectors, like RapL or protein kinase D (PKD), which can also mediate Rap1-mediated integrin activation.[31]

Another important integrin activating protein family are the kindlins. Kindlin1-3 also bind to the integrin β chain but at another site than talin.[32] Only kindlin2 is expressed ubiquitously and its KO is embryonically lethal.[33] Kindlin1 and -3 expression patterns, though, are restricted to epithelia and hematopoietic cells, respectively, and mice deficient for these proteins are born but also have severe phenotypes leading to early death.[34,35] How exactly kindlins are activated and how they activate integrins in turn is much less understood than the talin-dependent mechanisms, but recent data have shown that kindlins form dimers and that this dimerization is important for

kindlin-mediated integrin activation. Moreover, these kindlin dimers are potentially involved in integrin crosstalk and clustering.[36,37]

1.2.4. Integrin signaling (outside-in)

Apart from activating integrins from within the cell as a consequence of signaling events from, e.g. other receptors, integrins can also signal in the opposite direction – a process termed "outside-in signaling". Here, binding of an integrin to its ligand and the clustering of several integrins initiate a cascade of protein phosphorylations and the recruitment of different proteins to form the integrin adhesome (illustrated in figure **1.3**).[38]

One of the first events upon integrin clustering is the recruitment and autophosphorylation of focal adhesion kinase (FAK) or its homologue Pyk2 (protein tyrosine kinase 2). Phosphorylated FAK binds to SH2-domain containing proteins, like Src kinases. Src kinases also bind to β integrin tails, and can further phosphorylate FAK.[39]

Both FAK and Src are bound by paxillin, which is one of the central scaffold proteins at sites of integrin adhesion. Its numerous phosphorylation sites enable the further recruitment of proteins like integrin-linked kinase (ILK) or actin-binding proteins (e.g. vinculin, parvin or α-actinin). The latter ones form a crucial link between the membrane associated integrin-protein network and the actin cytoskeleton, which is important for stabilization and force transmission into the cell - a feature that is especially necessary during cell migration. Vinculin then can also interact with the Arp2/3 complex, which is involved in regulation of the actin cytoskeleton (see below).[39]

Further downstream, integrin activation then, on one hand, initiates the PI3K (phosphatidylinositol 3-kinase)/Akt pathway and activates extracellular signal-regulated kinase (ERK) and c-Jun N-terminal kinases (JNK) to control cell proliferation, differentiation, and survival.[40] On the other hand, integrin signaling also affects actin dynamics by recruiting regulators of Rho GTPases.[41]

The processes and players of integrin activation and signaling discussed above are a generalized summary of major pathways involved. Depending on the specific integrin expression and activation, the composition and signaling of the integrin adhesion complex can vary substantially[42–47] and the differences and consequences are by far not fully understood.

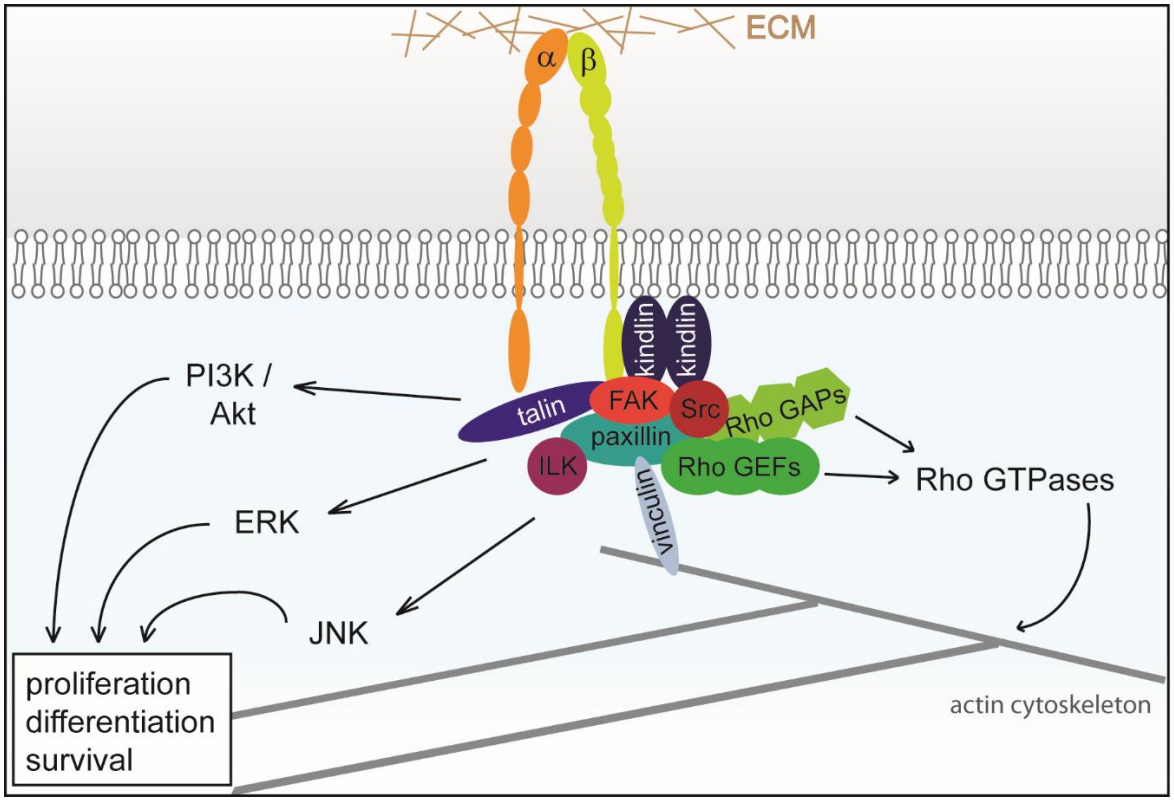

Figure 1.3 – Integrin Signaling
Upon ligand binding to the integrin other signaling molecules, including FAK and Src, and adaptor proteins, like paxillin, are recruited and initiate downstream signaling cascades via PI3K, ERK and JNK. The actin cytoskeleton is linked via adaptor proteins (vinculin) and further modified via Rho GTPases.

1.2.5. Integrin trafficking

Even though integrins are responsible for anchoring the cell within the ECM, they are constantly recycled from the plasma membrane into endosomal compartments and back. This way, the cell can react fast to changing stimuli and form new adhesions dynamically. Both active and inactive integrins can be endocytosed via several routes. Clathrin-dependent endocytosis is governed by proteins like ADP ribosylation factor (Arf) GTPases or dynamin, while clathrin-independent processes can involve clathrin-independent carriers, caveolae or macropinocytosis. Once integrins are localized to early endosomes they are sorted for either lysosomal degradation or recycling pathways back to the plasma membrane. In the case of integrins, two major pathways are described: The short loop, on one hand, transports integrins directly to the cell surface via the GTPase Rab4. The long loop, on the other hand, is regulated by Rab11 or Arf6 and involves trafficking via the perinuclear recycling compartment.[48] In addition to these two pathways, integrins can also be recycled to the cell membrane through retrograde transport via the Golgi apparatus.[49]

1.3. The actin cytoskeleton

The actin cytoskeleton is – similar to the bony skeleton of the human body – the basis for a cell's shape. It does not only determine morphology but also regulates dynamic modulations, when a cell adapts to changes in the environment.

Structurally, the actin cytoskeleton consists of globular actin (G-actin) that is organized into a double helix structure to form long filaments (F-actin). These filaments can occur as branched networks or in long bundles – depending on the specific function of actin at different subcellular localizations.[50]

Cortical actin, for instance, is found directly beneath the cell membrane, where it is crucial for general cell shape and dynamics of the plasma membrane. Lamellipodia, which are broad protrusions of migrating cells, contain a dense network of branched F-actin, while filopodia form finger-like protrusions, which explore the surroundings and are composed of actin bundles. Stress fibers help the cell to contract and are often directly connected to the ECM via integrins at specialized adhesion structures called focal adhesions (FA). Moreover, actin also regulates trafficking of intracellular compartments and vesicles. It has been described to be involved in V-ATPase recycling at lysosomes, formation of the autophagosome, or endocytic and exocytotic processes.[51]

1.3.1. Actin filament formation

The assembly of single G-actin molecules into filamentous actin is governed by actin nucleators or nucleation complexes. The main classes are Arp2/3 complexes and formins.

The Arp2/3 complex nucleates branched actin filaments, which are further stabilized by cortactin. Arp2/3 complex is regulated by members of the WASP/WAVE protein family. N-WASP (neuronal Wiscott-Aldrich Syndrome protein) is ubiquitously expressed and mice deficient for N-WASP are embryonically lethal[52]. WASP, however, is expressed by hematopoietic cells and loss or mutations of WASP lead to Wiskott-Aldrich syndrome, characterized by immunodeficiency and bleeding disorders[53]. Both WASP and N-WASP can be activated by direct binding of the Rho GTPase Cdc42 and/or binding to PIP_2 (phosphatidylinositol 4,5-bisphosphate). The WAVE proteins (WASP-family verprolin homologous proteins) act in a similar manner but are not activated by Rho GTPases directly. Instead, they are part of a regulatory complex (called WAVE regulatory complex or WRC), which is affected by Rho signaling.[50,54]

In contrast to the Arp2/3 complex, formins produce unbranched filaments of actin and occur usually as homodimers[50]. Formins are direct effectors of Rho GTPases and they can also act as elongation factors on actin filaments[50]. Several crosslinking proteins further interconnect single actin filaments to stabilize them. These include filamin, which crosslinks especially branched actin networks, and fimbrin or fascin, which stabilize parallel actin bundles.[50]

1.3.2. Rho GTPases

Rho GTPases form the major class of actin regulators. Like any other GTPase, Rho GTPases are controlled by both GTPase activating proteins (GAPs) and guanine nucleotide exchange factors (GEFs), which inactivate GTPase activity via hydrolysis of GTP to GDP or stimulate GTPases by exchanging GDP for GTP, respectively. The family of Rho GTPases comprises 20 different proteins, but the three best studied ones are RhoA, Rac and Cdc42. By distinct cellular localization and via different effector proteins Rho GTPases affect different aspects of actin dynamics. In a common but simplified scheme, Rac is primarily responsible for lamellipodia, Cdc42 controls filopodia and RhoA is involved in contraction-related processes especially at the uropod of migrating cells and in formation of stress fibers. However, there are functional overlaps of Rho GTPases and efficient regulation of actin dynamics is only possible by temporally and spatially controlled cooperation of all factors involved. [55]

The localized activation of Rho GTPases is regulated on one hand by direct recruitment to membranes via isoprenyl lipids on the GTPases themselves[56], and on the other hand by interactions with GEFs and GAPs at specific spots of activity[56]. These GTPase regulating proteins are often associated with or regulated by players of the integrin signaling complex.[56] Moreover, inactive Rho GTPases can be sequestered in the cytosol by guanine nucleotide dissociation inhibitors (GDI) that prevent membrane recruitment and GEF-mediated activation[57].

The effectors of Rho GTPases are just as diverse as their regulators. Apart from the already mentioned group of actin nucleators, several protein kinases are activated by Rho GTPases. Among these, P21-activated kinase (Pak) can affect the actin dynamics by phosphorylating LIM kinase (LIMK)[58] or myosin light chain kinase (MLCK)[59]. Especially RhoA is known to regulate myosin-related processes by activating rho-associated coiled-coil-containing protein kinase (ROCK). ROCK in turn stimulates phosphorylation of myosin light chain (MLC) and thereby increases contractility of actin fibers.[60]

Rho GTPases also affect cellular pathways that are not directly linked to actin remodeling, such as production of reactive oxygen species, lipid metabolism or transcriptional regulation. Furthermore, they also influence microtubuli and are involved in cell cycle regulation and cell division.[60] For our topic at hand, however, the central function of Rho GTPases in regulating dynamic changes of actin structures is of major interest.

1.4. Podosomes are cellular adhesion and invasion structures

Actin fibers are found in very different structures and are often directly linked to integrin-based adhesion complexes. This occurs typically at FA, which are found in most cell types and frequently form the end of a stress fiber.[61] FA are especially important for force application onto the substrate and its transduction onto the cytoskeleton during cell migration.[61] They are characterized by a local clustering of integrins and the subsequent signaling platform into a “comma”-like structure that mediates the connection of the ECM to the cytoskeleton.[61] Similar to FA, integrin-based adhesion complexes can be organized in focal complexes, which are smaller and more short-lived than FA, and fibrillar adhesions, which differ slightly in phosphorylation patterns and are often associated with fibronectin fibrils.[62]

However, in some cells additional (integrin-based) adhesion structures exist, which are called invadosomes. The term “invadosome” includes both podosomes and invadopodia, and there is an ongoing discussion in the scientific community as to whether podosomes and invadopodia describe the same structure or if they develop entirely independently.[63,64] The common denominator, however, is that podosomes per definition only occur physiologically, while invadopodia are exclusively found in pathological situations, for example after transformation of a cancer cell.

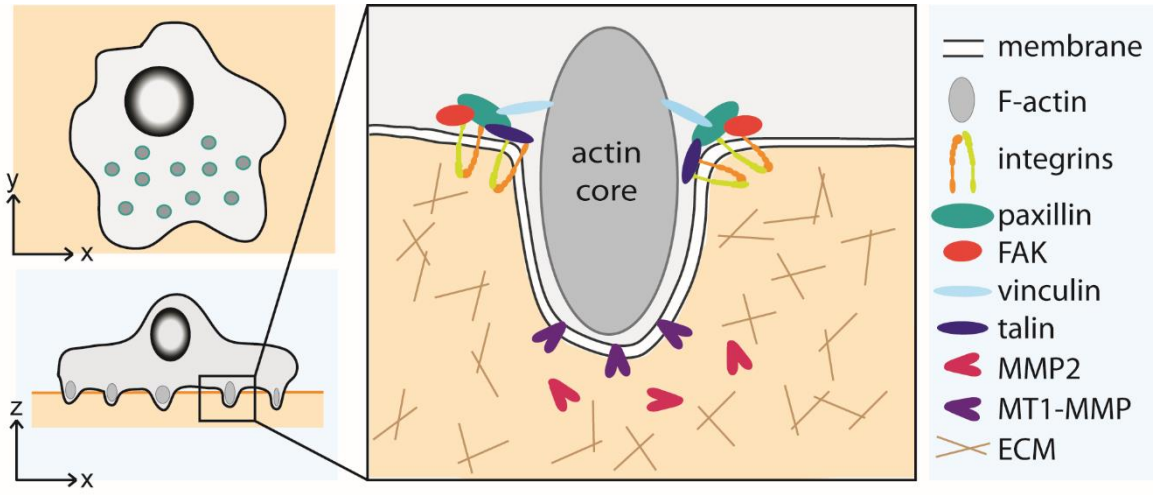

Figure 1.4 – Podosome Structure
Podosomes are ventral protrusions of the cell membrane containing an actin-rich core and a ring structure of adhesion proteins. They are able to degrade the underlying matrix by recruiting and secreting MMPs.

Structurally, all invadosomes form dotlike structures with a diameter of about 0.5-1 µm at the basal plasma membrane and protrude towards the substrate. They are composed of an actin-rich core that is surrounded by a ring of adhesion proteins (figure **1.4**). In addition to their role in cell adhesion, invadosomes are also able to degrade the underlying matrix and are therefore important for cellular invasion into tissue. Reported differences between invadopodia and podosomes relate to their protrusion depth (which is described to reach several µm for invadopodia and only ~1 µm for podosomes) and their life time of a few minutes in the case of podosomes compared to more than 1 h in invadopodia.[63] Furthermore, the exact composition of invadopodia and podosomes can be different[65], but these alterations may simply reflect cell type- or experiment-specific differences.

Podosomes are not present in all cells but are mostly restricted to cells of the myeloid lineage, like macrophages, dendritic cells (DCs) or osteoclasts. A few other cell types, including smooth muscle cells, fibroblasts or endothelial cells, have also been shown to form podosomes.[64] Invadopodia have been described in many different cancer cells and are considered a sign of increased invasiveness.[66] Moreover, transforming a cell line, such as fibroblasts, with e.g. constitutively active Src kinase will also lead to structures considered invadopodia[67] rather than podosomes.

1.4.1. Formation and composition of podosomes

The structure of podosomes is already very well understood. It contains a core of very dense actin filaments together with actin regulatory proteins, like cortactin, the Arp2/3 complex or WASP.[65]

The top of that core facing the cytoplasm is covered by a cap structure containing, for example, formins[68]. The core is surrounded by a ring-like accumulation of adhesion proteins: integrins and associated signaling and adapter proteins that connect the membrane to the core via actin fibers.[63] The adaptor protein Tks5 also localizes to the podosome ring and is so far the only protein that is exclusively found in invadosomes but not in other adhesion structures like FA.[69–71]

Moreover, single podosomes are also interconnected by unbranched actin cables (termed the "cloud"), which could explain why podosomes often appear in clusters.[72] Actin filaments found in podosomes and at podosome clusters contain a substantial amount of myosin IIa, which plays an important role in podosome protrusion and their function as mechanosensors.[63]

The initial signal for podosome formation is often coming via integrins or growth factor receptors for TGF-β, EGF or VEGF, which activate Src kinase, Rho GTPases or PI3K. Downstream of these, small actin puncta are formed first, followed by assembly of the ring proteins and the recruitment of matrix metalloproteases (MMPs), especially MT1-MMP but also MMP2 or MMP9. The localized release of these MMPs (and other proteases, like cathepsin or serine proteases) is the basis for the degradative activity at invadosomes.[64,73]

1.4.2. Podosome functions

The biological functions of podosomes are surprisingly diverse and reflect the many different cell types in which podosomes or invadopodia have been found. Classically, podosomes have been studied in the context of cell adhesion, migration and invasion – especially in immune cells[74–77]. The mesenchymal migration mode used, for example, by macrophages is based on integrin adhesion and protease activity and has been linked to podosome function.[75] Moreover, Carman and colleagues have shown that leukocytes use podosome-like structures for transcellular diapedesis through an endothelial cell layer *in vitro*.[74]

Very closely linked to migration and invasion of immune cells is the topic of cancer cell metastasis. The presence of invadopodia in tumor cells is typically associated with increased invasiveness and therefore a higher risk for formation of metastases.[66] Research on tumor cell invasion processes has provided some of the best *in vivo* studies of invadosomes: Leong and colleagues used chicken embryos to show the presence of Tks5 and WASP positive protrusions on extravasating breast cancer cells[78] and the relevance of invadopodia for cancer cell metastasis has been further

strengthened by Ngan and colleagues, who linked occurrence of metastases with invadopodia formation in a mouse model for breast cancer metastasis[79].

Osteoclasts are specialized cells of myeloid origin that are responsible for degradation of bone. Their podosomes fuse into a belt-like structured called “sealing zone”, which helps to seal off the degradation lacuna from the surrounding tissue and prevent spreading of proteases and acid.[80–82] Interfering with osteoclast podosomes, for example by loss of kindlin-3 or integrins, leads to osteopetrosis in mice and man due to dysfunctional osteoclasts.[83,84]

More recently, podosomes have been described to be mechanosensors[85–87], a function that is also associated with other adhesion structures, like FA[88]. The current model assumes that the podosome core protrudes further towards the substrate via increased actin polymerization. The force that is generated by the resistance of the matrix is then translated via actin and adaptor proteins to stretch-sensitive ring proteins, like talin or vinculin.[63]

Apart from these classical functions of invadosomes, several other aspects of podosome biology are being discussed. Podosome clusters have long been known to appear in smooth muscle cells[89] and endothelial cells[90,91], where they might be relevant for angiogenesis[92,93]. Moreover, podosome-like structures have also been described at neuronal growth cones[94], and at post-synaptic membranes of myotubes[95], although a complete functional explanation for the latter occurrence is still lacking. Both myotubes and osteoclasts are multinucleated cells, which develop by fusion of several single cells, and these processes also involve podosomes[96,97]. Furthermore, podosome-like structures have been postulated in antigen sampling by immune cells[98–100].

Taken together, podosomes are versatile structures that are relevant for many different cellular functions and are intimately connected to and dependent on both integrin-mediated adhesions and actin polymerization processes.

1.5. Cytohesins

The regulation of integrin-related signaling and actin dynamics is very complex and there are numerous players involved. Among these regulatory factors, the protein family of cytohesins has been studied for more than 20 years.

1.5.1. Cytohesin protein structure and expression patterns of cytohesin genes

The cytohesin (Cyth) protein family consists of four members: Cyth1, Cyth2 (also called ARNO), Cyth3 (or Grb1), and Cyth4. Evolutionary, the different cytohesins developed from one common ancestor. *Drosophila melanogaster*, for instance, has only one cytohesin homolog, called Steppke, which is most similar to the mammalian Cyth3.[101] The four cytohesins differ in their expression pattern: Cyth2 and Cyth3 are expressed ubiquitously, while Cyth1 and Cyth4 are reported to be found mostly in cells of the hematopoietic system and in the brain.[102–105] Their main function is the regulation of Arf GTPase activation via their GEF activity (figure **1.5 A**).[106] All four proteins share the same domain structure and a high sequence homology of ~70-85 %.[102]

On their N-terminus cytohesins contain a coiled-coil domain, which enables interaction with other proteins or dimerization. The coiled-coil domain is followed by a Sec7 domain that harbors the catalytic center for the GEF function, and finally, at the C-terminus, a pleckstrin homology (PH) domain required for association with membranes (see figure **1.5 B**). Moreover, cytohesins can also be phosphorylated at several residues close to their C-terminus.[106] The PH domain is especially interesting because it can occur in two different splice variants, which contain a stretch of either two or three glycins that determine the preference for certain phospholipids and therefore localization of cytohesins (figure **1.5 C**). The diglycine (2G) variants of cytohesins have a higher affinity for phosphatidylinositol (3,4,5)-trisphosphate (PIP_3) compared to PIP_2, while the triglycine (3G) variants bind to both PIP_2 and PIP_3 equally well.[107,108] As the concentration of PIP_2 is several magnitudes higher than the PIP_3 concentration in unstimulated cells[109], the 3G variants locate predominantly to PIP_2. PIP_3 is mostly generated locally upon stimulation of cells and concomitant activation of PI3K. Therefore, 2G-cytohesins can be specifically recruited to hotspots of cellular activity.

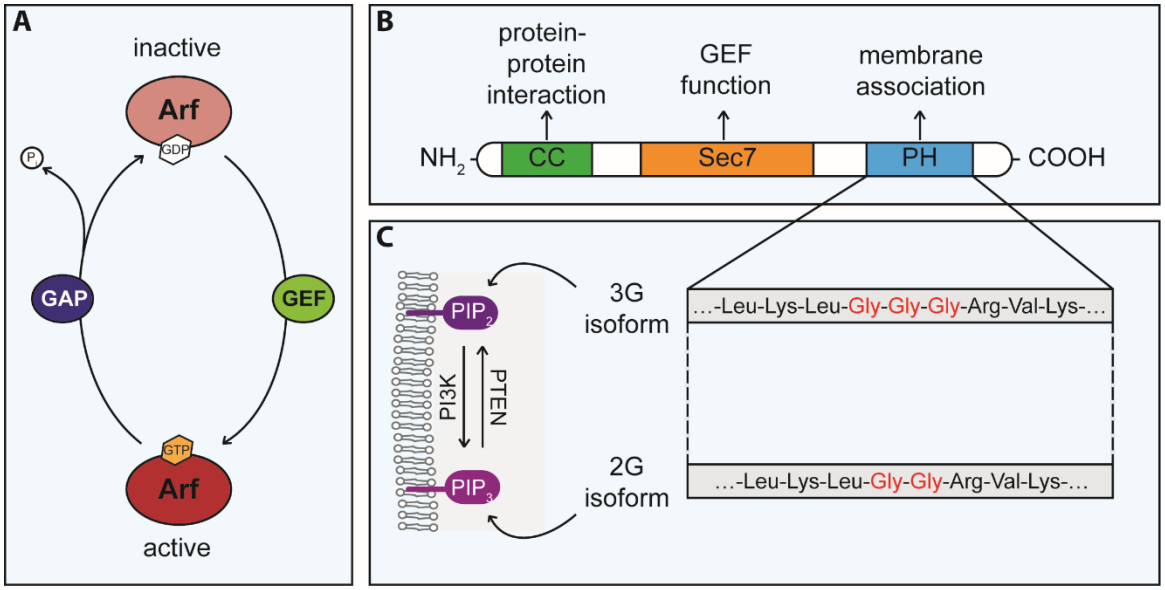

Figure 1.5 – Cytohesin structure and function

Cytohesins are GEFs for Arf GTPases and thereby facilitate their activation (**A**). Cytohesin domain structure: CC (coiled-coil domain), Sec7 domain, PH (Pleckstrin homology) domain (**B**). 2G and 3G isoforms of cytohesins have different affinities for PIP_2 and PIP_3 in the cell membrane (**C**).

1.5.2. Arf GTPases regulate membrane trafficking

With Arf GTPases being the main target of cytohesins, a closer look at these proteins will help to understand the functions of cytohesins. The family of Arf proteins belongs to the group of small GTPases and consists of six different members, Arf1-6, which localize to and are active at different membrane compartments within the cell. One major function of especially Arf1, Arf3, Arf4 and Arf5 is the regulation of membrane trafficking at or around the Golgi apparatus, while Arf6 is found predominantly at the plasma membrane. The main action of activated Arf proteins is the recruitment of further effector proteins to membranes. These can, for example, affect the local lipid composition of membranes, as illustrated by the Arf-dependent activation of phospholipase D (PLD) or PIP5K (phosphatidylinositol-4-phosphate 5-kinase). Other Arf effectors regulate more specific processes, e.g. budding of vesicles or clathrin-dependent endocytosis.[110]

Like other GTPases, Arf proteins are regulated by GEFs and GAPs. Cytohesins form one group of Arf GEFs, but there are also other Arf-specific GEF families, including BRAG or BIG proteins. Negative regulation of Arf activity is governed by GAPs, like ARAPs, which also serve as GAPs for RhoA, ACAPs, which have been shown to interact with β1 integrins, or GIT proteins, which can also associate with the Rho GEF PIX.[111,112]

In the context of adhesion-related processes, Arf6 is of primary interest as it is active at the cell membrane. Arf6 has been shown to regulate internalization of various adhesion receptors,

including β1 integrin or cadherin, and it affects actin remodeling processes via the Rho GTPase Rac1.[113,114] Furthermore, several studies have linked Arf function to podosomes. In osteoclasts, Arf6 activity and the Arf GAPs GIT2 or ARAP1 are important for sealing zone formation[115,116] and Donelly and colleagues could show that knock-down of Arf6 affects localization of MT1-MMP to invadopodia[117]. In a recent publication on the role of Cyth2 and Arf proteins for podosomes, Arf6, but not Arf1, was dispensable for podosome formation in THP-1 cells.[118] Indeed, Arf1 has also been reported to be involved in processes that are not directly linked to the Golgi, like composition of FA[119] or recruitment of the WRC to membranes[120]. This latter process also requires an interaction between Arf1 and Arf6 in order to locate Arf1 to the plasma membrane in the first place.

1.5.3. Biological roles of cytohesin proteins

Considering the relevance of Arf GTPases for very general cellular processes, it is not surprising that also cytohesins have been implicated in a variety of biological contexts. In line with the well-established role of Arfs in membrane trafficking, cytohesins affect dynamics and/or activation of several cell surface receptors, e.g. EGF receptor[121], VEGF receptor[122], LHCG receptor[123] and also the glucose transporter Glut4 downstream of insulin signaling[124]. Insulin-related signaling pathways have long been known to be regulated by cytohesins[125] and there are several *in vivo* studies showing the relevance of Steppke in Drosophila melanogaster[101] or of Cyth3 in mice[126,127] for insulin-mediated processes.

One major aspect of cytohesin research since the initial description of these proteins has been their involvement in cell adhesion and related processes and a special focus has been put onto Cyth1 and Cyth2. There is, however, only limited data on the role of Cyth3 in cell adhesion[128,129] and Cyth4 has not been studied functionally at all.

Cyth1 was discovered as an important regulator of LFA-1-dependent adhesion of T cells and a direct interactor of β2 integrins[103], and it was later shown to also affect β2 integrin-dependent phagocytosis[130,131] of neutrophils. However, Cyth1 also has effects on β1 integrins [132,133] and cadherin-based adherens junctions of epithelial cells[134]. In addition, Cyth1 is involved in migratory processes of mature DCs or HeLa cells.[108,135]

Cyth2 is also known to regulate integrins – although most reports focus on trafficking of especially β1 integrins, which is linked to effects on general adhesion behavior, FA formation and cell

spreading.[129,136] Moreover, the adaptor protein paxillin is a known binding partner of Cyth2 and both are important for migration of preadipocytes.[137] Cell migration is a common theme of Cyth2 biology[137–142] and is often connected to Cyth2-mediated regulation of Rho GTPases. Cyth2 can, for example, associate with the Rac GEF DOCK180 via the adaptor protein GRASP/tamalin[143] and RhoA activity is a major effector of cytohesin action on migration of mature DCs[135]. In line with these studies, Cyth2 has been shown to be important for formation of stress fibers and lamellipodia in HEK and HeLa cells.[144,145] More recently, Cyth2 has been linked directly to podosome formation in an Arf1 and RhoA dependent manner.[118]

In vivo data based on cytohesin knock-out mice is available for brain-related phenotypes. Both Cyth1 and Cyth2 have been reported to be important for myelination of neurons by Schwann cells, which is also regulated by adhesion processes and has been linked to phosphorylation of Cyth1 by the Src kinase Fyn.[104,146] Moreover, there are several studies showing that cytohesins possibly act protectively in neurodegenerative diseases.[147–149] Furthermore, Cyth2 modulates cellular protrusions (neurites) in neurons by binding to the actin-binding protein actinin-1[150] or via interaction with pallidin in early endosomes[151]. Therefore, also in the central nervous system the activities of cytohesins fit to the overall picture of regulators of cell adhesion, major actin rearrangement processes and/or membrane dynamics.

1.6. Aim of the project

Cell adhesion is a central factor in many biological settings and is therefore very tightly controlled. On a single cell level, integrin-mediated adhesions are directly linked to specific arrangements of the actin cytoskeleton, which in turn affect how a cell behaves within its environment. Cytohesins, and especially Cyth2, are proteins that regulate not only remodeling of actin structures, but also dynamics of receptors on the plasma membrane, including integrins. Therefore, they are of special interest when studying how integrin signaling affects the cytoskeletal organization.

Podosomes are at the crossroads of adhesion complex and actin dynamics and are recognized as relevant biological structures in many different settings. In order to answer how cytohesins are involved in mediating signaling input coming from integrins to changes of the actin cytoskeleton and podosome formation, we therefore set out to analyze the role of different cytohesins in podosome formation. As myeloid cells are typical representatives of podosome-forming cells, we made use of several cytohesin KO mice to generate primary cell cultures of bone marrow-derived dendritic cells (BMDCs). These cells form prominent podosome clusters without further stimulation and are thus an optimal model to study podosome-related signaling pathways. Given the well-established role of especially Cyth2 in actin-related processes and its recent description as a regulator of podosome formation in monocytes[118], a special focus will be given to this specific member of the cytohesin family.

2. Material and Methods

2.1. Material

2.1.1. Kits

Kit	Company (office)
Arf1 G-LISA Activation Assay Kit	Cytoskeleton (Denver, USA)
Arf6 G-LISA Activation Assay Kit	Cytoskeleton (Denver, USA)
DyLight 549 NHS ester	Thermo Fisher Scientific (Waltham, USA)
High capacity cDNA Reverse Transcription Kit	Invitrogen (Carlsbad, USA)
mMESSAGE mMACHINE SP6 Transcription Kit	Invitrogen (Carlsbad, USA)
NucleoSpin Gel&PCR Clean-up Kit	Macherey-Nagel (Düren, Germany)
Pierce BCA Protein Assay Kit	Thermo Fisher Scientific (Waltham, USA)
Pierce ECL Plus Western Blotting Substrate	Thermo Fisher Scientific (Waltham, USA)
Poly(A) Tailing Kit	Invitrogen (Carlsbad, USA)
Rho Pulldown Kit	Cytoskeleton (Denver, USA)
RNeasy Mini Kit	Qiagen (Venlo, Netherlands)

2.1.2. Enzymes

Enzyme	Company (office)
Collagenase IV	Sigma-Aldrich (Taufkirchen, Germany)
DNAse I	Thermo Fisher Scientific (Waltham, USA)
Dream Taq polymerase	Thermo Fisher Scientific (Waltham, USA)
Phusion high fidelity polymerase	New England Biolabs (Ipswich, USA)
Restriction enzymes (+ buffers)	Thermo Fisher Scientific (Waltham, USA)
Shrimp alkaline phosphatase	Fermentas (St. Leon-Rot, Germany)
T4 DNA ligase (+ buffer)	New England Biolabs (Ipswich, USA)

2.1.3. Buffers, media and supplements

Reagent	Company (office)
fetal calf serum (FCS), heat- inactivated	Sigma-Aldrich (St. Louis, USA)
Hank's balanced salt solution (HBSS) + Ca^{2+}	PAN-Biotech (Aidenbach, Germany)
LB-agar	Gibco (Karlsruhe, Germany)
Opti-MEM	Gibco (Karlsruhe, Germany)
Penicillin/Streptomycin (Pen/Strep)	PAA (Pasching, Austria)
phosphate-buffered saline (PBS)	PAN-Biotech (Aidenbach, Germany)
recominant murine GM-CSF	Peprotec (Hamburg, Germany)
VLE-RPMI 1640	Biochrom (Berlin, Germany)

2.1.4. DNA, RNA and protein standards

Product	Company (office)
Gene Ruler 1 kb DNA ladder	Thermo Fisher Scientific (Waltham, USA)
Gene ruler 100 bp DNA ladder	Thermo Fisher Scientific (Waltham, USA)
Precision Plus Protein All Blue Standard	Bio-Rad (Munich, Germany)
ssRNA ladder	New England Biolabs (Ipswich, USA)

2.1.5. Chemicals and Reagents

Reagent	Company (office)
6x DNA loading dye	Thermo Fisher Scientific (Waltham, USA)
Acetic acid	Carl Roth (Karlsruhe, Germany)
Acrylamide /Rotiphorese gel	Carl Roth (Karlsruhe, Germany)
Agarose	VWR (Radnor, USA)
Ammonium acetate	Carl Roth (Karlsruhe, Germany)
Ammonium chloride	Riedel-de Haen/Honeywell (Seelze, Germany)
Ammonium persulfate (APS)	Carl Roth (Karlsruhe, Germany)
Ampicillin	Carl Roth (Karlsruhe, Germany)
Antipain	Sigma-Aldrich (St. Louis, USA)
Aprotinin	Carl Roth (Karlsruhe, Germany)
Benzamidin	Sigma-Aldrich (St. Louis, USA)
β-mercaptoethanol	Carl Roth (Karlsruhe, Germany)
Boric acid	Carl Roth (Karlsruhe, Germany)
Bovine serum albumin (BSA)	Carl Roth (Karlsruhe, Germany)
Brefeldin A (BrefA)	Sigma-Aldrich (St. Louis, USA)
Bromophenol blue	Carl Roth (Karlsruhe, Germany)
Butanol	Carl Roth (Karlsruhe, Germany)
Caesium chloride	Carl Roth (Karlsruhe, Germany)
Chloroform	Carl Roth (Karlsruhe, Germany)
Collagen I (PureCol, type I bovine collagen)	Advanced BioMatrix (San Diego, USA)
Collagen IV (mouse)	Sigma-Aldrich (Taufkirchen, Germany)
Deoxynucleotides (dNTPs)	Thermo Fisher Scientific (Waltham, USA)
Developing solution (Adefo Citroline2000)	Adefo-Chemie (Neu-Isenburg, Germany)
Diamidinophenylindole (DAPI)	Sigma-Aldrich (Taufkirchen, Germany)
Diazabicyclooctane (DABCO)	Sigma-Aldrich (Taufkirchen, Germany)
Dithiothreit (DTT)	Carl Roth (Karlsruhe, Germany)
Ethanol, 96 % (EtOH)	Werner Hofmann Abteilung der Schmittmann GmbH (Düsseldorf, Germany)
Ethidium bromide	Carl Roth (Karlsruhe, Germany)
Ethylenediaminetetraacetic acid (EDTA)	Carl Roth (Karlsruhe, Germany)
Ethyleneglycotetraacetic acid (EGTA)	Sigma-Aldrich (Taufkirchen, Germany)
Fibrinogen (bovine)	Sigma-Aldrich (Taufkirchen, Germany)
Fibronectin (human), Alfa Aesar	Thermo Fisher Scientific (Waltham, USA)

Fibronectin (murine)	Oxford Biomedical Reseach (Oxford, UK)
Fixer (Adefofix)	Adefo-Chemie (Neu-Isenburg, Germany)
Gelatin solution, type B	Sigma-Aldrich (Taufkirchen, Germany)
Gelatin-FITC (gelatin from pig skin - FITC conjugate)	Life Technologies /Thermo Fisher Scientific (Waltham, USA)
Glucose	Carl Roth (Karlsruhe, Germany)
Glutaraldehyde, grade 1	Sigma-Aldrich (Taufkirchen, Germany)
Glycerophosphate	Sigma-Aldrich (Taufkirchen, Germany)
Glycine	Carl Roth (Karlsruhe, Germany)
Hydrochloric acid (HCl)	Carl Roth (Karlsruhe, Germany)
Igepal	Sigma-Aldrich (Taufkirchen, Germany)
Isopropanol	VWR (Radnor, USA)
Leupeptin	Carl Roth (Karlsruhe, Germany)
Methanol	VWR (Radnor, USA)
Methyl cellulose	Sigma-Aldrich (Taufkirchen, Germany)
Milk powder	Carl Roth (Karlsruhe, Germany)
Mounting medium (fluoroshield)	ImmunoBioScience (Mukilteo, USA)
Normal goat serum	R&D Systems (Minneapolis, USA)
Paraformaldehyde (PFA)	AppliChem (Darmstadt, Germany)
Phalloidin - AlexaFluor488	Thermo Fisher Scientific (Waltham, USA)
Phalloidin - TRITC	Sigma-Aldrich (Taufkirchen, Germany)
Phenol	AppliChem (Darmstadt, Germany)
Phenylmethylsulfonyl fluoride (PMSF)	Carl Roth (Karlsruhe, Germany)
Poly-L-lysine (PLL)	Sigma-Aldrich (Taufkirchen, Germany)
Ponceau S	Carl Roth (Karlsruhe, Germany)
Potassium acetate	Carl Roth (Karlsruhe, Germany)
Potassium bicarbonate	Sigma-Aldrich (Taufkirchen, Germany)
Recombinant mouse Icam-1 Fc chimera	R&D Systems (Minneapolis, USA)
Rhosin	Tocris (Bristol, UK)
RNA loading dye (2x)	New England Biolabs (Ipswich, USA)
Sodium acetate	Carl Roth (Karlsruhe, Germany)
Sodium chloride	Labochem International (Einhausen, Germany)
Sodium dodecyl sulfate (SDS)	Carl Roth (Karlsruhe, Germany)
Sodium fluoride (NaF)	Sigma-Aldrich (Taufkirchen, Germany)
Sodium hydroxide (NaOH)	Grüssing (Filsum, German)
Sodium pyrophosphate	Sigma-Aldrich (Taufkirchen, Germany)
Sodium vanadate	Sigma-Aldrich (Taufkirchen, Germany)
Saccharose	Carl Roth (Karlsruhe, Germany)
Tetramethylethylendiamine (TEMED)	Sigma-Aldrich (Taufkirchen, Germany)
Tris	Carl Roth (Karlsruhe, Germany)
Triton X-100	Carl Roth (Karlsruhe, Germany)
Trizol reagent	Thermo Fisher Scientific (Waltham, USA)
Tween20	Carl Roth (Karlsruhe, Germany)
Water, molecular biology reagent	Sigma-Aldrich (Taufkirchen, Germany)

2.1.6. Antibodies

Antibodies for flow cytometry

Target	Fluorochrome	Species	Clone	Dilution	Company
CD11a	PE-Cy7	rat	2D7	1:200	BD Bioscience (Heidelberg, Germany)
CD11b	BrilliantViolet605	rat	M1/70	1:200	Biolegend (San Diego, USA)
CD11b	FITC	rat	M1/70	1:200	Biolegend (San Diego, USA)
CD11c	APC	hamster	N418	1:200	eBiosciences (San Diego, USA)
CD11c	PE	hamster	N418	1:200	Biolegend (San Diego, USA)
CD16/CD32 (Fc-block)	-	rat	93	1:350	Biolegend (San Diego, USA)
CD18	APC	rat	C71/16	1:200	BD Bioscience (Heidelberg, Germany)
CD24	BrilliantViolet421	rat	M1/69	1:200	Biolegend (San Diego, USA)
CD29	PE-Cy7	hamster	eBioHMb1-1	1:200	eBiosciences (San Diego, USA)
CD45	PerCP Cy5.5	rat	30-F11	1:200	Biolegend (San Diego, USA)
CD45R	PE	rat	RA3-6B2	1:200	BD Bioscience (Heidelberg, Germany)
CD49a	APC	hamster	HMa1	1:100	Biolegend (San Diego, USA)
CD49d	FITC	rat	R1-2	1:100	BD Bioscience (Heidelberg, Germany)
CD49e	PE	hamster	HMa5-1	1:100	Biolegend (San Diego, USA)
CD49f	PE	rat	GoH3	1:100	BD Bioscience (Heidelberg, Germany)
CD51	PE	rat	RMV-7	1:100	Biolegend (San Diego, USA)
CD61	AlexaFluor488	hamster	2C9.G2	1:100	Biolegend (San Diego, USA)
CD64	PE/Dazzle 594	mouse	X54-5/7.1	1:200	Biolegend (San Diego, USA)
F4/80	APC	rat	BM8	1:200	Biolegend (San Diego, USA)
I-A/I-E	PerCP Cy5.5	rat	M5/114.15.2	1:200	Biolegend (San Diego, USA)
I-A/I-E	BrilliantViolet510	rat	M5/114.15.2	1:200	Biolegend (San Diego, USA)
integrin β5	FITC	mouse	KN52	1:100	eBiosciences (San Diego, USA)
integrin β7	PerCP Cy5.5	rat	FIB27	1:100	Biolegend (San Diego, USA)
Ly-6C	APC Cy7	rat	HK1.4	1:200	Biolegend (San Diego, USA)
Ly-6G	PE	rat	1A8	1:200	Biolegend (San Diego, USA)
Ly-6G	APC	rat	1A8	1:200	Biolegend (San Diego, USA)
MerTK	PE-Cy7	rat	DS5MMER	1:200	eBiosciences (San Diego, USA)

Antibodies for Western Blot

Target	Species	Clone	Dilution	Company
Akt	rabbit (polyclonal)	-	1:2000	Cell Signaling (Danvers, USA)
β-actin	rabbit (polyclonal)	-	1:1000	Sigma-Aldrich (Taufkirchen, Germany)
Cyth1	mouse	2E11	1:1000	Thermo Fisher Scientific (Waltham, USA)
Cyth2	mouse	H-7	1:500	Santa Cruz (Dallas, USA)
Cyth3	rat	8B4	1:20	E. Kremmer (Munich, Germany)
Cyth4	rat	1E11	1:20	E. Kremmer (Munich, Germany)
ERK1/2	rabbit (polyclonal)	-	1:1000	Cell Signaling (Danvers, USA)
GAPDH	mouse	6C5	1:5000	Acris (Herford, Germany)
Paxillin	mouse	165/paxillin	1:1000	Cell Signaling (Danvers, USA)
phospho-Akt (Ser473)	rabbit	D9E	1:1000	Cell Signaling (Danvers, USA)
phospho-Akt (Thr308)	rabbit (polyclonal)	-	1:1000	Cell Signaling (Danvers, USA)
phospho-ERK1/2 (Thr202/Tyr204)	rabbit (polyclonal)	-	1:1000	Cell Signaling (Danvers, USA)
phospho-Paxillin (Tyr118)	rabbit (polyclonal)	-	1:1000	Thermo Fisher Scientific (Waltham, USA)
phospho-Pyk2 (Tyr402)	rabbit (polyclonal)	-	1:500	Cell Signaling (Danvers, USA)
phospho-Src family (Tyr416)	rabbit (polyclonal)	-	1:1000	Cell Signaling (Danvers, USA)
Pyk2	mouse	5E2	1:1000	Cell Signaling (Danvers, USA)
tubulin	mouse	DM1A	1:1000	Sigma-Aldrich (Taufkirchen, Germany)

HRP-coupled secondary antibodies

Target	Species	Clone	Dilution	Company
mouse IgG	goat (polyclonal)	-	1:5000	Santa Cruz (Dallas, USA)
rabbit IgG	goat (polyclonal)	-	1:10000	Dianova (Hamburg, Germany)
rat IgG	goat (polyclonal)	-	1:2000	Santa Cruz (Dallas, USA)

Functional antibodies

Target	Species	Clone	Concentration	Company
β1 integrin	hamster	Hmb1-1	50 µg/ml	Biolegend (San Diego, USA)
β1 integrin	hamster	HA2/5	50 µg/ml	BD Bioscience (Heidelberg, Germany)
IgG isotype	hamster	HTK888	50 µg/ml	Biolegend (San Diego, USA)

Antibodies for immunofluorescent stainings

Target	Conjugate	Species	Clone	Dilution	Company
vinculin	-	mouse	hVIN-1	1:200	Sigma-Aldrich (Taufkirchen, Germany)
β2 integrin/ CD18	-	rat	M18/2	1:100	Biolegend (San Diego, USA)
paxillin	-	mouse	165/paxillin	1:100	Cell Signaling (Danvers, USA)
talin	-	rabbit (polyclonal)	-	1:50	Abcam (Milton, UK)
GFP	-	chicken (polyclonal)	-	1:100	Thermo Fisher Scientific (Waltham, USA)
mouse IgG	AlexaFluor647	goat (polyclonal)	-	1:200	Jackson Immunoresearch (West Grove, USA)
rat IgG	FITC	donkey (polyclonal)	-	1:200	Jackson Immunoresearch (West Grove, USA)
rabbit IgG	AlexaFluor488	goat (polyclonal)	-	1:100	Thermo Fisher Scientific (Waltham, USA)
chicken IgY	AlexaFluor488	goat (polyclonal)	-	1:300	Thermo Fisher Scientific (Waltham, USA)

Additional dyes

	Conjugate	Dilution	concentration	company
phalloidin	AlexaFluor488	1:200	1 µM	Thermo Fisher Scientific (Waltham, USA)
phalloidin	TRITC	1:400	2.5 µM	Sigma-Aldrich (Taufkirchen, Germany)
DAPI	-	1:1000	1 µg/µl	Sigma-Aldrich (Taufkirchen, Germany)

2.1.7. Oligonucleotides

Oligonucleotides for genotyping of cytohesin KO mice

target	primer name	sequence (5'→ 3')
murine Cyth1	mCyth1_wt for 1b	CCA CTA CTC CCA GCC GTT TTA T
	mCyth1_wt rev 2	GTT CGA GTG CAT GCT TTG CC
	mCyth1_neo for 4	AAC CAA ATT AAG GGC CAG CTC A
murine Cyth2	Pscd2 WT1 screen for	CAG AAA TGC CAG GGC TTT CTC AGC
	Pscd2 WT1 screen rev	GCA TAG GTT TCA GGG CTG GAA AAC AC
	Pscd2 TG249	GCA GAA AAC AGG TTA GCG ACT CCA
murine Cyth3	mCyth3_TG380	CAC ATG GGA CAC ACA ATC GC
	mCyth3_TG387	ACA GAC TTC GCT GTG GTG AG
	mCyth3_TG381	AAT AGG AAC TTC GGT TCC GGC

murine Cyth4	Cyth4 WT for	CTA CAC CTG GTT TGC CGG GA
	Cyth4 WT rev	CAG TGA GAA CAT GGG CCC CA
	Cyth4 KO rev	GGG AGT AGA GTT CCC AGG AGG
LysM-Cre	Cre8	CCC AGA AAT GCC AGA TTA CG
	MLys1	CTT GGG CTG CCA GAA TTT CTC
	MLys2	TTA CAG TCG GCC AGG CTG AC

All oligonucleotides were synthesized by MWG Eurofins (Ebersberg, Germany)

siRNAs

siRNA	**sequence of sense strand (5'→ 3')**	**supplier**
siRenilla	AAACAUGCAGAAAAUGCUG dTdT	Dharmacon (Lafayette, USA)
siItgb1 #1[152]	AGAUGAGGUUCAAUUUGAA dAdA	MWG Eurofins (Ebersberg, Germany)
siItgb1 #2[153]	CAAUCCGAAGUAUGAGGGA dAdA	MWG Eurofins (Ebersberg, Germany)
siItgb2 #1[154]	CUGCAUGUCCGGAGGAAAU dAdA	MWG Eurofins (Ebersberg, Germany)
siItgb2 #2[154]	GGUGAAAACGUAUGAGAAA dAdA	MWG Eurofins (Ebersberg, Germany)
siItga5_mm #1	GAAACAUGUGUACCUGGGU dTdT	MWG Eurofins (Ebersberg, Germany)
siItga5_mm #2	GUGUUUCAGGCUGCGCUGU dTdT	MWG Eurofins (Ebersberg, Germany)
siItgal_mm #1	GACUUCGUUGAGCUGAAUG dTdT	MWG Eurofins (Ebersberg, Germany)
siItgal_mm #2	UCGUCCCGCCUAUCAGGAA dTdT	MWG Eurofins (Ebersberg, Germany)
siItgam_mm #10	CAAUGUGACCGUAUGGGAU dTdT	MWG Eurofins (Ebersberg, Germany)
siItgam_mm # 12	CACGUGUUCCAAGUGGACA dTdT	MWG Eurofins (Ebersberg, Germany)
siItgax_mm #12	CUUGAGUUAUGAUAGUGUCA dTdT	MWG Eurofins (Ebersberg, Germany)
siItgax_mm #22	UGUGGCUAUCACACAGGCA dTdT	MWG Eurofins (Ebersberg, Germany)
siCyth2_mm #1[137]	GAGCUAAGUGAAGCUAUGA dTdT	MWG Eurofins (Ebersberg, Germany)
siCyth2_mm #2[151]	GCGAAUUUCUGUGAAGAAG dTdT	MWG Eurofins (Ebersberg, Germany)

Oligonucleotides for amplification and sequencing of cytohesin isoforms

target	primer name	sequence (5'→ 3')
murine Cyth1	mpscd1 for qPCR	CAA AGA CAA GCC TAC GGT GGA G
	mpscd1 rev_NotI	gcg ggg gcg gcc gc TCA GTG TCT CTT TGT GGA GGA GAC C
murine Cyth2	mpscd2 for_MluI	ggg gcg acg cgt ATG GAG GAC GGT GTC TAC GAG C
	mpscd2 rev qPCR	GAG CTG TCC CTT ATT GTT GGG AAT C
murine Cyth3	mpscd3 for qPCR	GAC AAG CCC ACC GCT GAG
	mpscd3 rev_NotI	gcg ggg gcg gcc gc CTA TTT CTT ATT GGC AAT CCT CC
murine Cyth4	mpscd4 for_MluI	ggg gcg acg cgt ATG GAT GTG TGT CAC ACA GAT C
	mpscd4 rev qPCR	GAT AAA GGC ATG CAA GAC AGA CGG

All oligonucleotides were synthesized by MWG Eurofins (Ebersberg, Germany)

2.1.8. Plasmids

pGEM-Fse vectors were used for *in vitro* transcription. The pGEM-Fse vector was based on the pGEM-T vector by Fermentas (St. Leon-Rot, Germany) and modified by Dr. Johanna Kolanus to contain an additional Fse restriction site. Cyth2-2G and Cyth2-3G constructs were inserted into pGEM-Fse vectors behind the SP6 RNA polymerase promoter.

2.1.9. Organisms

Organism	Source
Escherichia coli (E. coli), strain DH5α	
Cyth2$^{flox/flox}$ LysM-Cre mice	European Mouse Mutant Archive (EMMA), Italy
Cyth1 KO mice (Cytohesin-1 KO)[104]	National Institutes of Biomedical Innovation, Health and Nutrition (Japan)
Cyth3 KO mice[126]	KOMP Repository (UC Davis, USA)
Cyth4 KO mice	European Conditional Mouse Mutagenesis Program (EUCOMM)
Itga1 KO mice (bone marrow)[155]	Ambra Pozzi, Vanderbilt University (Nashville, USA)
CD18 null mice (bone marrow)[24]	Karin Scharffetter- Kochanek, Ulm University (Germany)
Itga4$^{flox/flox}$ Vav-cre mice (bone marrow)	Triantafyllos Chavakis, University Hospital Dresden (Germany)

2.1.10. Plastic ware and consumables

Item	Model	Company (office)
Cell culture dishes	Cellstar	Greiner Bio-one (Frickenhausen, Germany)
Cell scaper 25 cm	Cell Scraper 2-Posit. Blade 25	Sarstedt (Nümbrecht, Germany)
Cell strainer	EASYstrainer 70 µm	Greiner Bio-one (Frickenhausen, Germany)
	EASYstrainer 40 µm	Greiner Bio-one (Frickenhausen, Germany)
Coverslips	15 mm	Marienfeld (Lauda-Königshofen, Germany)
Dialysis cassette	Slide-a-Lyzer Dialysis Cassettes (10 k MWCO)	Thermo Fisher Scientific (Waltham, USA)
Elastomers	50 kPa, PDMS	Bernd Hoffmann and Rudolph Merkel (Forschungszentrum Jülich, Germany)
Electroporation cuvettes	4 mm	Biozym (Vienna, Austria)
Filter paper	Whatman	GE Healthcare (Chicago, USA)
Filter tips	10/200/1000 µl	Sarstedt (Nümbrecht, Germany)
Glass pasteur pipettes		Brand (Wertheim, Germany)
Microscope slides		Marienfeld (Lauda-Königshofen, Germany)
Microscopy channel slides	µ-slide VI$^{0.4}$ ibiTreat	Ibidi (Gräfelfing, Germany)
Needles	sterican	Braun Melsungen (Melsungen, Germany)
Neubauer chamber		Marienfeld (Lauda-Königshofen, Germany)
Nitrocellulose membrane	BioTrace NT nitrocellulose membrane	Pall Corporation (Pensacola, ??)
Parafilm		Bemis (Neenah, USA)
PCR tubes	200 µl Thin Wall Tubes	Axygen (Tewksbury, USA)
Petri dishes	10 cm	Greiner Bio-one (Frickenhausen, Germany)
Plastic tips	10/200/1000 µl	Carl Roth (Karlsruhe, Germany)
Radiographic films	amersham hyperfilm ecl	GE healthcare
Reaction tubes	0.5/1/2 ml	Starlab (Ahrensburg, Germany)
Serological pipettes	5/10/25 ml	Greiner Bio-one (Frickenhausen, Germany)
Syringes	Injekt 10 ml	Braun Melsungen (Melsungen, Germany)
Tubes for flow cytometry	5 ml	Sarstedt (Nümbrecht, Germany)
Tubes for ultracentrifugation	QuickSeal Polypropylene	Beckman (Munich, Germany)

2.1.11. Laboratory equipment

Device	Model	Company (office)
autoclave	DX-150	Systec (Linden, Germany)
CO_2 incubator	model C150	Binder (Great River, USA)
Centrifuges	8510R	Eppendorf (Hamburg, Germany)
	5415R	Eppendorf (Hamburg, Germany)
	Optima LE-80K ultracentrifuge	Beckman Coulter (Munich, Germany)
Electrophoresis chambers (agarose gels)		Polymehr (Paderborn, Germany)
Electrophoresis chambers (SDS-PAGE)	Mini Trans-Blot Cell	Bio-Rad (Munich, Germany)
Electroporator	Gene Pulser Xcell	Bio-Rad (Munich, Germany)
Flow cytometers	BD Canto II	BD Biosciences (Heidelberg, Germany)
	BD FACS Aria	BD Biosciences (Heidelberg, Germany
Gel documentation device	Gel Max	Intas (Göttingen, Germany)
Heating block	Thermomixer compact	Eppendorf (Hamburg, Germany)
Heating cabinet	EcoCell 55	MMM Medcenter (Munich, Germany)
Laminar flow hood	HeraSafe KS	Thermo Scientific (Waltham, USA)
Magnetic stirrer	ARE heating magnetic stirrer	VELP scientica (Usmate, Italy)
Microscopes	Eclipse TS100	Nikon (Tokyo, Japan)
	FluoView 1000	Olympus (Tokyo, Japan)
	LSM 880+ Airyscan	Zeiss (Jena, Germany)
Orbital shaker	New Brunswick innova44	Eppendorf (Hamburg, Germany)
pH meter	MP220	Mettler Toledo (Greifensee, Switzerland)
Pipette controler	AccuJet Pro	Brand (Wertheim, Germany)
Pipettes	Pipetman Classic	Gilson (Middleton, USA)
	ErgoLine	StarLab (Helsinki, Finland)
Plate reader	infinite M200	Tecan (Männedorf, Switzerland)
Power supplies	elite 300 plus	Schütt Labortechnik (Göttingen, Germany)
	EV-234	Consort (Turnhout, Belgium)
Rocker	WS-10	Edmund Bühler (Hechingen, Germany)
Roller mixer	RS-TR05	Phoenix Instrument (Garbsen, Germany)
Rotating wheel	Neolab Rotator	Neolab (Heidelberg, Germany)
Scales	AG285 (micro scale)	Mettler Toledo (Greifensee, Switzerland)
	JB2002-G	Mettler Toledo (Greifensee, Switzerland)
Spectrophotometer	NanoDrop 2000	Thermo Scientific (Waltham, USA)
Thermocyclers	C1000 Touch Thermal Cycler	Bio-Rad (Munich, Germany)
	MyCycler	Bio-Rad (Munich, Germany)
Vacuum pump	AC02	HLC BioTech (Bovenden, Germany)
Vortex mixer	UNIMAG ZX3	VELP scientica (Usmate, Italy)

2.2. Animal Experimental Techniques

2.2.1. Knock-out mice

Conditional Cyth2 knock-out (KO) embryos ($Cyth2^{flox/flox}$) were obtained from the European Mouse Mutant Archive (EMMA) in Italy. These mice were crossed with LysM-Cre mice[156], a generous gift from Prof. Irmgard Förster, to obtain a myeloid cell-specific KO. Cyth1 KO mice were initially described in 2012[104] and obtained from Osamu Suzuki at the National Institutes of Biomedical Innovation, Health and Nutrition, Japan. Cyth3 KO mice were generated and described by our laboratory.[126] Cyth4 KO mice were generated by Dr. Bettina Jux based on an ES cell line from EUCOMM (European Conditional Mouse Mutagenesis Program). As controls, wildtype (wt) animals from the same breedings were used. These mice were either Cre-negative $Cyth2^{flox/flox}$ or carried the respective wt cytohesin alleles.

$Cyth2^{flox/flox}$ LysM-Cre, Cyth1 KO and Cyth3 KO mice were on a C57BL/6J background, while Cyth4 KO mice used in this study had a mixed background of 50 % C57BL/6J and 50 % C57BL/6N. All mice were bred and kept in accordance with the German Animal Welfare Act at the Genetic Resources Center (GRC) of the LIMES Institute, Bonn University.

Experiments using integrin KO cells were performed with cells derived from bone marrow, which we obtained from collaborators. Cells from CD18 null mice[24] were a kind gift of Karin Scharffetter-Kochanek, Ulm University (Germany). Furthermore, we received bone marrow of $Itga1^{KO/KO}$ mice[155] from Ambra Pozzi, Vanderbilt University (Nashville, USA) and of $Itga4^{flox/flox}$ Vav-Cre mice[157,158] from Triantafyllos Chavakis, University Hospital Dresden (Germany).

2.2.2. Genotyping of cytohesin KO mice

In order to determine the genotype of cytohesin KO mice, deoxyribonucleic acid (DNA) from biopsies (tails tips or ear punches) was extracted by incubating the tissue in 200 µl of 50 mM sodium hydroxide at 96°C for 20 minutes followed by addition of 55 µl 1M Tris/HCl pH8.

Amplification of the different loci was achieved by polymerase chain reaction (PCR). The PCR reaction was assembled on ice in PCR tube strips as follows:

<u>For Cyth1, Cyth3 and Cyth4 loci:</u>

10 µl	OneTaq Reaction Mix (2x)
0.5 µl each	primers (10 pmol/µl stock)
2 µl	DNA
Ad 20 µl	H_2O

Thermocycler conditions for Cyth1 PCR:

Step	Temp	time	Cycles
Initial Denaturation	94°C	30 sec	x1
Denaturation	94°C	30 sec	
Annealing	64°C	30 sec	x30
Elongation	68°C	1 min	
	68°C	10 min	x1
	4°C	∞	

Thermocycler conditions for Cyth3 PCR:

Step	Temp	time	Cycles
Initial Denaturation	94°C	3 min	x1
Denaturation	94°C	3 min	
Annealing	63.5°C	45 sec	x30
Elongation	68°C	1 min	
	68°C	5 min	x1
	4°C	∞	

Thermocycler conditions for Cyth4 PCR:

Step	Temp	time	Cycles
Initial Denaturation	94°C	3 min	x1
Denaturation	94°C	3 min	
Annealing	63°C	45 sec	x35
Elongation	68°C	1 min	
	68°C	5 min	x1
	4°C	∞	

<u>For Cyth2 and LysM loci:</u>

2 µl	10x DreamTaq buffer
0.4 µl	10mM dNTPs
1 µl each	primers (10 pmol/µl stock)
0.2 µl	DreamTaq Polymerase
2 µl	DNA
Ad 20 µl	H_2O

Thermocycler conditions for Cyth2 PCR:

Step	Temp	time	Cycles
Initial Denaturation	95°C	3 min	x1
Denaturation	95°C	45 sec	
Annealing	64.5°C	45 sec	x35
Elongation	72°C	1 min	
	72°C	10 min	x1
	4°C	∞	

Thermocylcer conditions for LysM-Cre PCR:

Step	Temp	time	Cycles
Initial Denaturation	94°C	3 min	x1
Denaturation	94°C	0.5 min	
Annealing	62°C	0.5 min	x34
Elongation	72°C	1 min	
	72°C	10 min	x1
	10°C	∞	

After completion of the PCR protocol, the samples were subjected to agarose gel electrophoresis (2 % agarose in TAE buffer) to determine the size of the respective products (see 2.4.1.).

The expected sizes for the amplified loci were

Cyth1	~400 base pairs (bp)	Cyth1 wt
	~520 bp	Cyth1 KO
Cyth2	~530 bp	Cyth2 wt
	~690 bp	floxxed Cyth2
	~350 bp	Cyth2 KO
LysM	~350 bp	wt LysM
	~700 bp	LysM-Cre
Cyth3	~500 bp	Cyth3 wt
	~257 bp	Cyth3 KO
Cyth4	~286 bp	Cyth4 wt
	~560 bp	Cyth4 KO

2.2.3. Preparation of cell suspensions from primary organs for flow cytometry

Mice were euthanized by cervical dislocation and organs (spleen, lungs, lymph nodes (LN)) were dissected and stored in ice-cold phosphate-buffered saline (PBS). All organs were cut into small pieces before they were incubated in collagenase solution for 30 min (LN) or 45-60 min (spleen and lung) at 37°C. Afterwards, the cell suspension was homogenized by forcing the tissue through a 19 G needle and filtering through a 70 µm strainer. Cells were pelleted at 1350 rounds per minute (rpm) for 5 min at 4°C before they were either resuspended in FACS buffer (LN) or in ACK lysis buffer to lyse erythrocytes (spleen and lungs). Lysis was allowed to take place for 5 min at room temperature (RT) and stopped by adding 10x volume of PBS. Cells were then centrifuged again, before the pellet could be resuspended in FACS buffer.

For preparation of blood samples, blood was collected directly after euthanization and immediately mixed with ethylenediaminetetraacetic acid (EDTA) at a final concentration of about 10 mM to avoid coagulation. Samples were then subjected to erythrocyte lysis as described above.

Bone marrow cells were isolated as described in 2.3.1. and analyzed by flow cytometry directly.

Used buffers and solutions:

Collagenase solution	0.2 mg/ml collagenase IV, 100 U/ml DNAse I in HBSS + Ca^{2+}, 10 % fetal calf serum (FCS)
FACS buffer	5 % FCS in PBS
ACK lysis buffer	155 mM ammonium chloride, 10 mM potassium bicarbonate, 0.1 mM EDTA

2.2.4. Measurement of bone mineral density

Bone mineral density (BMD) as a functional read-out of osteoclast activity was measured using micro-computer tomography (µCT). After euthanization, femur and complete heads of 18 weeks old mice were placed into 4 % paraformaldehyde (PFA) solution for several days, before they were scanned with a µCT Skyscan 1174™ (Skyscan, Kontich, Belgien) with a slice size of 8 µm (femur) or 9 µm (skull) in collaboration with Prof. Christoph Bourauel from the Dental Clinic of Bonn University.

To determine the BMD, tree-dimensional segments with a thickness of 500 µm (equaling ~63 slices) of cortical bone from epiphysis and metaphysis of the distal femur, as well as sphenoid and parietal bone in the skull, were analyzed with CTAn Software (Bruker).

2.3. Cell Culture Methods

2.3.1. Generation of bone marrow-derived dendritic cells (BMDCs)

After euthanizing mice by cervical dislocation, femur and tibia of 8-15 weeks old mice were taken, and all muscle tissue was removed thoroughly. Bones were kept in PBS on ice after preparation and shortly disinfected with 70 % ethanol (EtOH) before being further handled under sterile cell culture conditions. Both ends of the bones were cut off and the bone marrow flushed out using a 27G needle and syringe filled with ice-cold PBS. The bone marrow was filtered through a 40 µM mesh and subsequently centrifuged at 280 g for 5 min at 4°C.

$5x10^6$ cells were resuspended in 10 ml of complete DC-medium (VLE-RPMI + 10 % FCS, 1 % Penicillin/Streptomycin (Pen/Strep) and 10 ng/ml recombinant murine granulocyte/monocyte colony-stimulating factor (GM-CSF)) and seeded into a 10 cm petri dish. After 2-3 days at 37°C and 5 % CO_2, 5 ml of fresh medium containing 10 ng/ml GM-CSF were added and after another 2-3 days 5 ml were removed from the plate, spun down at 280 g for 5 min and the pellet was resuspended in 5 ml of fresh medium (+GM-CSF) before it was pipetted back onto the plate.

After 6-9 days the adherent fraction (termed immature BMDCs or iDCs) was harvested by aspirating the cell culture medium, washing once with PBS and incubating with 5 ml of 2 mM EDTA/PBS for 10-15 min at 37°C. Adhesion proteins like integrins depend on Ca^{2+} ions and the chelation of Ca^{2+} by EDTA reduces the cells' adhesiveness. Cells that still adhered after EDTA treatment were gently scraped off the surface.

Cell concentrations were determined using a Neubauer chamber.

2.3.2. Transfection of BMDCs with mRNA

Immature BMDCs are not readily transfected with DNA constructs but they tolerate the introduction of ribonucleic acid (RNA). For this project, electroporation of messenger RNA (mRNA) therefore was the method of choice to express foreign proteins in BMDCs.

After harvest with PBS/EDTA (see above), cells were washed once with PBS to get rid of EDTA traces. Afterwards, cells were resuspended in Opti-MEM at 10^6 cells/200 µl. 10 µg of mRNA was placed into electroporation cuvettes (4mm) and mixed with 100 µl of cell suspension. The electroporation was performed with a Gene Pulser Xcell (Bio-Rad) using the following parameters:

1 pulse of 300 V, 6 ms (square wave protocol)

After transfection, cells were directly pipetted into pre-warmed cell culture medium containing FCS and GM-CSF, but no antibiotics.

mRNA transfections of cytohesins are not long lasting and protein expression reaches its maximum a few hours post transfection (hpt), before it decreases drastically within 24 h. Therefore, cells transfected with mRNA were analyzed already at 6 hpt.

2.3.3. RNA interference

In order to reduce expression of a given gene on protein level, RNA interference was used. This method is based on the endogenous microRNA system, where short RNAs bind to complementary sequences on mRNAs leading to recruitment of a protein complex and, ultimately, to silencing or degradation of the mRNA. That way, the mRNA pool available for protein translation is diminished. Artificial short RNAs called “small interfering RNA” (siRNA) can be experimentally introduced into cells and use the same mechanism as endogenous microRNAs.[159]

After harvest with PBS/EDTA (see above), cells were washed once with PBS to get rid of EDTA traces. Afterwards, cells were resuspended in Opti-MEM at 1-2x10^6 cells/100 µl. 10 µg of siRNA was placed into electroporation cuvettes (4mm) and mixed with 100 µl of cell suspension. The electroporation was performed with a Gene Pulser Xcell (Biorad) using the following parameters:

2 pulses of 1000 V, 0.5 ms (square wave protocol)

After transfection, cells were directly pipetted into pre-warmed cell culture medium containing all growth factors except for antibiotics. Cells transfected with siRNA were used at 24 hpt unless stated otherwise.

2.3.4. Immunofluorescence staining of cells

In order to visualize proteins within the cell, immunofluorescence (IF) staining was performed. iDCs were seeded on pre-coated surfaces (coverslips or plastic ware that is suitable for laser scanning microscopy) for at least 6 h at 37°C and 5 % CO_2. After crosslinking proteins by fixation of cells with PFA and washing off residual PFA with three PBS washes, cells were permeabilized with 0.2 % TritonX100 in PBS for 5 min at RT and then washed again 3x with PBS before they were

covered with blocking solution (3 % BSA in PBS) for 30 min at RT to block unspecific binding sites. Subsequently, the primary antibody solution (antibodies diluted in 3 % BSA/PBS) was added dropwise (30 µl) to parafilm-covered glass slides and coverslips were placed upside-down onto each drop. The glass slide was then placed into a humid chamber and cells incubated for 1 h at RT in the dark. Afterwards, primary antibody was washed off 3x with PBS and the coverslips then incubated in a similar manner for another 45-60 min in secondary antibody solution (antibodies diluted in PBS) at RT in the dark. The coverslips were then transferred back into a 12-well plate, washed 3x with PBS, and mounted onto glass slides using a 15 µl drop of fluoroshield containing 50 mg of diazabicyclooctane (DABCO) per ml. After drying overnight (o.n.) at RT in the dark, glass slides were kept at 4°C until imaging using confocal laser scanning microscopy.

2.3.5. Podosome formation assay

iDCs were harvested and seeded at 50 000 cells/coverslip in complete DC-medium onto coverslips coated with different proteins. Cells were allowed to adhere and form podosomes in an overnight incubation at 37°C and 5 % CO_2 (~16-20 h) before they were fixed by adding PFA directly into the medium to a final concentration of 4 %. After 20 min at RT, the coverslips were washed 3x with PBS to remove residual PFA. Afterwards, cells were stained with an antibody against vinculin and fluorescently labelled phalloidin, which is a toxin binding with high affinity to F-actin. That way one can visualize podosome rings and cores, respectively (see 2.3.4.).

Images were taken using a confocal laser scanning microscope (FluoView 1000, Olympus, or LSM880+ Airyscan, Zeiss) at 60x or 63x magnification and podosomes were quantified using ImageJ 1.52i software (National Institutes of Health, Bethesda, MD).

2.3.6. Blocking integrin function with specific antibodies

To analyze podosome formation in the presence of blocking antibodies, ibidi µ-slide $VI^{0.4}$ (ibiTreat) slides were coated with FN or gelatin (50 µg/ml) for 1 h at RT and washed with 1 ml of PBS per channel. Cells in VLE-RPMI (10 % FCS, 1 % Pen/Strep, 10 ng/ml GM-CSF) were mixed with Hmb1-1 or HA2/5 antibody or isotype control antibodies at 50 µg/ml to obtain a final cell concentration of $8x10^5$ cells/ml. Channels were flushed with 500 µl of pre-warmed VLE-RPMI (10 % FCS, 1 % Pen/Strep, 10 ng/ml GM-CSF) and 100 µl of cell suspension was seeded per channel. After incubation o.n. at 37°C and 5 % CO_2, medium was carefully replaced by 100 µl of pre-warmed PFA

solution (4 % PFA in PBS). After fixation for 20 min at RT, PFA was washed off with PBS and the cells were stained for podosomes using antibodies against vinculin and fluorescently labelled phalloidin (see 2.3.5.). In addition, secondary antibodies directed against the functional antibodies were added to the antibody cocktail.

Images were taken using a confocal laser scanning microscope (LSM880+ Airyscan, Zeiss) at 63x magnification, before podosomes were quantified using ImageJ 1.52i software (National Institutes of Health, Bethesda, MD).

2.3.7. Matrix-degradation assay

To assess degradative capacities of podosome-containing cells a slightly modified version of a protocol by Chen and colleagues[160] was used. By coating with a fluorescently labeled matrix protein and seeding cells on top, degradation of matrix by the cells was visible as dark holes within the fluorescent surrounding. Staining of cell nuclei furthermore allows to determine the total degraded area per cell.

For coating of pre-activated coverslips (see 2.5.2.) with either gelatin (20 % FITC-gelatin, 80 % unlabeled gelatin, at 200 µg/ml in PBS) or FN (undiluted FN-Dylight549, 100 µg/ml in PBS, see 2.5.1.), the lid of a 12-well plate was covered with parafilm and 60 µl drops of the respective coating solution were applied on top. Next, the coverslips were placed upside down onto the solution and incubated for 15 min (gelatin) or 1h (FN) at RT in the dark. Subsequently, coverslips were placed back into a 12-well plate and washed 2x with PBS. To quench potential fluorescence of the glutaraldehyde, the coverslips were incubated in VLE-RPMI + 10 % FCS for 30 min at RT before a final round of 2 PBS washes.

Cells were seeded at 50.000 cells per coverslip in complete DC medium and cultured for 24 h at 37°C and 5 % CO_2. The assay was stopped by adding PFA at a final concentration of 4 % to the medium. Following incubation for 20 min at RT in the dark, PFA was washed off 3x with PBS. Before continuing with the IF staining protocol (see 2.3.4.), free aldehydes were quenched with 150 mM glycine/PBS for 5 min followed by another three washing steps using PBS. For degradation assays cells were stained with the DNA-specific dye diamidinophenylindole (DAPI) and phalloidin and imaged using a laser scanning microscope (FluoView 1000, Olympus) at 20x magnification. To improve the signal of the matrix coating, the pinhole was opened to a non-confocal width.

Degradative activity was quantified by measuring the total degraded matrix area (visible as areas without fluorescent signal) in relation to total cell number (based on the DAPI staining) using ImageJ 1.52i software (National Institutes of Health, Bethesda, MD). In detail, gelatin or FN images were processed with a gaussian blur filter (sigma 1 µm), and thresholded until only degraded areas were visible. Using the "analyze particles" tool, the total degraded area was measured and set in relation to the total cell number as determined by the DAPI staining of nuclei.

2.3.8. Flow Cytometry

Flow cytometry is used to measure protein levels on the cell surface or within the cell. After staining a given cell suspension with specific antibodies that are conjugated to a fluorophore, cells are subjected to a laser beam to measure fluorescence intensity of every single cell.

After harvesting or isolating cells, the cell suspension was placed on ice and handled on ice or at 4°C at all times. 0.1-1 x 10^6 cells were first spun down at 280g for 5min (at 4°C) and the cell pellet subsequently resuspended in 50-100 µl PBS containing Fc-block (anti CD16/CD23 antibody) at a 1:350 dilution to avoid unspecific binding of antibodies to Fc receptors. After 15 min at 4°C, an equal volume of staining solution containing the respective antibodies in PBS was added (final dilution 1:100 to 1:200) and further incubated for 20 min at 4°C in the dark. To wash off unbound antibody, 1 ml of cold PBS was added to each tube and the cells were pelleted at 280 g for 5 min at 4°C. Finally, cells were resuspended in 100-200 µl of ice-cold PBS and fluorescence was measured with a BD Canto II (BD Biosciences).

2.3.9. Time course adhesion assay

In order to induce adhesion-related signaling at a defined time point the following procedure was used. BMDCs were harvested and resuspended thoroughly in normal culture medium at 5x10^6 cells/ml. After adding the same volume of a 10 % methyl cellulose solution (in VLE-RPMI), the cells were surrounded by a viscous matrix that prevented them from adhering to the vessel surface or to each other. Methyl cellulose is used for similar purposes in colony forming cell assays to isolate single cells[161] and is able to retain adhesive properties of cells[162]. After 1-2 h incubation at 37°C and 5 % CO_2, the methyl cellulose mix was diluted by adding 10x volume of normal culture medium and the cells were directly seeded into pre-coated 6-well plates at 800 000 cells/well. Afterwards, the cells were placed back at 37°C and 5 % CO_2 for 5-360 min.

For analysis of integrin cell surface expression by flow cytometry, the cells were placed on ice at the indicated time points and an equal volume of ice-cold PBS was added to prevent changes to the integrins at the cell surface. The liquid containing non-adherent cells was transferred to fresh tubes and 500 µl of ice-cold 2mM EDTA/PBS were added to the remaining adherent fraction. After incubating for 20 min on ice, cells were scraped off and added to the non-adherent cell fraction. Finally, cells were stained for flow cytometry as described above (2.3.8.).

To generate protein lysates, cell lysis was performed directly in the well as described below (2.5.5.).

2.3.10. Integrin internalization assay

In order to study internalization dynamics of integrins, cells adhering to different substrates were first stained with an unlabeled antibody against defined integrins. During the following incubation, more and more integrins were internalized together with bound antibody. Next, cells were harvested and stained with secondary antibodies that would only recognize the remaining antibody-bound integrins on the cell surface.

In detail, cells grown on 6-well plates at 400 000 cells/well were pre-incubated in starvation medium (0.5 % FCS, 1 % Pen/Strep and 10 ng/ml GM-CSF in VLE-RPMI) for 1h at 37°C and 5 % CO_2. Then, medium was replaced by 0.5 ml of ice-cold staining solution (primary antibodies diluted in PBS; hamster anti-CD49e-biotin 1:200, rat anti-CD18 1:250 and hamster anti-CD49a 1:200) and cells were stained for 1 h at 4°C. Afterwards, unbound antibody was washed off with PBS and cells were incubated in starvation medium for 1-3 h at 37°C and 5 % CO_2.

At the indicated time points the cells were placed on ice and an equal volume of ice-cold PBS was added to prevent changes in integrin cell surface expression. The liquid containing non-adherent cells was transferred to fresh tubes and 500 µl of ice-cold 2mM EDTA/PBS was added to the remaining adherent fraction. After 20 min on ice, cells were scraped off and added to the non-adherent cell fraction.

Afterwards, cells were stained for flow cytometry as described above (2.3.8.), but with the following adaptations: Blocking solution contained 10 % normal goat serum in 3 % BSA/PBS, but no Fc-blocking antibody, and secondary antibodies from goat or fluorescently labelled streptavidin were used for staining.

2.3.11. Integrin recycling assays using Brefeldin A

Apart from being internalized and recycled to the cell surface, integrins on the cell surface are also replenished by de-novo synthesis from the endoplasmic reticulum (ER) via the Golgi apparatus. To exclude this Golgi-dependent source of newly synthesized integrins, cells seeded o.n. onto pre-coated 6-wells at 500 000 cells/well in DC medium were incubated in starvation medium (0.5 % FCS, 1 % Pen/Strep in VLE-RPMI) containing 5 µg/ml Brefeldin A (BrefA), an inhibitor of the Golgi apparatus, for 2-6 h at 37°C and 5 % CO_2. Control samples contained 0.1 % EtOH instead of BrefA.

At the indicated time points the cells were placed on ice and an equal volume of ice-cold PBS was added to prevent changes to the integrin cell surface expression. The liquid containing non-adherent cells was then transferred to fresh tubes and 500 µl of ice-cold 2mM EDTA/PBS was added to the remaining adherent fraction. After incubating for 20 min on ice, cells were scraped off and added to the non-adherent cell fraction. Afterwards, cells were stained for flow cytometry as described above (2.3.8.).

2.4. Molecular Biology

2.4.1. Agarose gel electrophoresis

To determine the size of nucleic acids, gel electrophoresis was performed. DNA and RNA samples were mixed with the respective loading dye and RNA samples were additionally heated to 65°C for 5 min. A 1-2 % solution of agarose in TAE buffer (for DNA) or TBE buffer (for RNA) was prepared by heating in a microwave until agarose was fully dissolved. After cooling down, 2 µl of ethidium bromide were added per 100 ml of agarose and cast into plastic trays. When the gel was polymerized, samples were loaded into the wells and separated at 95-120 V for 30-45 min. In order to estimate the size of a specific band, DNA or RNA standards were run on the same gel. Ethidium bromide, which intercalates into DNA/RNA fragments, was visualized using Gel Max (Intas).

TAE buffer (1x)	40 mM Tris, 20 mM acetic acid, 1 mM EDTA, pH 8
TBE buffer (1x)	89 mM Tris (pH 7.8), 89 mM boric acid, 2 mM EDTA

2.4.2. Enzymatic digestion and ligation of plasmid DNA

Plasmid DNA was digested with the bacterial restriction enzymes MluI and NotI using specific buffers as recommended by Fermentas. 3 µg of DNA were incubated with 1 µl of each restriction enzyme in a total volume of 30 µl for 1h at 37°C. Afterwards, 1 µl of alkaline phosphatase was added to samples containing the desired vector backbone and incubated for another 10 min at 37°C, followed by heat inactivation of the enzyme for 5 min at 75°C. Dephosphorylation of DNA fragments was performed to prevent re-ligation, which requires at least one phosphorylated end to occur. Digested samples were run on agarose gels to verify successful digestion and to separate digestion products. DNA fragments of the expected size were cut out of the gel and were purified using the NucleoSpin Gel&PCR Clean-up kit by Macherey Nagel according to manufacturer's instructions. DNA concentrations were determined using a NanoDrop 2000 (Thermo Scientific).

To ligate the desired DNA fragment into the backbone of choice, 50 ng of backbone together with 150 ng of insert were mixed with 1x ligase buffer containing T4 ligase (2 units/µg plasmid) in a total volume of 20 µl and incubated for 1h at RT.

2.4.3. Transformation of bacteria

The ligated plasmid was introduced into chemo competent DH5α *Escherichia coli* (E. coli) by heat shock transformation. In detail, 10-100 ng of plasmid DNA was added to 80 µl of bacteria, mixed gently and incubated on ice for 10 min. During subsequent incubation at 37°C for 5 min the bacteria took up the plasmid and were immediately placed back onto ice. 1ml of lysogeny broth (LB) medium (without antibiotics) was added to the transfected E. coli to recover for 30 min at 37°C shaking. Afterwards, bacteria were spun down for 2 min at 13 000 rpm and resuspended in 100 µl of LB medium. To select for bacteria containing the vector of choice, transformed bacteria were plated onto agar plates containing a selection antibiotic (100 µg/ml ampicillin). After incubation at 37°C for 16 h, single colonies were picked and incubated in 3-4 ml LB medium containing ampicillin o.n. at 37°C.

2.4.4. Isolation of plasmid DNA from bacteria

In order to isolate plasmid DNA amplified by dividing E. coli, bacteria were cultured in LB medium containing the respective selection antibiotics o.n. at 37°C and 180 rpm.

For small volumes of 3-4 ml bacterial suspension in LB medium, bacteria were pelleted for 2min at 5000 rpm and resuspended in 200 µl of solution I. Lysis of bacteria was performed by adding 400 µl of solution II and incubating for 3 min at RT. Cell lysis was stopped by adding 300 µl of neutralizing solution III. After centrifugation for 12 min at 13 000 rpm, the supernatant without the genomic bacterial DNA was transferred to a fresh tube and 400 µl of phenol-chloroform (1:1 mixture, lower phase) was added. After thorough vortexing, samples were centrifuged for 5 min at 13 000 rpm and the upper, aqueous phase containing plasmid DNA was transferred to fresh tubes. DNA was precipitated by adding 600 µl of isopropanol and washed twice by adding 1 ml of 70 % EtOH and centrifuging for 10 min at 13 000 rpm. Pellets were air dried for a few minutes and resuspended in 50 µl of H_2O containing 0.1 µg/µl RNAse A.

Larger volumes of 1 l bacterial culture were processed similarly, but in addition plasmid DNA was further purified by caesium chloride gradient-centrifugation according to Glisin and colleagues[163]. Bacteria were pelleted for 20 min at 4200 rpm and resuspended in 40 ml of solution I. Lysis was initiated by adding 80 ml of solution II for 5 min at RT and stopped by adding 40 ml of solution III. After centrifugation for 10 min at 4200 rpm and 4°C, the supernatant was transferred into a fresh vessel containing 100 ml of isopropanol. DNA was precipitated for 10 min at 5000 rpm and 4°C and the pellet dried for several minutes.

For caesium chloride gradient centrifugation, DNA pellets were resuspended in 3.5 ml of solution I and mixed with 5.5 g caesium chloride, 100 µl igepal (10 %) and 500 µl ethidium bromide (2 % solution). After another round of centrifugation for 5 min at 4500 rpm and RT, the supernatant was transferred into ultracentrifugation vessels and centrifuged for 3.5h at 80 000 rpm and RT. The bright pink phase containing plasmid DNA was recovered and ethidium bromide was removed by several washing steps with butanol (saturated with 1 M NaCl). Finally, DNA was precipitated by adding 1 volume of 1 M ammonium acetate and 3 volumes of 96 % EtOH and pelleted for 5 min at 4500 rpm and RT. After washing with 70 % EtOH, the DNA pellet was allowed to dry o.n. and dissolved in 0.5-1 ml H_2O.

Solution I	10 mM EDTA, 25 mM Tris, 50 mM glucose, pH 8
Solution II	0.2 M sodium hydroxide, 1 % SDS (w/v), pH 13
Solution III	3 M potassium acetate, 2 M acetic acid, pH 5

2.4.5. *In vitro* transcription

In vitro transcription was performed using the mMESSAGE mMACHINE kit by Life Technologies according to manufacturer's instructions. In short, plasmids containing the SP6 promoter preceding the gene of interest were linearized using NotI or MluI restriction enzymes for 2h. Complete digestion was verified by gel electrophoresis. The plasmid was purified from residual enzymes and salts by adding 1/20 volume of 0.5 M EDTA, 1/10 volume of 3 M Na acetate and 2 volumes 96 % EtOH and incubating for 15 min at -20°C. Following the precipitation step, the DNA was pelleted by centrifugation for 15 min at maximum speed and 4°C. Supernatant was removed and the pellet dried at RT. After resuspension in H_2O, DNA concentrations were determined with a NanoDrop2000 (Thermo Scientific).

For *in vitro* transcription, the reaction mix (consisting of 10 µl 2x NTP/CAP, 2 µl 10x reaction buffer, 1 µg DNA and 2 µl enzyme mix in a total volume of 20 µl) was assembled at RT and the samples were incubated for 2 h at 37°C. Afterwards, remaining DNA was digested by adding 1 µl of TURBO DNAse to the transcription reaction and incubating for 15 min at 37°C.

As mRNA is more stable when it contains a polyA tail, the transcribed mRNA was poly-adenylated using a Poly(A) Tailing Kit. The transcription reaction (20 µl) was topped up with 36 µl H_2O, 20 µl 5x E-PAP buffer, 10 µl 25 mM $MnCl_2$ and 10 µl ATP and mixed well. Before addition of

4 µl E-PAP enzyme, 0.5 µl of the reaction mix were saved as a control for gel electrophoresis. Poly-adenylation was performed by incubation for 1h at 37°C.

Another 0.5 µl of the now poly-adenylated mRNA was removed and analyzed together with the non-adenylated (saved) sample on a 1.2% agarose/TBE gel (see 2.4.1). While the non-adenylated mRNA should have the expected size based on the number of nucleotides, a smear of different sizes is expected for the poly-adenylated sample since poly-adenylation results in RNAs containing polyA-tails of varying lengths.

Poly-adenylated mRNA was finally purified with the RNeasy kit according to manufacturer's instructions. Final yield of mRNA ranged between 50-60 µg of RNA per sample (determined with NanoDrop2000) and was aliquoted into ready-to use sizes that were stored at -20°C until being used for mRNA transfection of cells.

2.4.6. Isolation of cellular mRNA and cDNA synthesis

The RNA fraction of cells was isolated using Trizol Reagent. Cells were harvested as described above, pelleted for 5 min at 280 g and 4°C and directly resuspended in 1 ml of Trizol reagent. Afterwards, samples were either processed directly or stored at -80°C until further use.

After 5 min at RT 200 µl of chloroform were added per tube and vortexed well. After 3-10 min at RT, samples were centrifuged for 5 min at 12 000 g. Following centrifugation, two clear phases are visible: the lower organic phase contains the protein fraction, while RNA is dissolved in the upper aqueous phase. DNA accumulates at the border between the two phases forming a whitish layer. To proceed with RNA isolation, the upper phase was carefully transferred to a fresh tube and the nucleic acids were precipitated by adding 500 µl of isopropanol. After 5-15 min at 4°C, the RNA was pelleted for 10 min at 12 000 g and 4°C. Following two washing steps with 1 ml of 75% EtOH and centrifugation for 10 min at 12 000 g and 4°C, the RNA pellet was dryed for a few minutes and dissolved in RNAse-free water. RNA concentrations were determined using NanoDrop2000 and samples were stored at -20°C until further use.

Reverse transcription of RNA into cDNA was done using the High capacity cDNA Reverse Transcription Kit according to manufacturer's instructions. 0.1-1 µg of RNA were incubated with DNAse (1U DNAse per µg RNA) in DNAse buffer in a final volume of 10 µl for 10 min at 37°C. DNAse was inactivated by heating to 95°C for 3 min. Subsequently, 10 µl of the cDNA transcription mix

were added. Reverse transcription was performed for 120 min at 37°C, followed by 5 min at 85°C to inactivate the enzyme. cDNA samples were then stored at -20°C.

2.4.7. Analysis of cytohesin isoform expression

In order to determine the expression of cytohesin isoforms (2G or 3G) in iDCs, cDNA of wt iDCs was generated (see 2.4.6.) and the sequence coding for the PH domain of each cytohesin was amplified by PCR. Since samples were to be sent for sequencing, the accurate and less error-prone phusion polymerase was used for PCR. As positive controls, pure 2G or 3G cytohesin isoforms from DNA plasmid constructs were used. The PCR master mix was assembled as follows:

10 µl	5x phusion HF buffer
1 µl	10 mM dNTPs
2.5 µl	of each primer
2.5 µl	cDNA
31 µl	H_2O
0.5 µl	Phusion DNA polymerase

The following primer pairs were used for amplification:

Cyth1	mpscd1 for qPCR + mpscd1 rev_NotI
Cyth2	mpscd2 for_MluI + mpscd2 rev qPCR
Cyth3	mpscd3 for qPCR + mpscd3 rev_NotI
Cyth4	mpscd4 for_MluI + mpscd4 rev qPCR

Thermocycler conditions:

Step	Temp	time	Cycles
Initial Denaturation	98°C	30 sec	x1
Denaturation	98°C	30 sec	
Annealing	60°C	30 sec	x39
Elongation	72°C	1 min	
	72°C	10 min	x1
	4°C	∞	

Afterwards, samples were run on a 2 % agarose/TAE gel and bands of the correct size were excised and purified using the NucleoSpin Gel&PCR Clean-up kit by Macherey-Nagel according to manufacturer's instructions. Samples were sent for Sanger sequencing by MWG Eurofins using the respective forward primer (Cyth1, Cyth3 and Cyth4) or the reverse primer (Cyth2). Relative frequencies of 2G/3G isoforms were then determined by sequence trace decomposition using TIDE software (www.tide.deskgen.com) based on the Sanger chromatograms.[108,164]

2.4.8. RNA sequencing

iDCs were kept in suspension using methyl cellulose (see 2.3.9.) for 1 h, before they were seeded onto FN- or gelatin-coated 6-well plates at 10^6 cells/well in VLE-RPMI medium (5 % FCS, 1 % Pen/Strep, 10 ng/ml GM-CSF). After 7 h at 37°C and 5 % CO_2, medium was removed, and cells were directly resuspended in 1 ml Trizol. Samples were kept at -80°C until further processing for RNA sequencing, which was conducted by the group of Prof. Joachim Schultze (Department for Genomics & Immunoregulation, LIMES Institute, Bonn University).

RNA was isolated with Trizol according to the manufacturer's instructions. The quality of RNA was assessed by visualization of 28S and 18S band integrity on a Tapestation 2200 (Agilent). Only samples with a RIN score above 9 were further processed. 10 ng of RNA were converted into cDNA libraries according to the TruSeq RNA library preparation kit v2. Size distribution of cDNA libraries was determined using the Agilent high sensitivity DNA assay on a Tapestation 2200 (Agilent). cDNA libraries were quantified using KAPA Library Quantification Kits (Kapa Biosystems). After cluster generation on a cBot, 75 bp single read sequencing was performed on a HiSeq1500.

After base calling and de-multiplexing using CASAVA version 1.8.2, the 75 bp single-end reads were aligned to the mouse reference transcriptome mm10 from UCSC by kallisto v0.44.0 using default parameters. Data was imported into DESeq2 (v.1.10.1)[165] using the TXimport (v1.2.0) package. DESeq2 was used for the calculation of normalized counts for each transcript using default parameters.

2.5. Protein Biochemistry

2.5.1. Fluorescent labelling of fibronectin

In order to obtain fluorescently labelled fibronectin for matrix-degradation assay, the DyLight 549 NHS ester kit by Thermo Scientific was used. The Dylight549 dye contains amine-reactive N-hydroxysuccinimide (NHS) esters that form covalent bonds with primary amines in proteins. Lyophilized fibronectin was dissolved for 30 min at 37°C to a final concentration of 1 mg/ml in PBS. Afterwards, Dylight 549 NHS ester was added at 10x molar excess and the mixture was incubated for 1 h at RT in the dark. Unbound dye was removed by dialysis: The dye-fibronectin solution was filled into Slide-a-Lyzer Dialysis Cassettes (10 k molecular weight cutoff), and the cassette was placed into 1 l of autoclaved aqua bidest. During 2 h of gentle stirring at 4°C in the dark the unbound dye diffused into the surrounding water, while the FN-bound dye was too big to diffuse through the pores of the dialysis cassette. This dialysis step was repeated in autoclaved aqua bidest for another 2 h and an o.n. dialysis round, before the FN-Dylight549 was recovered from the dialysis cassette. The labelled fibronectin was aliquoted into suitable volumes (200 µl) and stored at -20°C until use.

2.5.2. Coating procedure of glass coverslips

To enhance binding of different extracellular matrix proteins to the glass surface, coverslips were first coated with 50 µg/ml poly-L-lysine (PLL) in PBS for 10 min at RT via absorption. After a short washing step with PBS the amine groups of the lysines were activated with 0.5 % glutaraldehyde/PBS for 10 min at RT. Subsequently, the glutaraldehyde was washed off thoroughly by rinsing the coverslips 5x with PBS. To sterilize the coverslips again, they were transferred into 70 % EtOH and incubated for 20 min at RT before being washed with PBS for another 3x. These pre-activated coverslips could be stored at 4°C in PBS for 1-2 weeks.

Due to the pre-activation of the PLL other proteins are linked covalently and the coating is much more efficient.[166] Coating proteins were diluted to a final concentration of 50 µg/ml (unless stated otherwise) using either PBS (for Fibronectin (FN), fibrinogen and gelatin) or 0.25 % acetic acid (for collagen I and collagen IV). 200 µl of the protein solutions were placed onto the pre-activated coverslips and incubated for 1 h at RT. After a short washing step with PBS, the coverslips were either used directly or stored for up to 1 week at 4°C in PBS.

2.5.3. Analysis of RhoA GTPase activity with pulldown assays

To assess the fraction of active RhoA protein in a cell the Rho Pulldown Kit from Cytoskeleton was used according to manufacturer's instructions. The principle of the pulldown assay is to assess GTPase activity based on an affinity-tagged effector protein that serves as bait and is only bound by the active form of the GTPase. In the case of RhoA, the Rho-binding domain of the Rho effector protein Rhotekin was used. Cell lysates are incubated with a Rhotekin-GST fusion protein bound to glutathione-sepharose beads and all active Rho molecules are immobilized to the beads via Rhotekin. After a short washing protocol, the active Rho-fraction is enriched and can be eluted with a reducing buffer. The relative amount of active RhoA is quantified by SDS PAGE using total RhoA protein from the input lysate as control.

In detail, 1-2x10^6 cells were seeded onto pre-coated 10 cm cell culture dishes, which bind both FN and gelatin without being pre-activated, and were cultured in standard medium o.n. For some experiments, the Rho inhibitor Rhosin was added at a final concentration of 30 µM during the overnight incubation.

For harvest, the dishes were placed on ice, washed once with 5ml of ice-cold PBS buffer and then lysed in the respective lysis buffer. After a short centrifugation step (1 min at 14 000 rpm at 4°C), supernatants were transferred to fresh tubes, immediately shock-frozen in liquid nitrogen and stored at -80°C until use. A small aliquot of the lysate was retained and used to determine protein concentrations using BCA assay (see 2.5.6.).

250-300 µg of protein were added to 50 µg Rhotekin-beads and incubated for 1h at 4°C on a rotating wheel. Afterwards, the beads were washed once with wash buffer, resuspended in 15 µl of 2x Laemmli sample buffer containing 5 % β-mercapto-ethanol and heated for 2 min at 95°C.

2.5.4. Analysis of Arf GTPase activity with G-LISA

Activity of Arf1 and Arf6 GTPases was determined using the Arf1/6 G-LISA Activation Assay Kits (Cytoskeleton) according to manufacturer's instructions. A G-LISA uses the principle of an enzyme-linked immunosorbent assay (ELISA) to assess GTPase activity. For that, a plate is pre-coated with an Arf-binding protein, which is bound by only active Arf molecules in the lysate. After a washing procedure, bound Arf protein is detected by an Arf-specific primary antibody and a horse-radish peroxidase (HRP)-coupled secondary antibody. Total amounts of active Arf proteins are then determined by colorimetric analysis.

In detail, iDCs at 1-2x10^6 cells/plate were cultured o.n. on FN- or gelatin-coated cell culture dishes (10 cm) in standard DC medium. For harvest, the medium was aspirated, and the plates were immediately placed on ice. After a washing step with ice-cold PBS, cells were lysed in 100 µl of lysis buffer containing protease inhibitors and were transferred to a fresh tube using a cell scraper. Before aliquoting and snap-freezing the lysates in liquid nitrogen, insoluble debris was pelleted for 1 min at 14 000 rpm and 4°C. Samples were stored at -80°C until further use. A small aliquot of lysate was used to determine protein concentrations.

10 µg of protein was mixed with binding buffer and incubated on a pre-coated 96-well plate for 30 min at 4°C on an orbital shaker (300 rpm). Afterwards, plates were washed twice with wash buffer and the samples were incubated in antigen presenting buffer for 2 min at RT. After another three washing steps, primary antibody against Arf1 or Arf6 was allowed to bind for 45 min at RT on a shaker at 400 rpm. Next, samples were washed 3x with wash buffer and incubated with secondary antibody for another 45 min at RT on a shaker at 400 rpm. Finally, unbound antibody was removed by three vigorous washing steps and HRP detection reagent was added for 10 min at RT. The reaction was stopped by adding HRP Stop buffer and absorbance was measured at 490 nm.

2.5.5. Generation of protein lysates

Protein lysates were usually taken from cells grown in 6-well dishes that were pre-coated for 1 h at RT with either FN or gelatin diluted to 50 µg/ml in PBS. To remove all media containing protein, cells were washed once with ice-cold PBS, which was thoroughly aspirated, before 50-100 µl of MRC lysis buffer containing different protease inhibitors (10 µg/ml aprotinin, 10 µg/ml leupeptin, 2 µg/ml antipain, 1 mM benzamidine and PMSF (phenylmethylsulfonyl fluoride) at a 1:1000 dilution of a saturated stock) was added. The lysates were autoclaved aqua bidest transferred to fresh tubes using a cell scraper and were kept on ice for 15-30 min. After a final centrifugation for 10 min at 10 000 rpm and 4°C, the supernatant containing the protein fraction was transferred to fresh tubes and stored at -20°C until further use.

MRC lysis buffer	50 mM Tris-HCl pH 7.5, 1 mM EGTA pH 8.0, 1 mM EDTA pH 8.0, 10 mM glycerophosphate, 50 mM sodium fluoride, 5 mM sodium pyrophosphate, 1 mM sodium vanadate, 0.27 M saccharose, 1 % Triton

2.5.6. Determination of protein concentration with BCA assays

To determine protein concentrations, a commercial BCA assay was used. The underlying principle for this assay is the reduction of copper ions by protein in an alkaline environment.[167] By adding bicinchoninic acid (BCA) to the protein solution a purple-colored reaction product is formed, which absorbs at 562 nm.

3 µl of protein lysate were added to each well of a 96-well plate and 200 µl BCA solution (20 µl of solution B in 1 ml of solution A) were pipetted on top. For the reference standard curve, BSA was diluted with lysis buffer to defined concentrations of 0.07-5.0 mg/ml. After 10 min at 65°C, the absorbance at 562 nm was measured using infinite M200 (Tecan), and protein concentration of each sample was determined based on the BSA standard curve.

2.5.7. SDS-PAGE and Western Blotting

To analyze protein content in a given sample, proteins from a lysate were separated according to their molecular weight by SDS-PAGE, and transferred onto nitrocellulose membranes via western blotting[168] to be finally detected with specific antibodies.

For SDS-PAGE, polyacrylamide gels were cast using the Mini Trans-Blot Cell system by Bio-Rad (see table below). Depending on the expected molecular weight of the protein of interest, different percentages of polyacrylamide (8-12 %) were used for the resolving gel. Above the resolving gel, a shorter layer of stacking gel containing 5 % acrylamide enabled the accumulation of proteins in a precise band, before separation in the resolving gel.

Protein lysates were first denatured by adding protein buffer, which contains SDS and dithiothreitol (DTT), and incubating for 5 min at 96°C. Next, 20 µg of denatured protein were loaded onto the gel and separated by electrophoresis at 80-120 V in Laemmli Running Buffer. During the first 30 min a lower voltage (80 V) was used to improve accumulation of protein in the stacking gel. Separation of proteins then occurred at 120 V.

After successful separation, proteins were transferred onto nitrocellulose membranes by western blotting. For that, a wet blotting system (Mini Trans-Blot Cell by Bio-Rad) was used, where the polyacrylamide gel was placed between two sponges together with a layer of filter paper and the nitrocellulose membrane. Blotting was performed in ice-cold transfer buffer at 4°C for 120 min at 80 V. Finally, blotting success was verified by visualizing protein bands with a 0.1 % ponceau solution in 5 % acetic acid.

For detection of specific proteins, membranes were first blocked in 5 % milk powder in tris-buffered saline with Tween (TBST), before they were incubated in primary antibody diluted in 3 % BSA/TBST or 5 % milk powder/TBST o.n. at 4°C. After three washing steps of 10 min in TBST, a secondary HRP-coupled antibody was diluted in TBST and added to the membrane for 1h at RT. Additional three washing steps in TBST were performed to remove all unbound antibody. After adding the HRP substrates luminol and peroxide (part of the enhanced chemiluminescence (ECL) solution), the chemiluminescent reaction enables detection of the protein of interest using radiographic films.

Membranes were regenerated to be used with another primary antibody by heating in stripping buffer for 15 min. Afterwards, remaining stripping buffer was carefully washed off, and the membranes could be incubated in blocking solution again.

	Stacking gel	**Resolving gel**	
	5 %	**10 %**	**12 %**
H_2O	1.4 ml	1.9 ml	1.6ml
30 % acrylamide	330 µl	1.7 ml	2.0 ml
1.5 M Tris pH 8.8	-	1.3 ml	1.3 ml
1 M Tris pH 6.8	250 µl	-	-
10 % SDS	20 µl	50 µl	50 µl
10 % APS	20 µl	50 µl	50 µl
TEMED	2 µl	2 µl	2 µl

Protein buffer	100 mM Tris-HCl (pH 6.8), 4 % SDS, 1 % bromophenol blue, 20 % glycerin, 200 mM DTT
Laemmli Running Buffer	25 mM Tris, 250 mM glycine, 0.1 % SDS
Transfer buffer	20 % methanol in 200 mM glycine, 25 mM Tris-Base, 0.002 % SDS
TBST	0.05 M Tris, 140 mM sodium chloride, 0.05 % Tween20, pH 7.9
Stripping buffer	2 % SDS, 0.7 % β-mercapto-ethanol, 63 mM Tris pH 6.8

2.5.8. Semiquantitative Analysis of Protein Expression

Quantification of protein expression based on films generated from chemiluminescent detection of HRP-coupled antibodies was done using the gel plugin in ImageJ 1.52i software (National Institutes of Health, Bethesda, MD). In short, specific protein bands were selected and transferred into a histogram, which could be used to determine the area under the curve. By setting the protein of interest in relation to a loading control ("house-keeping gene" or total protein), semi quantitative values were obtained.

2.6. Statistical Analysis

Data generated with the methods above are represented as mean values of several independent experiments or mice. Error bars indicate either standard deviation (SD) or standard error of the mean (SEM). Details can be found in the figure legends.

Statistical significance was analyzed using the GraphPad Prism 8.1.1 software (GraphPad Software, San Diego, USA). The statistic test used for each experiment is indicated in the figure legends. A p-value below 5 % was considered significant.

3. Results

Integrins and integrin-related signaling processes are important factors in podosome formation and function[73] and cytohesins are known to regulate both cell adhesion and actin-dependent processes[106,129,143–146]. Even though one member of the cytohesin protein family, Cyth2, has recently been described to be involved in podosome biology[118], it is unclear so far, if and how cytohesins mediate specific integrin-derived influences on podosome formation. Moreover, the relevance of the complete cytohesin family for podosome formation has not been addressed either. Therefore, we set out to examine the role of all four cytohesins in integrin-mediated formation of podosomes.

3.1. Cyth2 regulates podosome formation and function in a matrix-dependent manner

In order to study the effect of cytohesins on podosome formation, we used immature BMDCs (iDCs) from different cytohesin KO mice. These cells are part of the myeloid lineage and form podosome clusters constitutively, which makes them an ideal model for podosome research. As Cyth2 full-KO mice die shortly after birth (Bettina Jux, unpublished data), we used a conditional (floxed) allele of Cyth2 together with a LysM-driven Cre recombinase to generate loss of Cyth2 in myeloid cells[156]. KO mice of Cyth1[104], Cyth3[126] and Cyth4 (unpublished data), however, are viable and could therefore be used for this study directly. All KOs resulted in a clear loss of the respective cytohesin on protein level in iDCs (figure **3.1**).

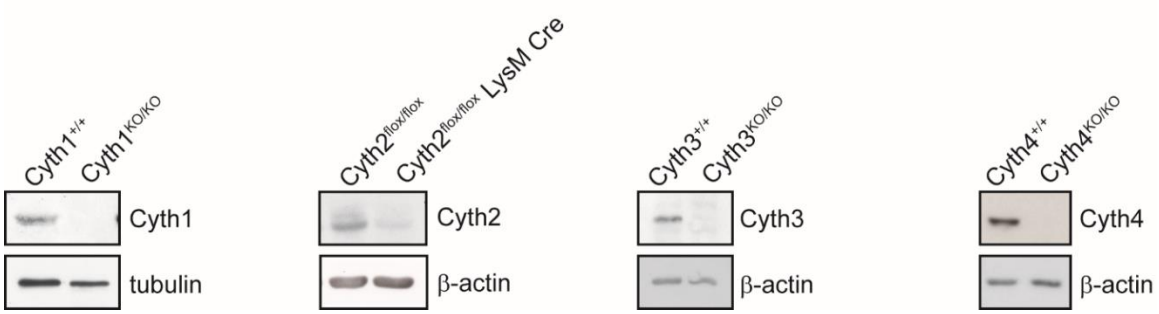

Figure 3.1 – BMDCs derived from different cytohesin KO mice are deficient for cytohesins
Analysis of protein expression by iDCs from Cyth1 KO mice, Cyth2$^{flox/flox}$ LysM-Cre mice, Cyth3 KO mice and Cyth4 KO mice showed KO efficiency for each cytohesin.

3.1.1. Cyth2 is the only cytohesin family member involved in podosome formation of iDCs on specific substrates

To analyze the ability of different cytohesin KO iDCs to form podosomes, we seeded cells onto fibronectin (FN)-coated coverslips and stained them for key podosome markers. Figure **3.2 A** shows a confocal airyscan image of podosomes in iDCs, illustrating the classical composition of actin-rich cores surrounded by ring-like structures containing adhesion-related proteins, like vinculin. In contrast, FAs are characterized by streak-like accumulations of vinculin. Quantification of podosome frequencies revealed that only loss of Cyth2 affected podosome formation in iDCs, while KO of Cyth1, Cyth3, or Cyth4 had no effect compared to wildtype (wt) cells (figure **3.2 B**). Cyth2 KO iDCs cultured on FN displayed a significant reduction in podosome formation (figure **3.2 B**), which was further confirmed on single cell level by quantifying podosomes per cell (figure **3.2 C**).

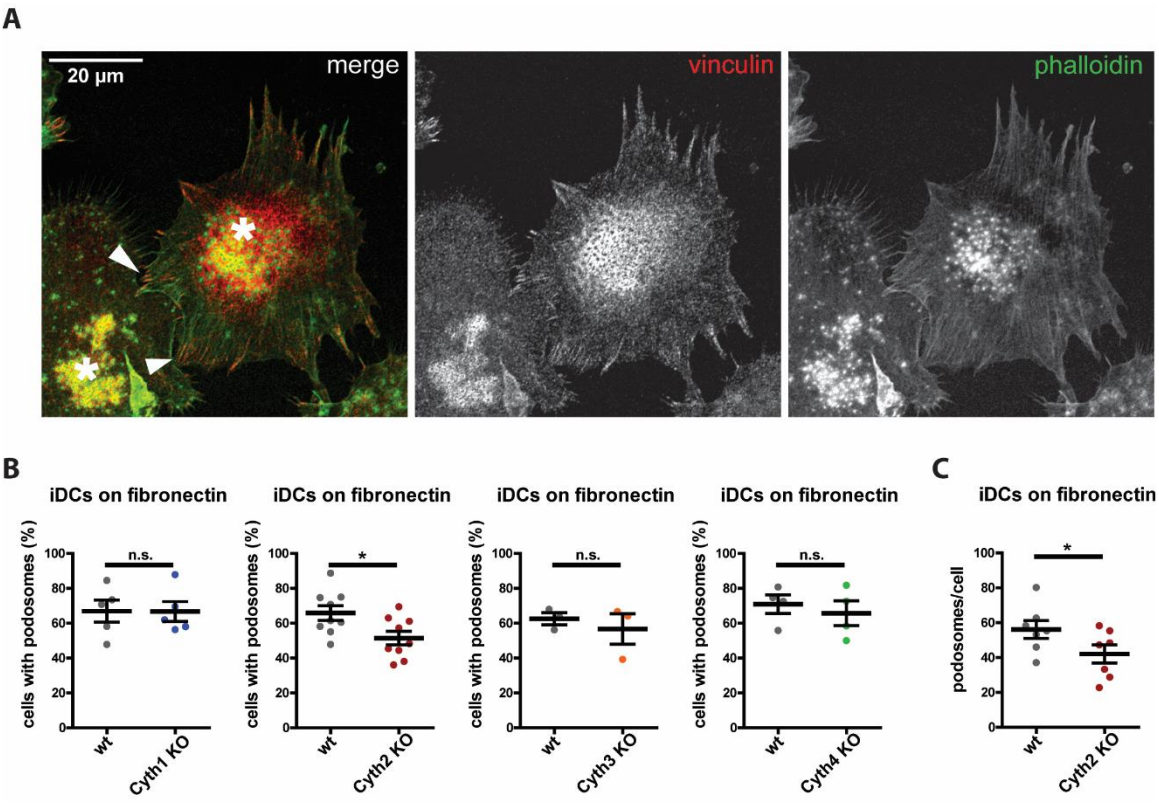

Figure 3.2 – Cyth2 enhances podosome formation on fibronectin
iDCs were cultured on FN and stained for podosomes with phalloidin and an antibody against vinculin. (**A**) Exemplary confocal airyscan image. Star indicates podosome cluster, arrows indicate focal adhesions (FA). (**B**) Quantification of podosome frequencies of iDCs from different cytohesin KO mice. (**C**) Quantification of podosomes per cell. (Error bars represent mean +/- SEM; Statistics: Wilcoxon matched-pairs signed rank test: n.s. (not significant) p>0.05; * p<0.05)

One of the key functions of podosomes is their ability to degrade the underlying matrix and therefore facilitate invasion into tissue.[64] To assess the degradative capacity of podosomes, cells were seeded onto coverslips coated with fluorescently-labelled gelatin. Degradation of this gelatin coating could then be determined by quantifying the loss of fluorescence after 24 h (figure **3.3 A**). Interestingly, Cyth2 KO iDCs degraded more gelatin than their wt counterparts (figure **3.3 B**), which is in contrast to their behavior in terms of podosome formation. However, given that the key difference between both experiments was the substrate used for coating (FN versus gelatin), we next analyzed whether podosome occurrence on gelatin-coated surfaces was equally elevated. As shown in figure **3.4 A**, Cyth2 deficient iDCs indeed formed more podosomes, when they were cultured on gelatin, which corresponds well with their increased degrading activity on this substrate. Similar to the results on FN, none of the other cytohesin KO iDCs showed any effect on podosome formation on gelatin (figure **3.4 A**) and the elevated podosome incidence in Cyth2 KO iDCs was also detectable on single cell level (figure **3.4 B**).

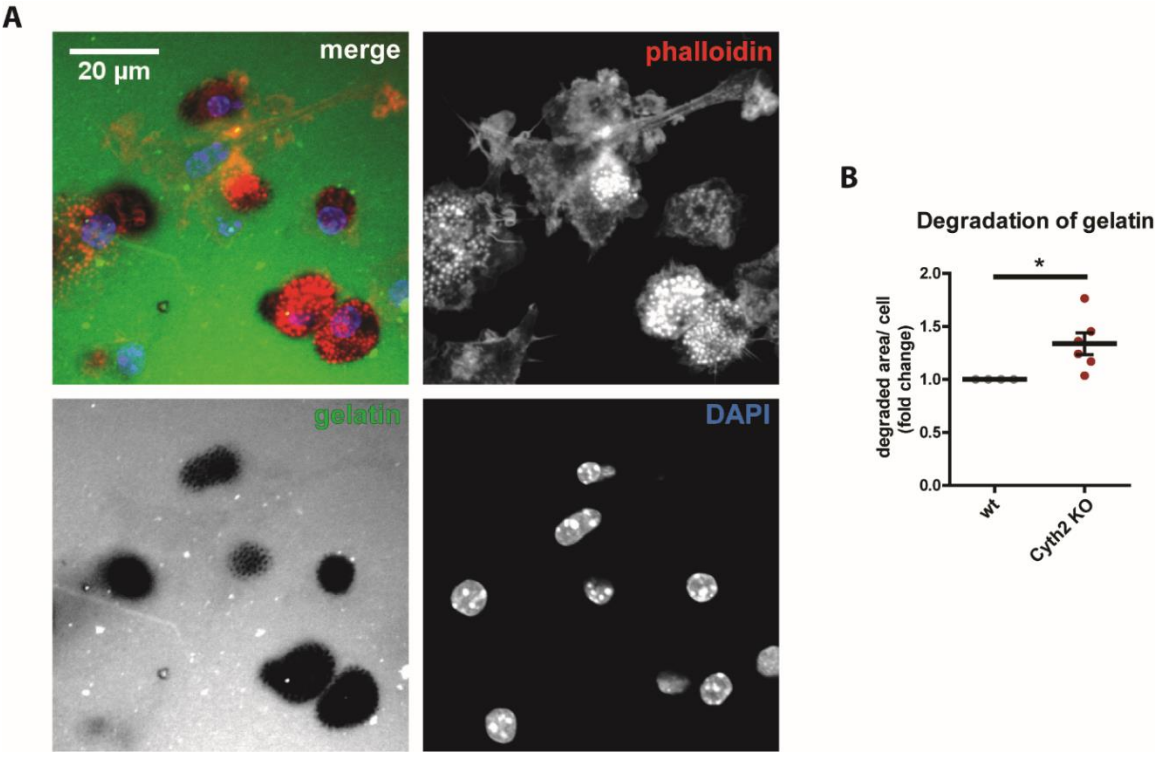

Figure 3.3 – Degradation of gelatin is increased in Cyth2 KO iDCs
iDCs cultured on fluorescently labelled gelatin for 24 h were stained with phalloidin and DAPI. (**A**) Exemplary images of degraded gelatin around podosome clusters. (**B**) Quantification of degradation by Cyth2 KO and wt iDCs. (Error bars represent mean +/- SEM; Statistics: Wilcoxon matched-pairs signed rank test: * $p<0.05$)

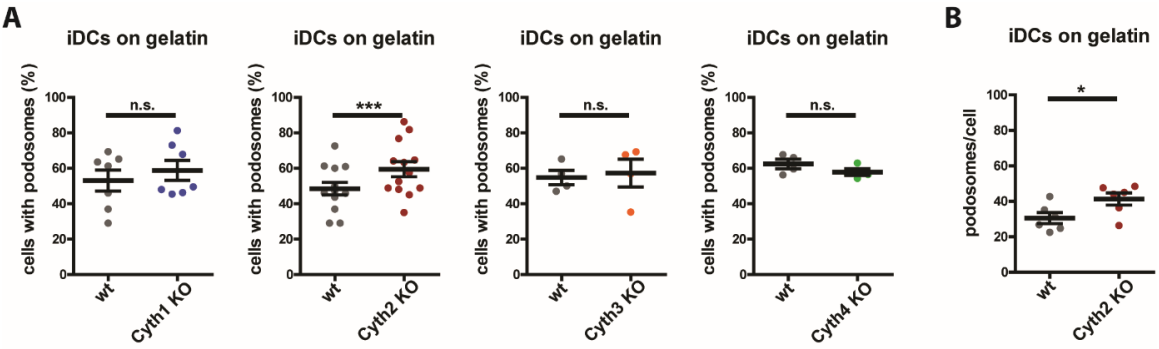

Figure 3.4 – Cyth2 reduces podosome formation on gelatin

iDCs were cultured on gelatin and stained for podosomes. (A) Quantification of podosome frequencies of iDCs from different cytohesin KO mice. (**B**) Quantification of podosomes per cell. (Error bars represent mean +/- SEM; Statistics: Wilcoxon matched-pairs signed rank test: n.s. (not significant) $p>0.05$; * $p<0.05$; *** $p<0.001$)

Vice versa, degradation of fluorescently labelled FN was decreased compared to wt cells (figure **3.5**), which is in line with the reduced occurrence of podosomes in Cyth2 KO cells on that specific coating material. The loss of one single protein (Cyth2) therefore has opposing effects on podosome formation depending on the underlying coating substrate.

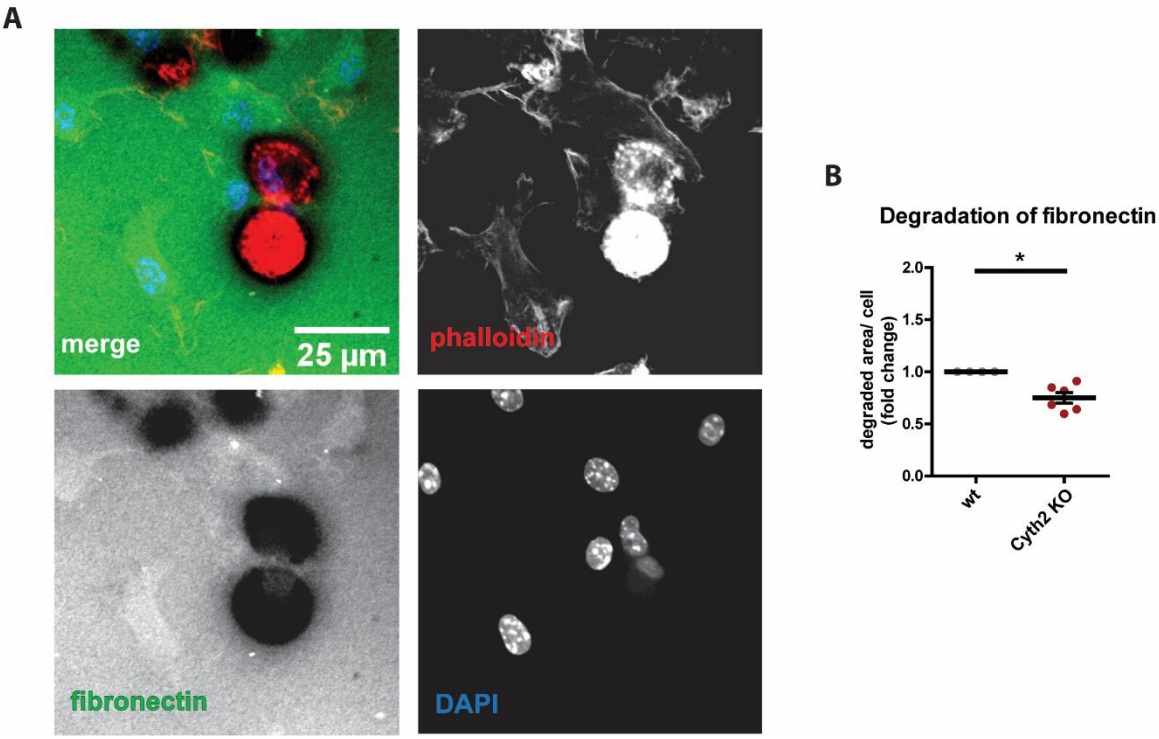

Figure 3.5 – Degradation of fibronectin is decreased in Cyth2 KO iDCs

iDCs cultured on fluorescently labelled FN for 24 h were stained with phalloidin and DAPI. (**A**) Exemplary images of degraded FN around podosome clusters. (**B**) Quantification of degradation by Cyth2 KO and wt iDCs. (Error bars represent mean +/- SEM; Statistics: Wilcoxon matched-pairs signed rank test: * $p<0.05$)

We next asked whether similar effects also occur on other matrix proteins and quantified podosome formation on Icam-1, fibrinogen, collagen I and collagen IV (figure **3.6**). While podosome frequencies on Icam-1 and fibrinogen did not change in presence or absence of Cyth2, culturing wt and Cyth2 KO iDCs on collagen IV had an effect similar to gelatin-coatings: Loss of Cyth2 increased podosome formation on this substrate. Podosome formation on collagen I also did not result in significant differences between wt and Cyth2 deficient cells, although the tendency points in the same direction as the samples on collagen IV. It has to be noted, though, that general adhesion of iDCs to collagen I was impaired (data not shown), which complicated quantification of podosomes and resulted in increased spread of values. Gelatin is primarily a mixture of hydrolyzed collagens[169], so observing a similar effect on collagen IV further strengthens the relevance of our data.

As we had cultured murine iDCs on FN derived from human plasma, we also made sure that our FN-dependent effect was no species-related artefact. However, on murine FN we could observe a similar reduction in podosome numbers of Cyth2 KO iDCs compared to wt cells (figure **3.6**). Deregulation of podosome formation by loss of Cyth2 is therefore independent of species-related differences in FN.

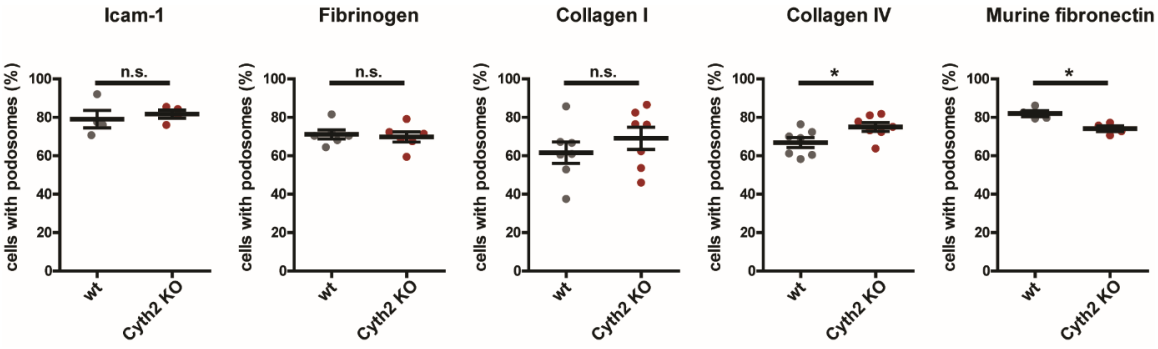

Figure 3.6 – Cyth2 is only involved in podosome formation on specific matrices
iDCs cultured on coverslips coated with different matrices (Icam-1, fibrinogen, collagen I, collagen IV and murine FN) were stained with phalloidin and an antibody against vinculin and podosome frequencies were quantified. (Error bars represent mean +/- SEM; Statistics: Wilcoxon matched-pairs signed rank test: n.s. (not significant) $p>0.05$; * $p<0.05$)

Taken together, among the family of cytohesin proteins, only Cyth2 is involved in podosome formation and function. This regulatory role of Cyth2 on podosome formation depends on the presence of specific substrates and can even have opposing effects depending on the underlying matrix protein.

3.1.2. Cell spreading and formation of focal adhesions is not affected by loss of Cyth2

Podosomes are one type of specialized adhesion structures but cell adhesion can also be mediated by FAs.[62] As depicted in figure **3.7**, loss of Cyth2 did not influence the occurrence of FAs in iDCs on any substrate significantly indicating that the effect of Cyth2 is specific for podosomes. Moreover, general deregulation of adhesion processes would affect the cells' immediate interaction with the underlying matrix resulting in altered spreading behavior. Cell area of Cyth2 KO iDCs on different matrices, however, was not significantly different from wt control cells (figure **3.8**) – with the exception of collagen IV coatings, which led to a slight increase in spreading of iDCs, when Cyth2 was lacking. Overall, the effects we observed in Cyth2 KO iDCs seemed to be specific for podosomes, while other adhesion structures and general cell adhesion were unaffected.

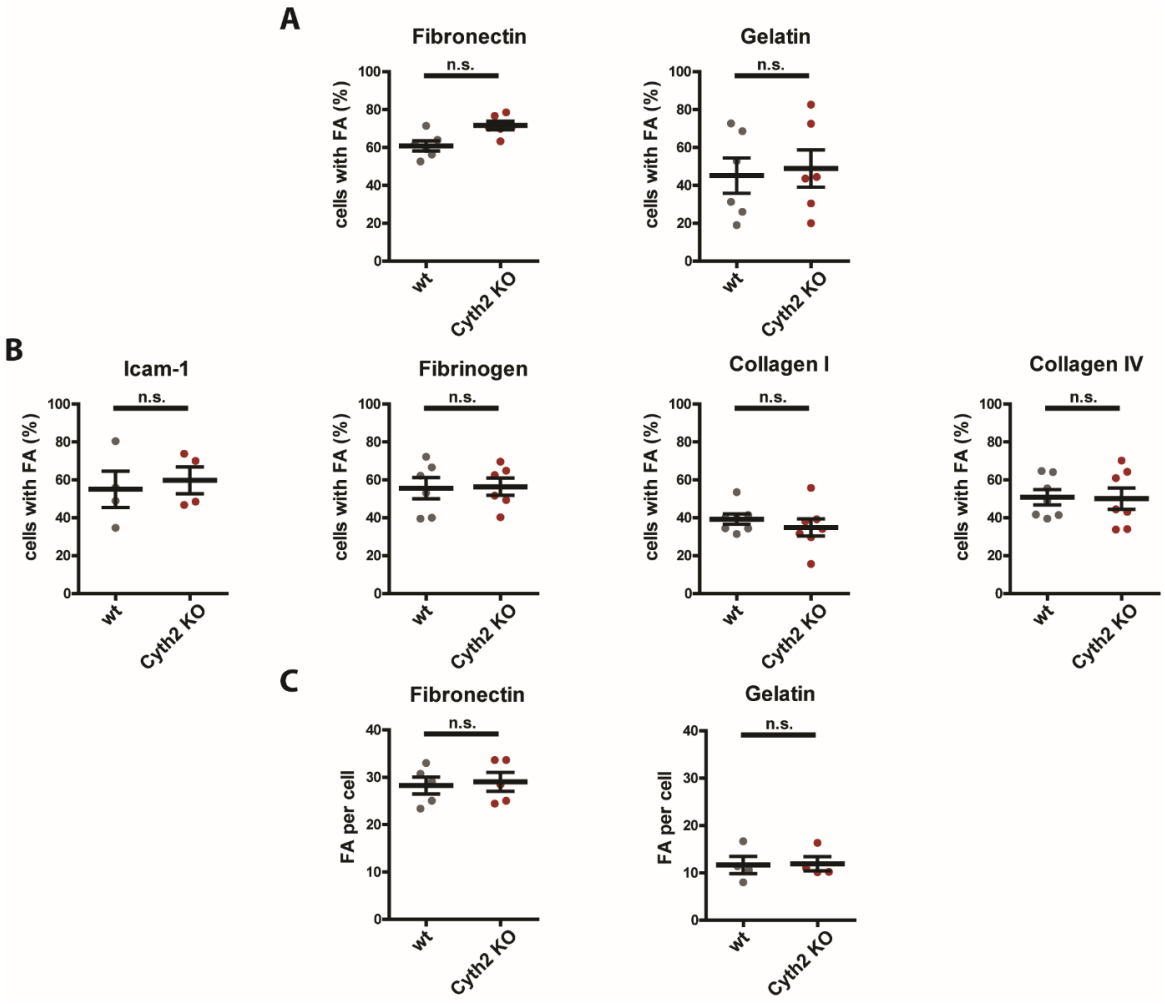

Figure 3.7 – Focal adhesions are not affected by loss of Cyth2
iDCs cultured on different matrices were stained with phalloidin and an antibody against vinculin. (**A**) Quantification of FA frequencies of wt and Cyth2 KO iDCs on fibronectin and gelatin. (**B**) Quantification of FA frequencies of wt and Cyth2 KO iDCs on Icam-1, fibrinogen, collagen I and collagen IV. (**C**) Quantification of FA numbers per cells of iDCs on fibronectin or gelatin. (Error bars represent mean +/- SEM; Statistics: Wilcoxon matched-pairs signed rank test: n.s. (not significant) $p>0.05$; * $p<0.05$)

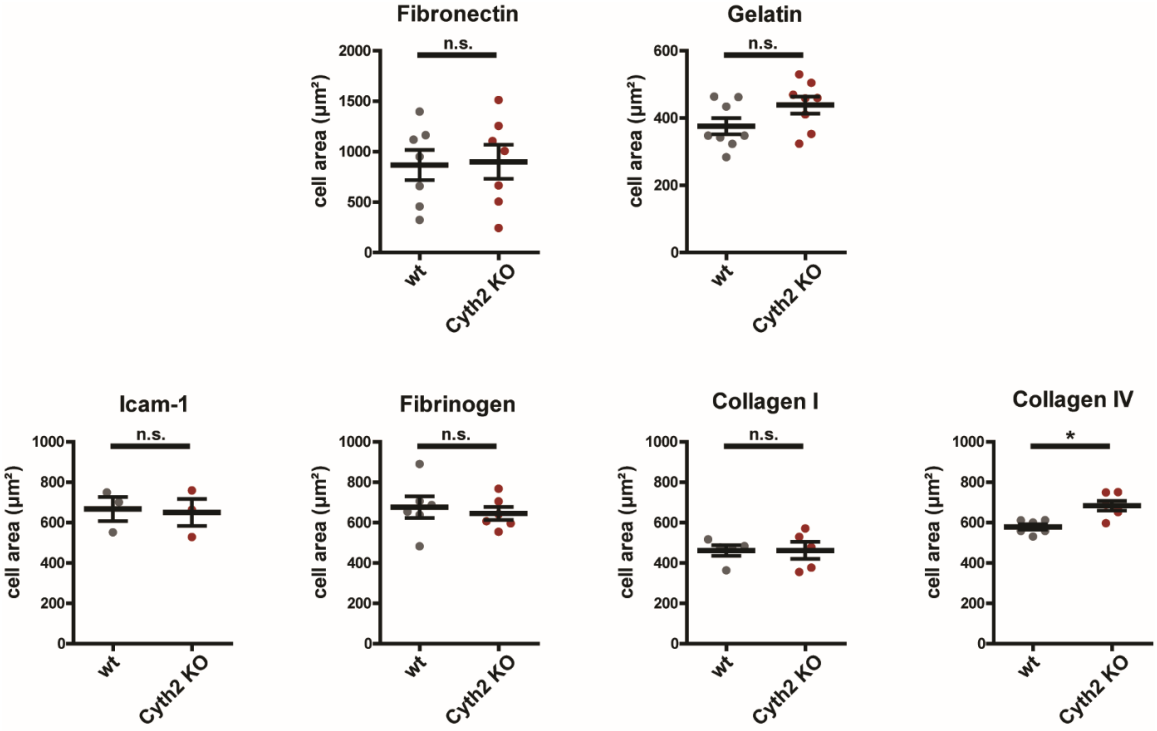

Figure 3.8 – Cell spreading of Cyth2 KO iDCs on different matrices
iDCs cultured on coverslips coated with different matrices were stained with phalloidin and an antibody against vinculin. Cell spreading (cell area) of wt and Cyth2 KO iDCs on fibronectin, gelatin, Icam-1, fibrinogen, collagen I and collagen IV was quantified by determining total cell area. (Error bars represent mean +/- SEM; Statistics: Wilcoxon matched-pairs signed rank test: n.s. (not significant) $p>0.05$; * $p<0.05$)

3.1.3. Cell adhesion strength and behavior of iDCs is differentially affected by fibronectin and gelatin matrices

Loss of Cyth2 has different effects on podosome formation by iDCs on FN compared to gelatin. These two coating substances, however, are inherently different in their biochemical composition, which might have consequences for their biophysical properties as well as for how they are perceived by cells. Cell spreading is a very broad indicator for adhesion strength and can differ substantially between iDCs cultured on different substrates (figure **3.9 A**). Especially for cells adhering to FN vs gelatin the difference is significant, with an average cell area of roughly 870 µm² (±397 µm²) and 380 µm² (±63,2 µm²), respectively (illustrated in figure **3.9 B**). In addition, both FA and podosome numbers per cell, as well as podosome frequencies are reduced in cells cultured on gelatin compared to FN (figure **3.9 C+D**). Moreover, in comparison to FN, general adhesion onto gelatin is delayed: FN enables adhesion within a few minutes, while iDCs need 30-60 min to attach to gelatin (data not shown). These data already indicate that adhesion processes on FN and gelatin are different and these differences have to be considered when analyzing the role of Cyth2 in these processes.

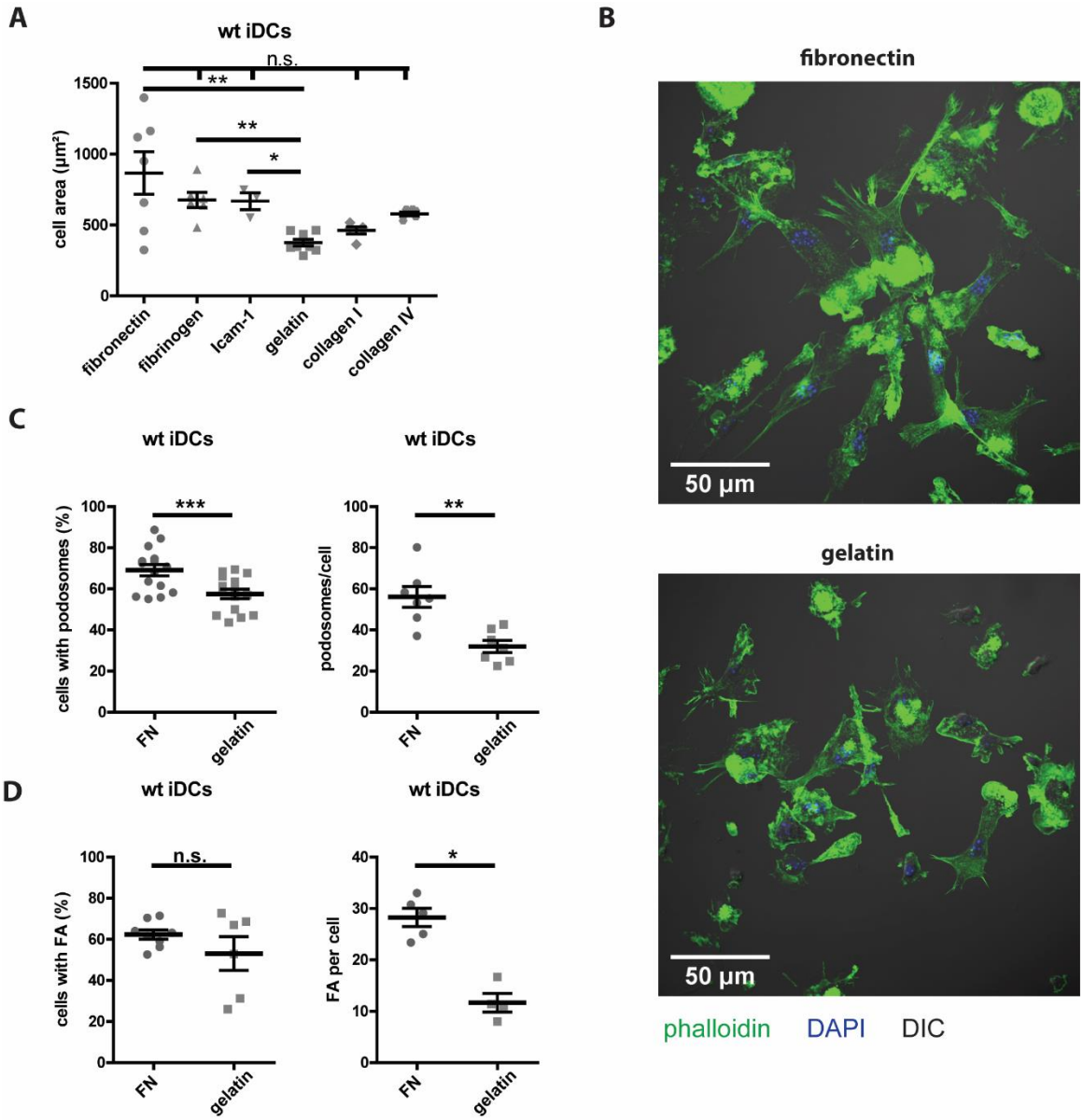

Figure 3.9 – Differences in adhesion behavior of iDCs on FN and gelatin

(**A**) Cell spreading of wt iDCs cultured on coverslips coated different matrices (Statistics: Kruskal-Wallis test with Dunn's multiple comparison test). (**B**) Staining of wt iDCs on FN or gelatin. (**C**) Podosome formation of wt iDCs cultured on FN or gelatin (Statistics: Wilcoxon matched pairs signed rank test). (**D**) FA formation of wt iDCs cultured on FN or gelatin. (Statistics: Wilcoxon matched pairs signed rank test)

(Error bars represent mean +/- SEM; n.s. (not significant) $p>0.05$; * $p<0.05$; ** $p<0.01$; *** $p<0.001$)

3.1.4. Altered mechanosensing does not explain the differences in podosome formation on fibronectin and gelatin

In principal, the reduced spreading of iDCs on gelatin vs FN indicates that gelatin coating produces a softer matrix compared to FN coatings. Given the established role of podosomes as mechanosensors[63], it is possible that merely the biophysical differences between FN and gelatin are responsible for the different podosome formation of (a) wt cells on these two substrates and (b) of Cyth2 KO compared to wt iDCs. In order to test this hypothesis, we made use of elastomers, a polydimethyl-siloxane (PDMS)-based gel of defined stiffness. Glass or cell culture plastics have an elasticity of several GPa (Young's modulus)[170], while elastomers come in a more physiological range of a few kPa[171] (50 kPa in our case). Coating elastomers with FN generates a surface with the same biological properties as FN-coating on glass or plastic, but with a decreased stiffness. This way, the elasticity of the FN-coated surface is more similar to gelatin-coated plastic. If Cyth2 KO iDCs on this soft FN behave as if they were seeded on gelatin-coated plastic, the differential podosome formation is most likely due to the different elasticity of FN and gelatin and not caused by other factors.

As figure **3.10 A** illustrates, cell spreading was reduced on FN-coated elastomers compared to plastic in both wt and Cyth2 KO iDCs (figure **3.10 B**), which is in line with reduced mechanical strain. Also, podosome formation in iDCs decreased on soft matrix (figure **3.10 C**), just as it did on gelatin. However, podosome formation was decreased in both wt and Cyth2 deficient cells and did not show the counter-regulation observed on gelatin (figure **3.4**). Therefore, the reduced podosome levels in Cyth2 KO iDCs on FN could be caused by disturbed mechanosensing but this does not explain the opposing effect of Cyth2 deficient cells on gelatin. Thus, there must be additional differences between FN and gelatin leading to differential dependence on Cyth2. Moreover, cells on collagen IV show the same dependency on Cyth2 for podosome formation as cells on gelatin (figure **3.6**). Still, cell spreading as well as podosome levels of wt cells on collagen IV are more similar to FN than to gelatin (figures **3.9A, 3.6** and **3.2**). Mechanical properties might therefore play a role in the altered adhesion behavior and podosome formation on FN and gelatin in wt cells but the regulation of podosome formation by Cyth2 seems to be more complex.

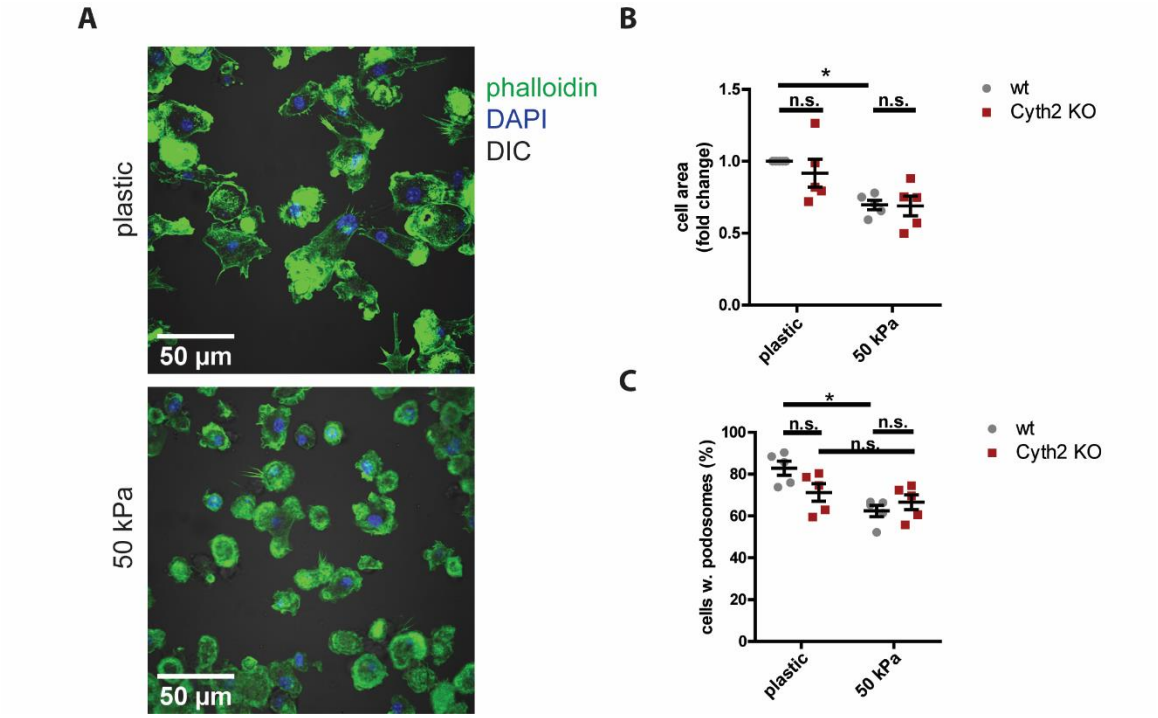

Figure 3.10 – Substrate rigidity affects podosome formation

Cells were seeded on FN-coated plastic dishes or elastomers and stained with phalloidin and DAPI. (**A**) Exemplary images of wt iDCs on rigid and soft FN-matrices. Cell spreading (**B**) and podosome quantification (**C**) of wt and Cyth2 KO iDCs on FN-coated cell culture plastic or 50 kPa-elastomers.

(Error bars represent mean +/- SEM; Statistics: 2way ANOVA with Bonferroni's or Tukey's multiple comparison test; n.s. (not significant) $p>0.05$; * $p<0.05$)

3.2. Integrin expression and dynamics are not altered in Cyth2 KO iDCs

Loss of Cyth2 in iDCs has very different effects on podosome formation depending on the underlying substrate. In some cases (Icam-1 or fibrinogen coating) Cyth2 seems to be dispensable, while other coatings either lead to an increase or a reduction of podosome frequencies. Having a closer look at the respective coating material, it becomes clear that they are recognized by different integrin classes. Icam-1 and fibrinogen are classical ligands for β2 integrins, while FN and gelatin or collagens are bound especially by β1 integrins (figure **1.1**).[11] Therefore, we decided to focus on the role of integrins in Cyth2-mediated regulation of podosome formation.

3.2.1. Integrin cell surface expression of iDCs is not affected by loss of Cyth2

Even though there are 24 different integrin dimers described, the actual integrin expression of every cell type is restricted to a certain repertoire.[10] For that reason, we first wanted to know, which integrins are expressed by iDCs at all. Using an RNA sequencing data set that we had generated with the group of Prof. Schultze at the LIMES Institute, we could narrow down the relevant integrins to 7 different α chains and 6 different β chains, which can occur as 11 different integrin dimers (figure **3.11 A**). The overall expression levels of these integrins varied substantially with the β2 integrins being the strongest expressed group, followed by β1 integrins. Especially α6, β3, β5 and β7 integrins were expressed at very low levels. Furthermore, RNA levels of all integrins did not change in Cyth2 KO iDCs and were not affected by the underlying matrix – apart from α1 integrin, which was slightly upregulated in cells cultured on gelatin.

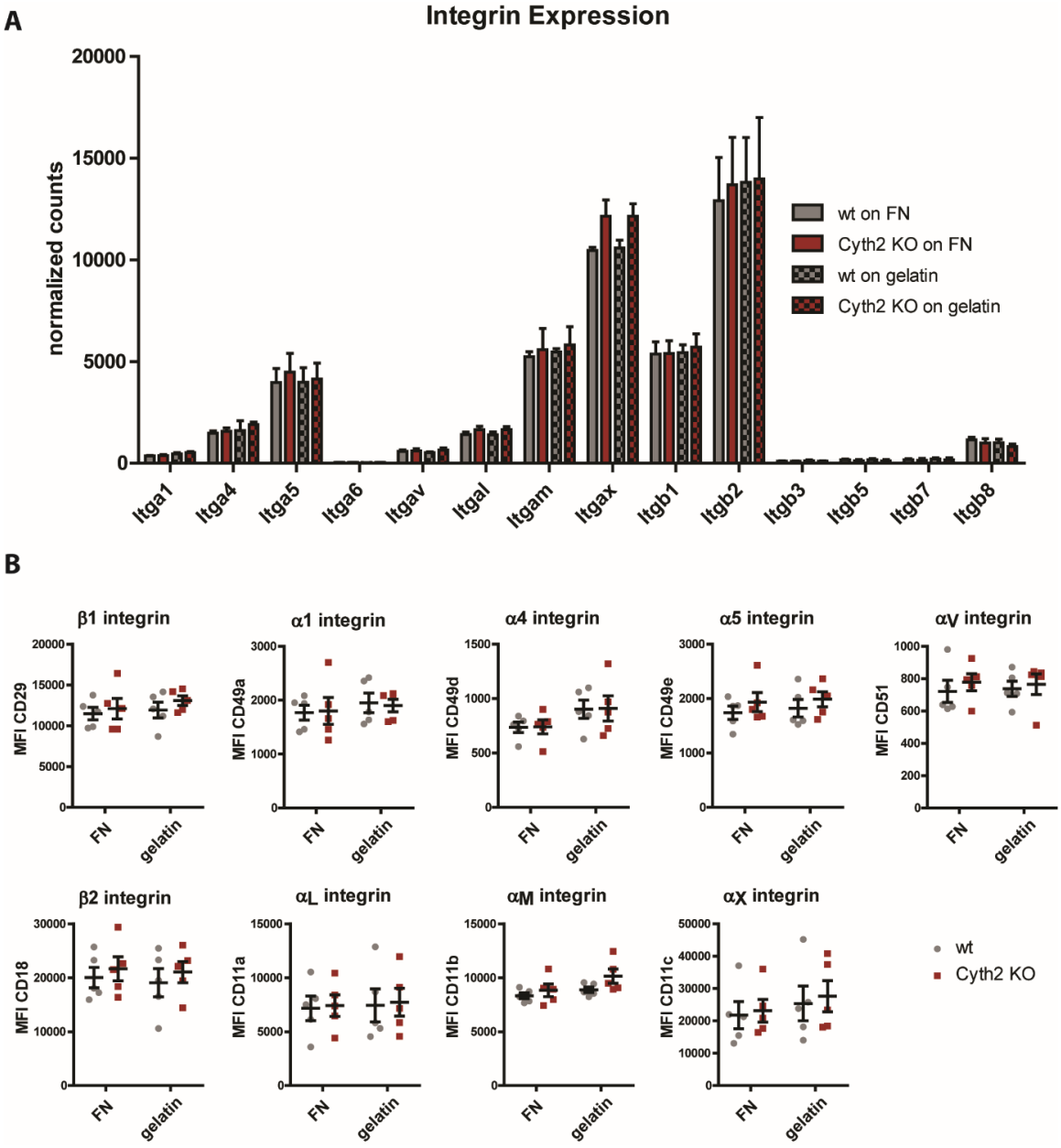

Figure 3.11 – Basal integrin expression in iDCs is not affected by Cyth2

(A) RNA expression of integrins in wt and Cyth2 KO iDCs cultured on FN or gelatin for 7h (n=4) based on an RNA sequencing data set. Other integrin mRNAs were below 50 counts. Error bars represent mean +/- SD. (**B**) Flow Cytometry of iDCs on FN or gelatin (o.n. adhesion) and quantification of median fluorescence intensity (MFI) of integrins on the cell surface (n=5). (Error bars represent mean +/-SEM.)

We also sought to confirm these RNA data on protein level and analyzed integrin expression on the cell surface by flow cytometry. As figure **3.11 B** shows, we could detect αL, αM, αX and β2 integrins, as well as α1, α4, α5 and β1 integrins on the surface of iDCs. Furthermore, we also found low levels of αv integrin, but hardly any β3 integrin. α6, β5 and β7 integrins were not detectable at all in iDCs on either FN or gelatin-coated surfaces (data not shown). β8 integrin was identified on RNA level but as there is no antibody available for flow cytometry, we could not confirm these results on protein level. Given that β8 integrins always occur together with the αv integrin chain[172]

and αv levels were quite low, we assumed that also β8 integrins do not participate much in iDC adhesion to FN or gelatin. Therefore, we conclude that the two major integrin classes expressed by iDCs are β1 and β2 integrins (summarized in figure **3.12**). In terms of interaction with FN especially α4β1 and α5β1 and to some extent also the αv integrins are of interest, while gelatin or collagen could be sensed via α1β1 or αXβ2 integrins (compare figure **1.1**). Moreover, KO of Cyth2 did not affect integrin expression in iDCs cultured on either FN or gelatin, nor did the underlying coating manifest itself in different expression levels of integrins (figure **3.11 B**).

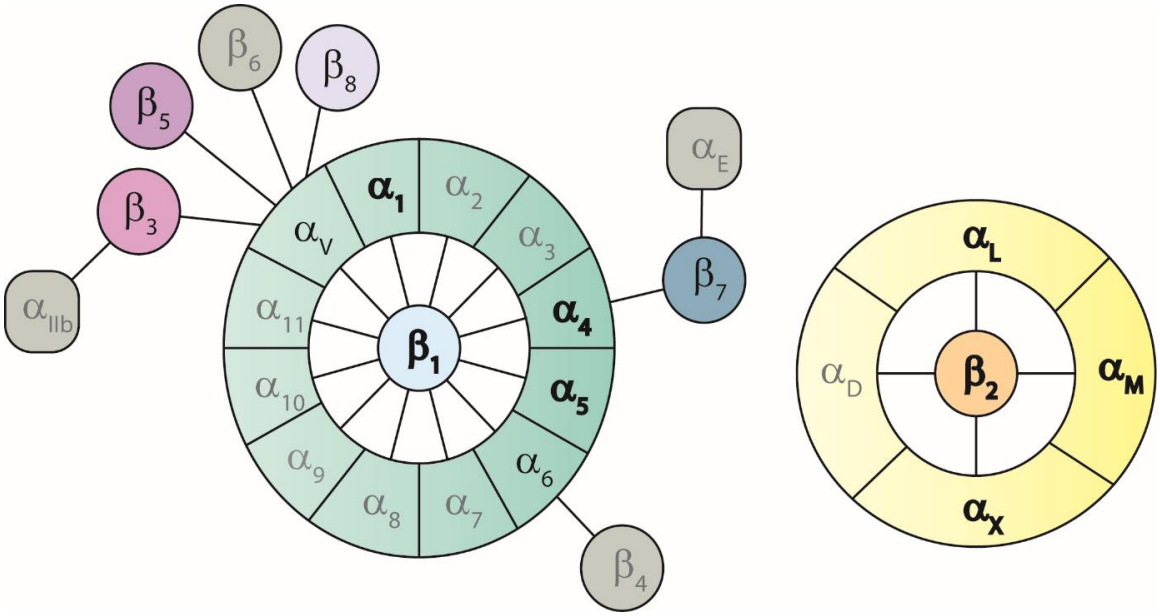

Figure 3.12 – Integrin receptor expression in iDCs
iDCs express a limited number of integrins: Several β2 integrins (αLβ2, αMβ2, αXβ2) and β1 integrins (α1β1, α4β1, α5β1). αV integrins are expressed at very low levels and α6, β3,β5 and β7 integrins are not detectable on the cell surface.

As we had just found β1 and β2 integrins as the major integrins expressed by iDCs, we next examined whether these integrin chains localize to iDC podosomes at all. Immunofluorescence stainings showed that both integrin classes are found in the podosome ring structure (figures **3.13** and **3.14**). There were, however, no apparent differences in integrin localization between wt and Cyth2 KO iDCs or between cells cultured on FN or gelatin.

In summary, iDCs express several different integrins, but the majority of integrins on the cell surface consists of β1 and β2 integrins. Both integrin classes localize to podosome rings. However, the loss of Cyth2 does not affect integrin expression under steady state conditions, i.e. in cells cultured o.n. on the respective ligands. Moreover, coating with FN or gelatin does not alter integrin expression either.

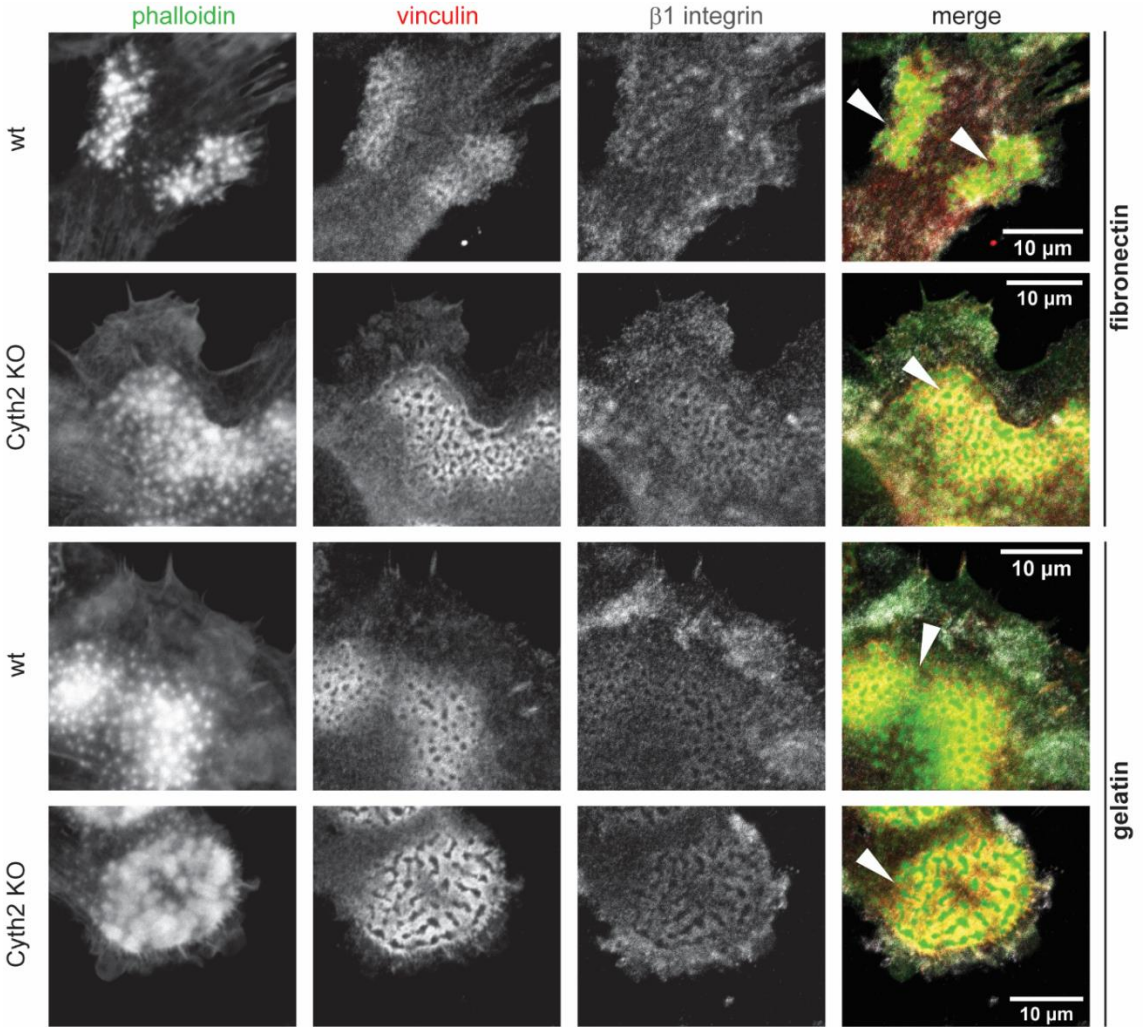

Figure 3.13 –β1 integrins localize to podosome rings

Confocal images of wt and Cyth2 KO iDCs cultured on FN or gelatin in the presence of anti-β1 integrin antibody (clone Hmb1-1) that were stained with phalloidin and antibodies against vinculin and anti-rat secondary antibodies. Arrows indicate podosome clusters. Scale bar represents 10 µm.

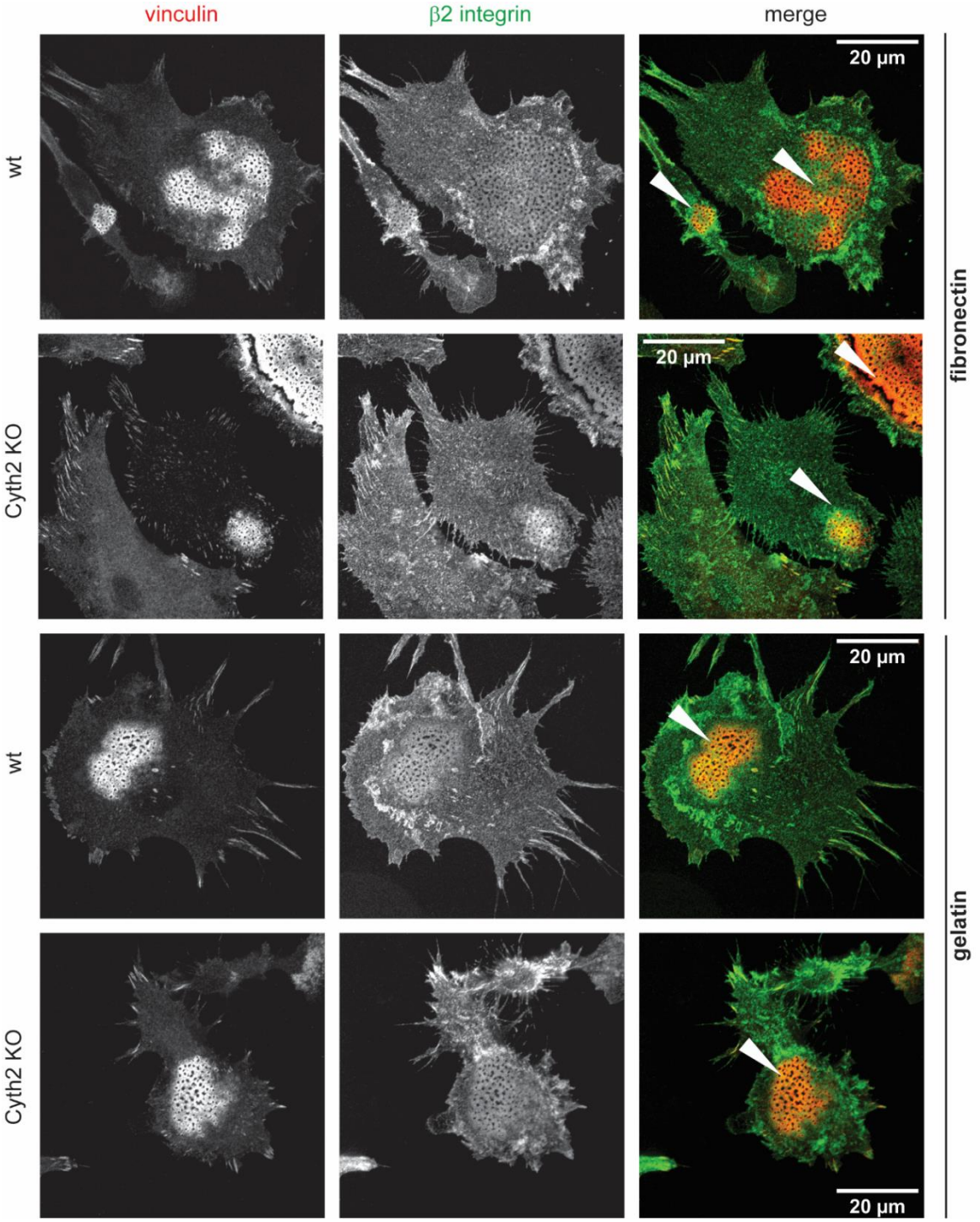

Figure 3.14 –β2 integrins localize to podosome rings

Confocal airyscan images of wt and Cyth2 KO iDCs cultured on FN or gelatin that were stained with antibodies against vinculin and β2 integrin. Arrows indicate podosome clusters. Scale bar represents 20 µm.

3.2.2. Cyth2 is not involved in integrin surface expression dynamics in iDCs

Integrins are very dynamic and they are constantly endocytosed to become degraded in lysosomes or to be recycled to the cell surface. That way, a cell is able to adapt quickly to changes in the environment or in intracellular signaling.[49] Given that especially Cyth2 has been described to regulate integrin recycling in epithelial cells[129,136], it is possible that, while steady state expression levels of integrins are not different between wt and Cyth2 KO cells, integrin dynamics are differentially regulated in the presence or absence of Cyth2.

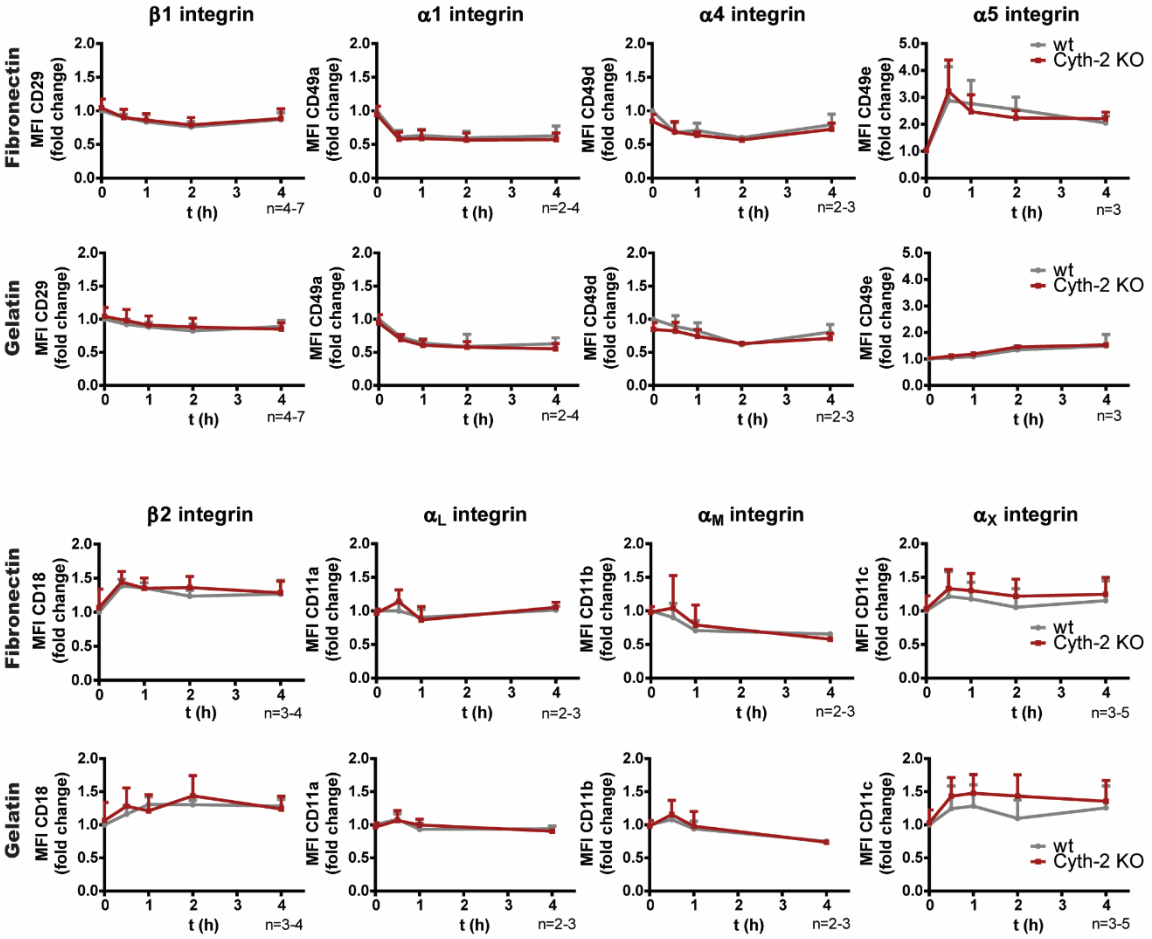

Figure 3.15 – Integrin dynamics upon adhesion are independent of Cyth2
Wt and Cyth2 KO iDCs were kept in suspension for 1h and then seeded onto FN- or gelatin-coated surfaces (t=0h). At indicated time points, cell surface expression of integrins was measured by flow cytometry. (Error bars represent mean +/- SD)

To analyze whether stimulation of integrins by specific ligands directly affects integrin expression on the cell surface, we first aimed at generating an unstimulated state of integrins on iDCs. We achieved this by culturing iDCs in a viscous methyl cellulose solution that prevented cells from getting into contact with each other or with the vessel walls. Thereby, formation of adhesions and

stimulation of integrin signaling was avoided. After dilution of the methyl cellulose, cells could be seeded onto ligand-coated surfaces, which induced a precise and time-controlled activation of integrins. As seen in figure **3.15**, integrin levels indeed responded to the adhesion process, but there was no difference between wt and Cyth2 KO cells. Nevertheless, integrin dynamics on gelatin were often slightly delayed compared to the situation on fibronectin. This was especially apparent in the case of α5 integrins, which form the major FN-receptors of iDCs together with the β1 integrin chain[11]. On FN, α5 integrin levels were strongly upregulated as early as 30 min post adhesion, while they rose much more slowly on gelatin. This again illustrates how different adhesion processes on these two coating materials can be.

Next, we had a closer look into integrin internalization by staining integrins on the cell surface with unlabeled antibodies. During incubation periods of different lengths, integrins are internalized and thereby antibody levels on the surface are reduced gradually. By counterstaining with a secondary antibody, the reduction of integrin levels on the cell surface can be quantified. We focused especially on α5 integrins, which are the most strongly expressed FN-binding integrins on iDCs, and α1 integrins, which are the only classical collagen receptor of these cells. β2 integrins served as controls. However, internalization of neither α1, nor α5 nor β2 integrins was affected by loss of Cyth2 (figure **3.16**). Moreover, internalization rates on FN and gelatin were also similar.

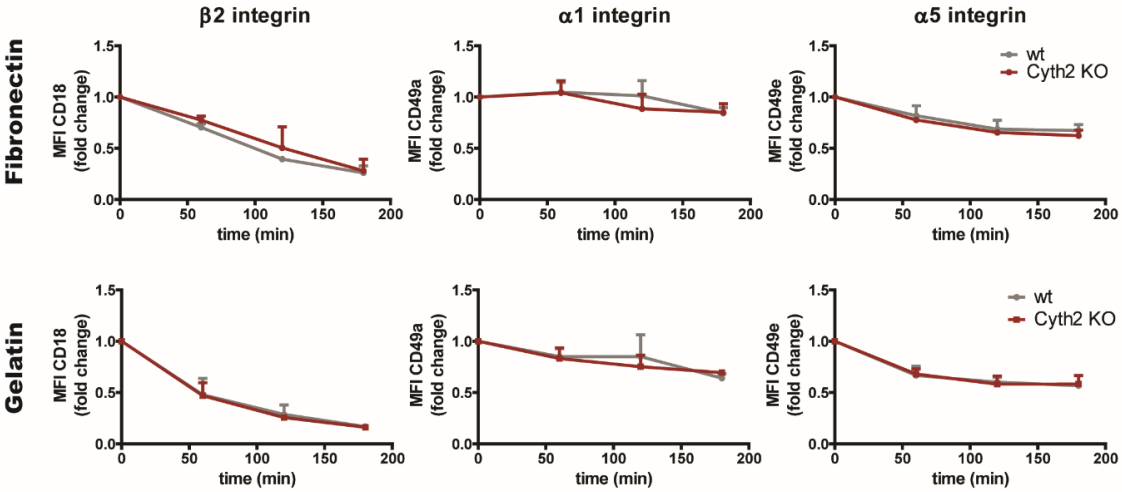

Figure 3.16 – Integrin internalization is not affected by loss of Cyth2

Wt and Cyth2 KO iDCs cultured on FN or gelatin were stained with unlabeled antibodies for β2, α1 and α5 integrin. At the indicated time points cells were harvested and remaining antibodies on the cell surface were stained with a secondary antibody and visualized by flow cytometry. Graphs show mean of 3 independent experiments. (Error bars indicate mean +/- SD)

Integrin levels on the cell surface are not only determined by integrin recycling from endosomes but also via the secretory pathway involving the Golgi apparatus. This includes both reconstitution with newly synthesized integrins from the ER and retrograde transport routes of recycled integrins.[48,49] In order to exclude this source of integrin molecules, we treated cells with Brefeldin A (BrefA). BrefA stabilizes the complex of Arf GTPases and certain GEFs (but not cytohesins) and thereby prevents cycling of Arfs between different activation states.[173] This leads to disintegration of the Golgi apparatus and therefore blocks vesicle transport from the Golgi to the cell membrane. Figure **3.17** shows that BrefA treatment leads to gradual reduction of integrins on the cell surface, as integrin recycling alone is not sufficient to maintain integrin levels. KO of Cyth2, though, does not alter the dynamics of this effect, nor does the coating material.

Taken together, we could not observe any effect of Cyth2 on integrin expression or dynamics in iDCs that would explain the differences in podosome formation on different integrin ligands. Yet, we again noticed that adhesion processes in general are regulated differently on FN vs gelatin.

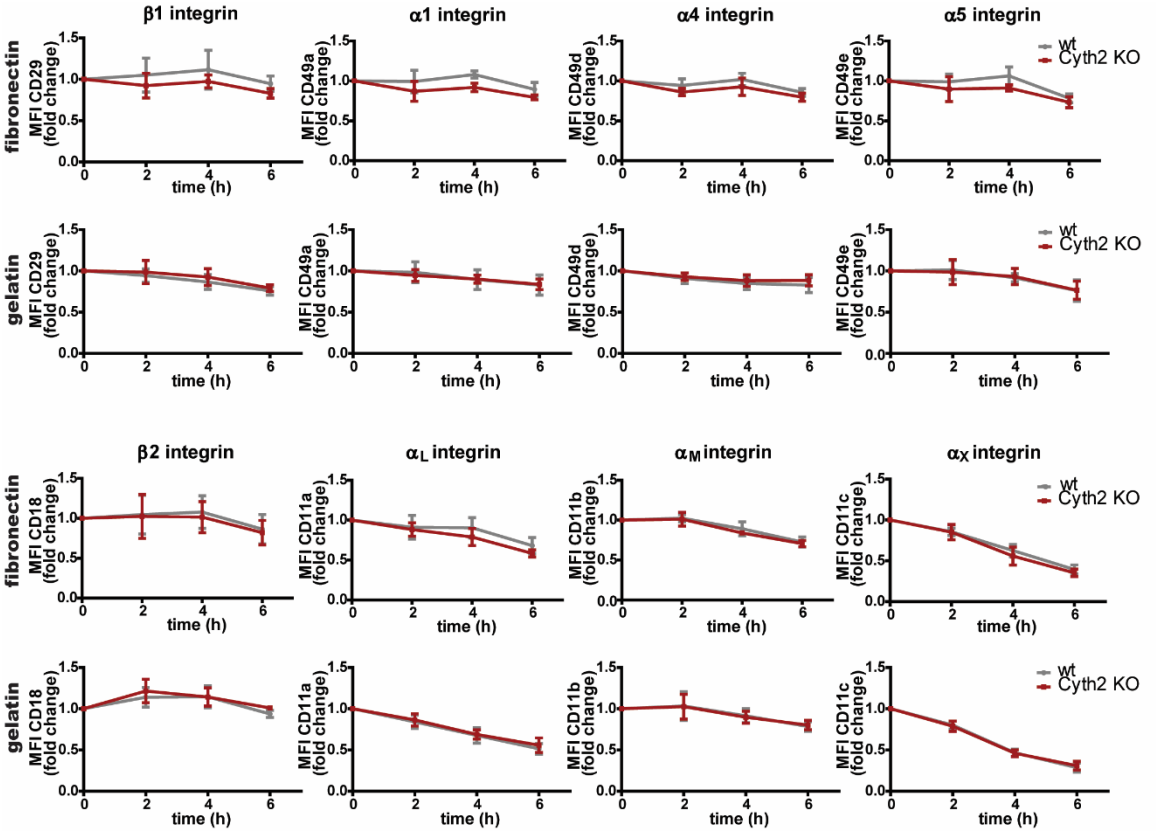

Figure 3.17 – Integrin recycling is not altered in Cyth2 KO iDCs

Wt and Cyth2 KO iDCs were cultured on FN or gelatin and treated with 5 µg/ml BrefA for 2/4/6 h, before they were harvested and analyzed for integrin cell surface expression by flow cytometry. Graphs show mean of 3 (FN) or 4 (gelatin) independent experiments. (Error bars represent mean +/- SD)

3.3. The effects of Cyth2 on podosome formation are mediated via specific integrins

So far, we could determine that Cyth2 regulates podosome formation in iDCs depending on the underlying matrix. Integrins are the most likely candidates to regulate this matrix-specific effect as they are known to distinguish between different ECM proteins.[11] However, their expression and dynamics seemed not to be affected by Cyth2. Therefore, we decided to investigate the involvement of single integrins in podosome formation by iDCs in more detail.

3.3.1. β2 integrins are a major structural component of podosomes in iDCs

Although our previous results using fibrinogen or Icam-1 coatings indicate that β2 integrins are most likely not involved in Cyth2-mediated podosome formation, β2 integrins are still by far the major integrin class expressed by iDCs. They occur together with αL, αM or αX integrin chains. As they are only found in cells of hematopoietic origin[10], their role in invadosome formation is not studied quite as extensively as other integrins, but it has been found localized to the ring structure of invadosomes[174,175]. One study, though, examined the role of β2 integrins specifically in iDCs and claimed that these integrins are required for podosome formation on several coating substrates.[77]

In order to verify if these results are also relevant in our system, we obtained bone marrow cells of CD18 null mice from Prof. Karin Scharffetter Kochanek at Ulm University and analyzed podosomes of iDCs generated from these cells. As figure **3.18 A** shows, these Itgb2 KO iDCs do not express β2 integrin or any of the respective alpha chains on their surface. Podosome frequencies of Itgb2 KO cells were drastically reduced on surfaces coated with FN, gelatin or the β2 integrin-specific ligand fibrinogen compared to controls (figure **3.18 B**). General adhesion behavior, however, was only impaired, when KO cells were cultured on fibrinogen. Adhesion onto FN or gelatin was still possible, even though cell spreading was slightly reduced compared to wt cells (figure **3.18 C**). Therefore, β2 integrin seems to be only required for adhesion onto classical β2-integrin ligands, but mostly dispensable for adhesion onto β1-specific integrin ligands like FN or gelatin/collagen. β2 integrins, however, seem to be a crucial structural component of podosomes irrespective of the underlying matrix.

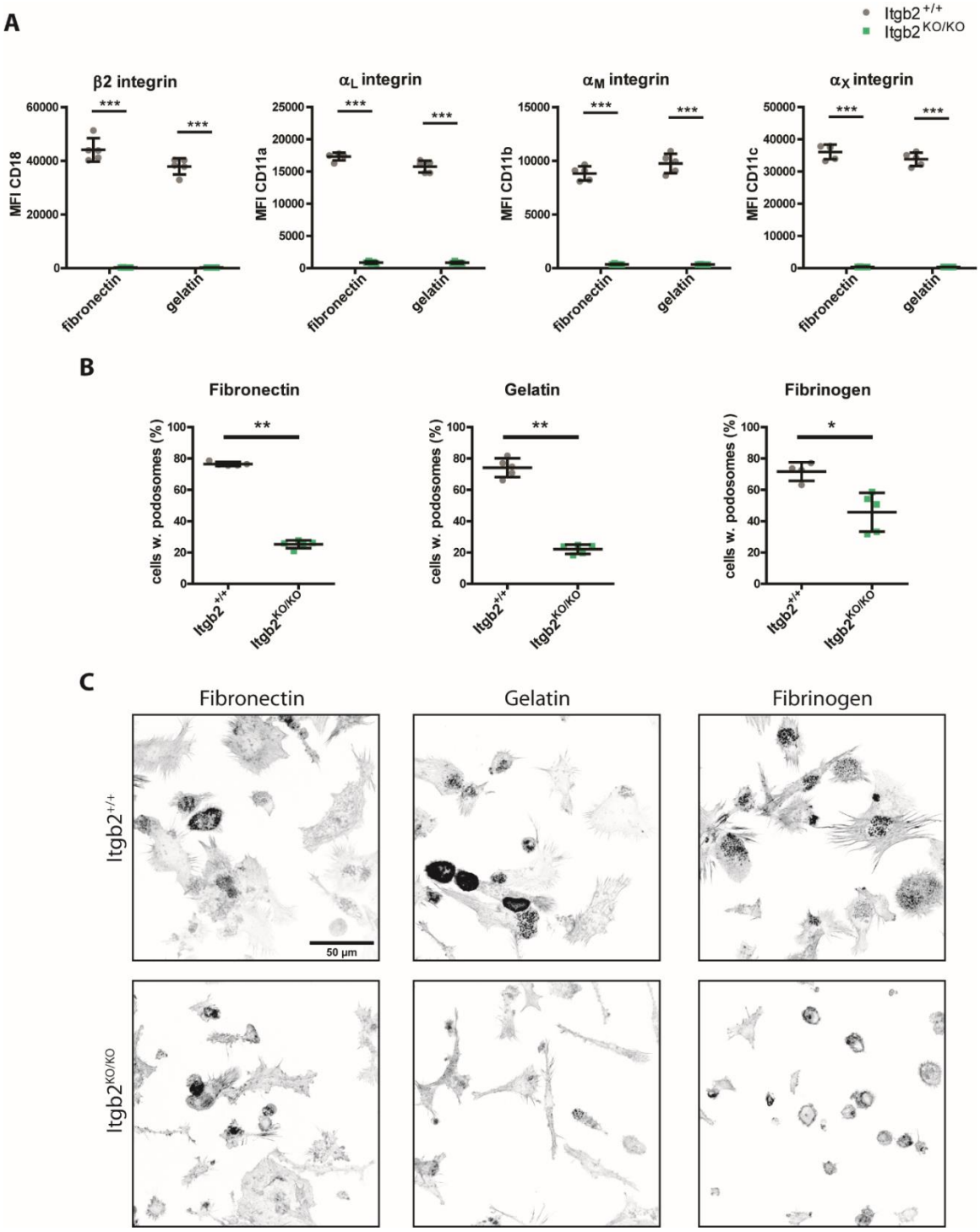

Figure 3.18 – β2 Integrins are crucial components of podosome structure

iDCs from CD18 null mice (Itgb2$^{KO/KO}$) and control mice were seeded onto FN, gelatin and fibrinogen. (**A**) Cell surface of expression of β2, αL, αM and αX integrins. (Statistics: 2way ANOVA with Bonferroni' multiple comparison test) (**B**) Quantification of podosomes on FN, gelatin and fibrinogen. (Statistics: Mann-Whitney test) (**C**) phalloidin staining of Itgb2$^{+/+}$ and Itgb2$^{KO/KO}$ iDCs on FN, gelatin and fibrinogen. (Error bars represent mean +/- SD; * p<0.05; ** p<0.01, *** p<0.001)

As the complete loss of β2 integrins has such a dramatic effect on the cells' ability to form podosomes, we decided to induce only partial reduction of β2 integrin expression by siRNA-

mediated knockdown (kd). Moreover, this approach enabled us to study the role of Cyth2 in β2 integrin-related processes. Figure **3.19 A** shows that kd of Itgb2 with two different siRNAs leads to a reduction of β2 integrin surface expression to 50-60 % of control cells. In contrast to the full-KO of β2 integrins, podosome formation in β2 integrin kd cells (both wt and Cyth2 KO cells) was only mildly affected compared to control cells (figure **3.19 B**). Nevertheless, both wt and KO podosome levels were altered in opposite directions leading to an assimilation at an intermediate level. This effect was more robust on FN than on gelatin, which could be due to the lower number of experiments performed on gelatin.

Neither FN nor gelatin are typical ligands for β2 integrins but there are reports that discuss especially αXβ2 integrin as a receptor for collagen[176]. For that reason, we further analyzed kd of the β2-associated alpha chains, αL, αM and αX, which reduced surface expression levels to roughly 50 % of controls (figure **3.19 C, E, G**). On FN, the reduction of αL, αM and αX chains had no significant effect on podosome formation. Still, the values showed a slight tendency in the same direction as the Itgb2 kd samples (figure **3.19 D, F, H**). This was also the case on gelatin with respect to αL and αM integrin and might reflect concomitant reductions of β2 integrin surface levels after kd of the alpha chains. Kd of αX integrin, however, resulted in a more pronounced assimilation of wt and Cyth2 KO podosome levels on gelatin. In the case of siItgax #22, we even observed a reversal of wt and Cyth2 KO podosome numbers, although this siRNA produced a weaker knock down than siItgax #12 (figure **3.19 G**). Therefore, one cannot exclude potential off-target effects and has to be careful with the interpretation of this result. A final conclusion is thus difficult to draw and would require further experiments.

Nonetheless, interfering with β2 integrins can abolish the Cyth2 KO-induced difference in podosome formation. Considering the central role of β2 integrins for podosomes in general (as illustrated in figure **3.18**), it is possible that even a moderate reduction of β2 integrin levels by siRNA-mediated kd might disturb the podosome formation machinery in a way that the mild regulatory effects of Cyth2 are masked. Moreover, kd of the β2-associated α integrin chains does not enhance this β2 integrin effect on FN. Only αX integrin could be involved in regulating podosome formation on gelatin, but our results are too ambiguous to allow for a final conclusion. Therefore, we conclude that on FN β2 integrins are most likely not involved in the differential regulation or podosome formation by Cyth2. On gelatin, though, the αxβ2 integrin might play a role.

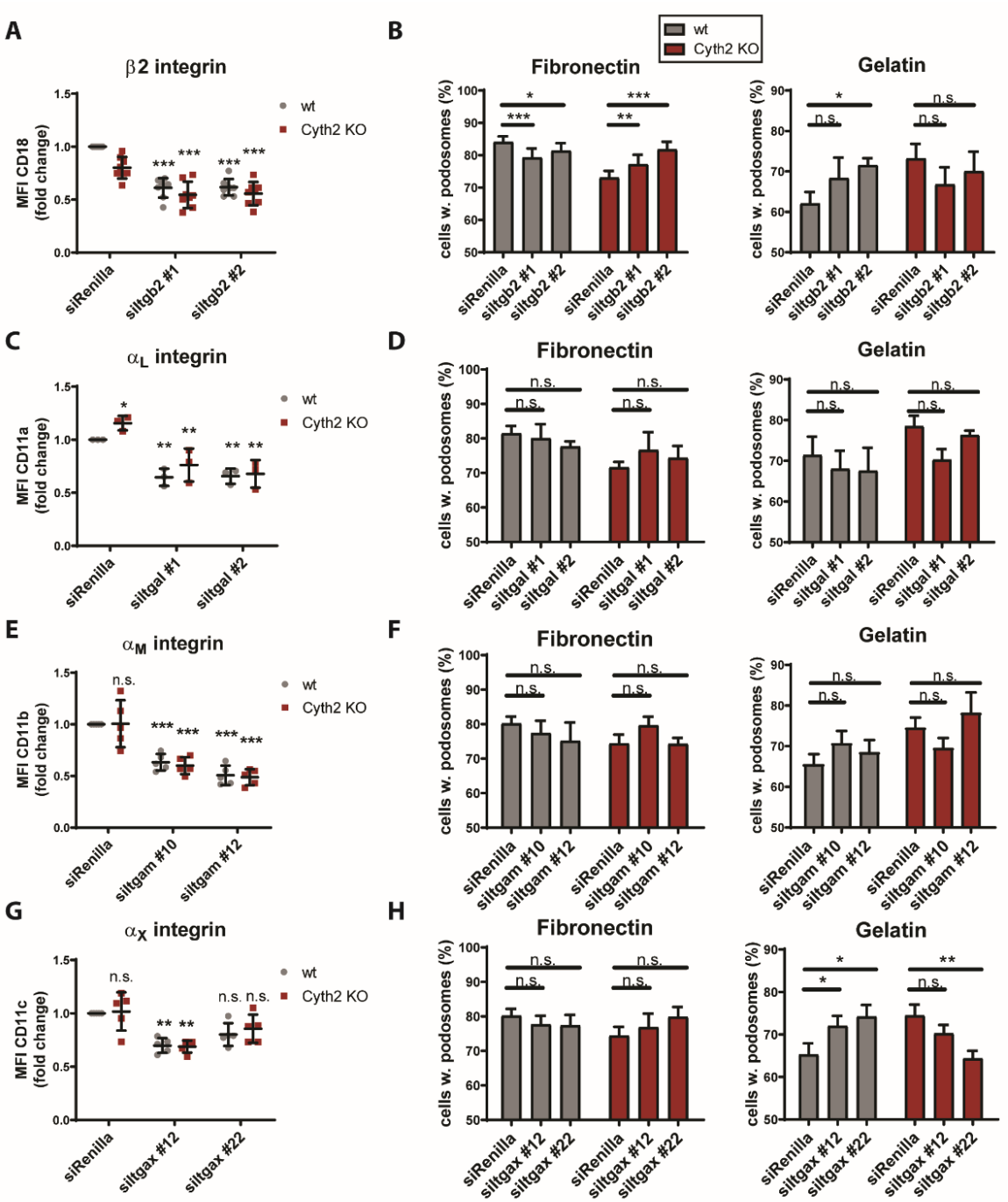

Figure 3.19 – Knock-down of β2 integrins abolishes Cyth2-mediated differences on podosome formation by iDCs
Kd of Itgb2, Itgal, Itgam and Itgax (**A, C, E, G**) in iDCs was verified by flow cytometry at 24 hpt. (**B**) Podosome formation on FN (n=7) or gelatin (n=4) was quantified 24 hpt with siRNAs against Itgb2. (**D, F, H**) Podosome formation on FN or gelatin was quantified 24 hpt with siRNAs against Itgal (n=3), Itgam (n=5) and Itgax (n=5) (Statistics: 2way ANOVA with Dunnett's multiple comparison test. Error bars represent mean +/- SEM; n.s. (not significant) p>0.05; * p<0.05; ** p<0.01; *** p<0.001)

3.3.2. Cyth2 is an important regulator of α5β1 integrin signaling function in podosome formation

Our previous experiments with different coating substrates (figures **3.2, 3.4** and **3.6**) indicated that Cyth2 is involved in podosome formation specifically on β1 integrin ligands. iDCs express predominantly α1β1, which recognizes collagen, and α4β1 and α5β1, which are receptors for FN. In order to elucidate which integrin might be responsible for the differential effects of Cyth2 on either FN or gelatin, we interfered with different β1 integrins using either siRNA-mediated kd approaches or cells derived from specific KO mice.

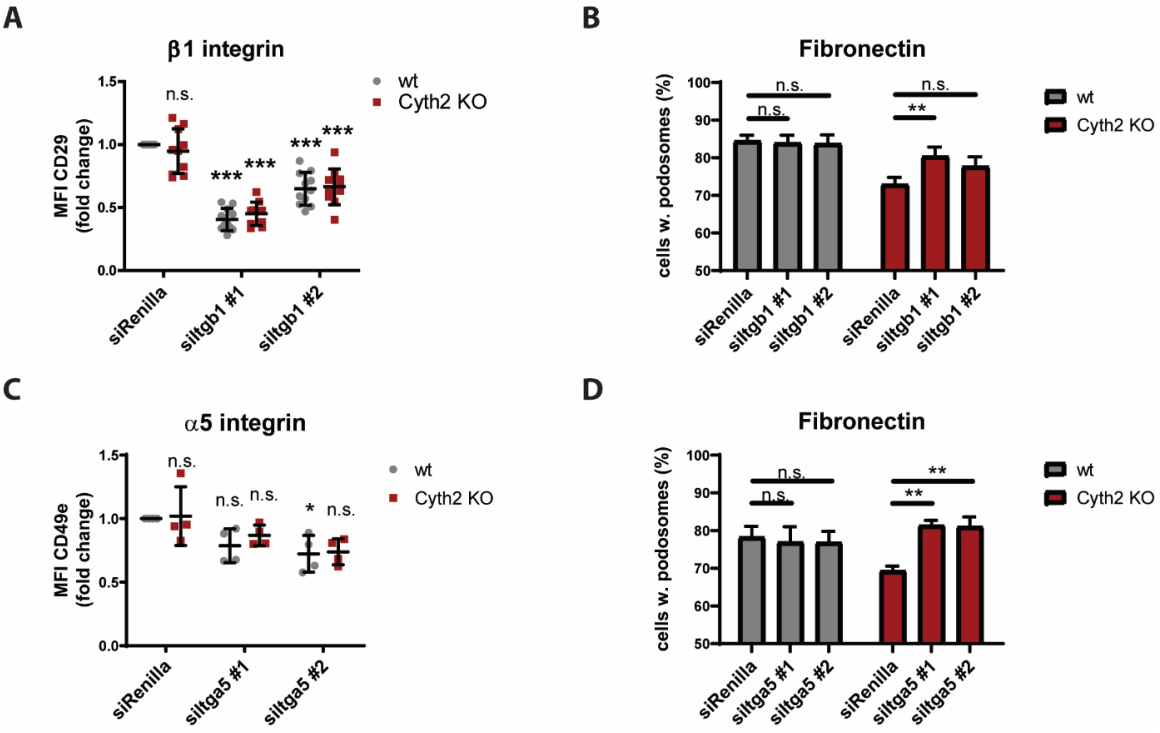

Figure 3.20 – Signaling via α5β1 integrins mediates podosome reduction by Cyth2 on FN
(**A**) Itgb1 was knocked down in wt and Cyth2 KO iDCs and kd efficiency was determined by flow cytometry. (**B**) Podosome formation after kd of Itgb1 on FN (mean of 8 independent experiments). (**C**) Itga5 was knocked down in wt and Cyth2 KO iDCs and kd efficiency was determined by flow cytometry. (**D**) Quantification of podosome formation after kd of Itga5 on FN (mean of 4 independent experiments). (Statistics: 2way ANOVA with Dunnett's multiple comparison test; Error bars indicate mean +/- SEM. n.s. (not significant) p>0.05; * p<0.05; ** p<0.01 *** p<0.001)

To test for the involvement of β1 integrins in podosome formation, we knocked down β1 integrins in iDCs with two different siRNAs and verified the kd success by flow cytometry (figure **3.20 A**). Itgb1 siRNA #1 resulted in a 50-60 % reduction of surface levels of β1 integrin compared to controls, while Itgb1 siRNA #2 was less efficient and reduced integrin expression by only 30 %. Next, we analyzed podosome formation on different matrices. On FN, kd of β1 integrins in wt cells did not affect podosome frequencies at all (figure **3.20 B**). However, Cyth2 KO cells that received Itgb1 siRNA #1 displayed podosome numbers comparable to wt cells and podosome formation in

KO cells treated with Itgb1 siRNA #2 at least showed a similar tendency. The strength of these effects correlates well with the kd efficiencies of the respective siRNAs.

As the main receptor for FN in iDCs is $\alpha5\beta1$ and $\alpha5$ integrins were strongly upregulated upon adhesion onto FN (figures **3.11** and **3.15**), we speculated that kd of the $\alpha5$ integrin chain might be even more specific than kd of the common $\beta1$ integrin. Both Itga5 siRNAs showed only mild kd efficiencies (figure **3.20 C**), but the reduced podosome formation by Cyth2 KO iDCs on FN was rescued completely by both siRNAs (figure **3.20 D**). Wt iDCs, however, were again not affected by kd of $\alpha5$ integrins. Moreover, blocking $\beta1$ integrin function with two independent blocking antibodies (clones Hmb1-1 and HA2/5) also rescued the reduction of podosome formation in Cyth2 KO cells on FN (figure **3.21**). These results indicate that in wt cells signaling through $\alpha5\beta1$ integrins has no immediate effect on podosome formation on FN. Nevertheless, once Cyth2 is missing, signals from $\alpha5\beta1$ integrins inhibit podosome formation. Therefore, we conclude that under wt conditions Cyth2 seems to block these inhibitory signals coming from $\alpha5\beta1$ integrins.

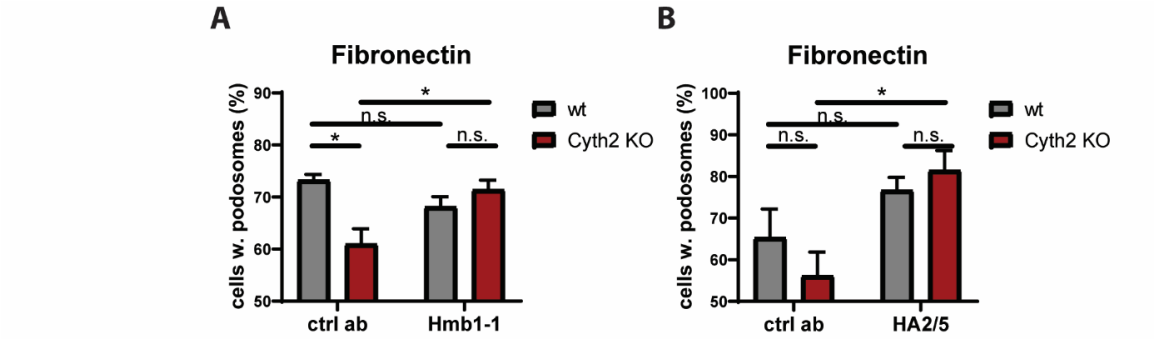

Figure 3.21 – Blocking β1 integrin function rescues the Cyth2 KO effect on podosome formation on FN
(**A**) Podosome formation on FN after treatment with integrin $\beta1$ blocking ab (Hmb1-1) (n=3). (**B**) Podosome formation on FN after treatment with integrin $\beta1$ blocking ab (HA2/5) (n=3). (Statistics: 2way ANOVA with Tukey's multiple comparison test; Error bars indicate mean +/- SEM. n.s. (not significant) $p>0.05$; * $p<0.05$; ** $p<0.01$ *** $p<0.001$)

Furthermore, we analyzed the effect of $\beta1$ and $\alpha5$ integrin kd on podosome formation on gelatin. Here, reduction of $\beta1$ integrin expression levels abolished the difference between wt and Cyth2 deficient cells as well, but this seemed to be mostly due to wt cells increasing their podosome numbers (figure **3.22 A+B**). Kd of $\alpha5$ integrins similarly affected mostly wt cell cultured on gelatin (figure **3.22 C+D**), even though the effects were not statistically significant.

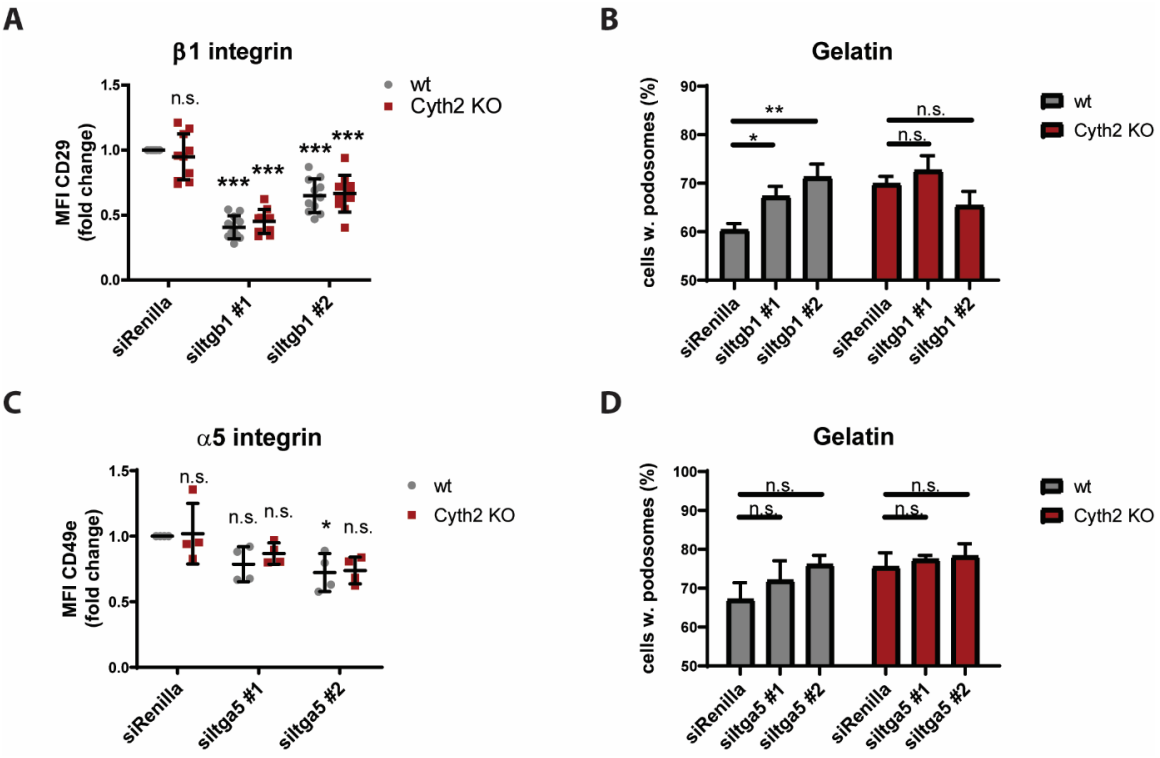

Figure 3.22 – Loss of β1 integrins mimics Cyth2 KO effect on podosome formation on gelatin
(A) Itgb1 was knocked down in wt and Cyth2 KO iDCs and kd efficiency was determined by flow cytometry. (**B**) Podosome formation after kd of Itgb1 on gelatin (mean of 4-5 independent experiments). (**C**) Itga5 was knocked down in wt and Cyth2 KO iDCs and kd efficiency was determined by flow cytometry. (**D**) Quantification of podosome formation after kd of Itga5 on gelatin (mean of 4 independent experiments). (Statistics: 2way ANOVA with Dunnett's multiple comparison test; Error bars indicate mean +/- SEM. n.s. (not significant) p>0.05; * p<0.05; ** p<0.01 *** p<0.001)

In addition, we used function-blocking antibodies directed against β1 integrin to further assess the role of β1 integrins in podosome formation on gelatin (figure **3.23**). Both Hmb1-1 and HA2/5 antibodies showed a tendency for elevation of wt podosome formation to the level of control KO cells. Even though the effects observed on gelatin were not as robust as on FN, these data also support the notion that, in contrast to the situation on FN, interfering with α5β1 integrins rather mimics the loss of Cyth2 on gelatin. This would further mean that the inhibitory effect of α5β1 integrins on podosome formation is mediated via Cyth2 on gelatin. Thus, if either Cyth2 or α5β1 integrins are missing, this inhibition does not take place anymore and podosome levels increase.

Taken together, we observed that specifically on FN deregulation of podosome formation by loss of Cyth2 is mediated via α5β1 integrins. This specific way of involvement of α5β1 integrins, however, is not relevant on gelatin. Rather, it seems like the connection between Cyth2 and α5β1 integrin signaling is different, when cells are cultured on gelatin.

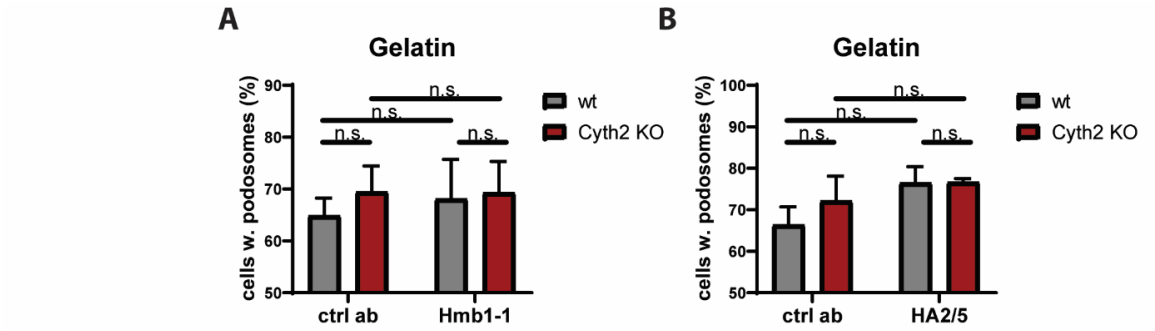

Figure 3.23 – Blocking β1 integrin function slightly increases podosome numbers in wt cells on gelatin
(**A**) Podosome formation on gelatin after treatment with integrin β1 blocking ab (Hmb1-1) (n=3). (**B**) Podosome formation on gelatin after treatment with integrin β1 blocking ab (HA2/5) (n=3). (Statistics: 2way ANOVA with Tukey's multiple comparison test; Error bars indicate mean +/- SEM. n.s. (not significant) p>0.05; * p<0.05; ** p<0.01 *** p<0.001)

3.3.3. α1 and α4 integrins do not affect podosome formation in iDCs

α5β1 is the highest expressed FN-specific integrin in iDCs. Nevertheless, FN can also be recognized by α4β1 integrins[11], which are also found on the surface of iDCs. We generated iDCs from Itga4$^{flox/flox}$ Vav-Cre bone marrow, which we received from Prof. Triantafyllos Chavakis at the University hospital Dresden. These iDCs were deficient for α4 integrin (figure **3.24 A**). At the same time, this loss of α4 integrin also reduced the expression of β1 integrin, while other integrin expression levels were not altered (data not shown). Podosome formation on FN or gelatin, however, was not affected by the presence or absence of α4 integrin (figure **3.24 B**). Therefore, α4 integrin signaling seems not to be important for podosome formation on these integrin ligands.

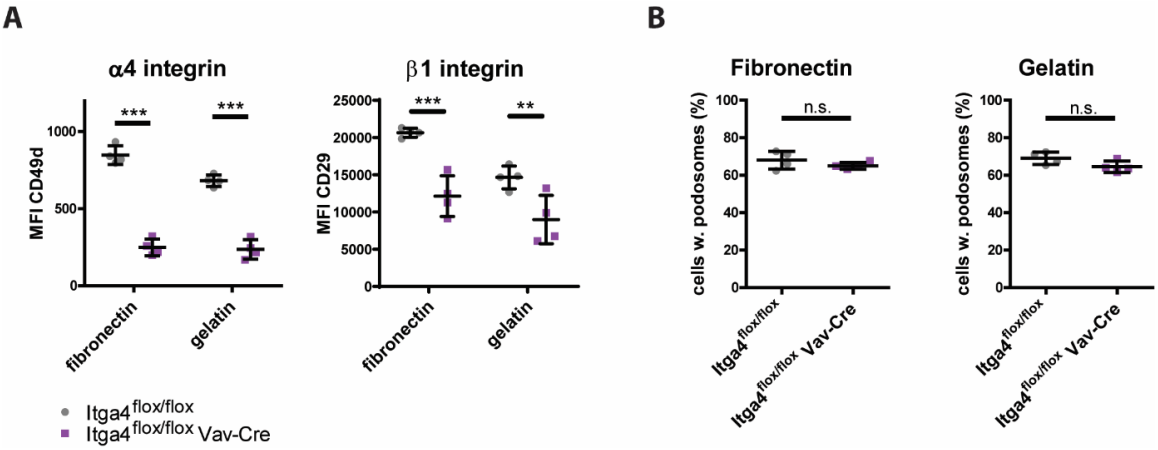

Figure 3.24 – α4 integrins are not required for podosome formation in iDCs
iDCs generated from Itga4$^{flox/flox}$ Vav-Cre mice have reduced levels of α4 and β1 integrin (**A**), but normal podosome formation capacity on FN or gelatin (**B**). (Statistics: 2way ANOVA with Bonferroni's multiple comparison test or Mann–Whitney test; error bars indicate mean +/- SD; n.s. (not significant); p>0.05; * p<0.05; ** p<0.01; *** p<0.001)

The involvement of α5β1 integrins in podosome formation on gelatin was unexpected considering the classical binding specificity of α5β1 integrins and also statistically not as clear as on FN. Therefore, it is possible that another β1 integrin is more relevant for podosome formation on gelatin. α1β1 integrins are the only classical collagen receptor expressed by iDCs and as the full-KO of α1 integrin in mice has no critical phenotype[155], we could use bone marrow from Itga1 KO mice (a kind gift of Prof. Ambra Pozzi at Vanderbilt University, Nashville, USA) to analyze podosome formation. As shown in figure **3.25 A**, the loss of α1 integrin also resulted in a mild reduction of β1 integrin surface levels, while again expression of other integrins did not change (data not shown). Culturing of Itga1$^{KO/KO}$ iDCs on FN, gelatin, collagen I or collagen IV, however, did not result in differences in podosome formation in comparison to wt controls (figure **3.25 B**). Consequently, α1 integrin is dispensable for podosome formation by wt iDCs.

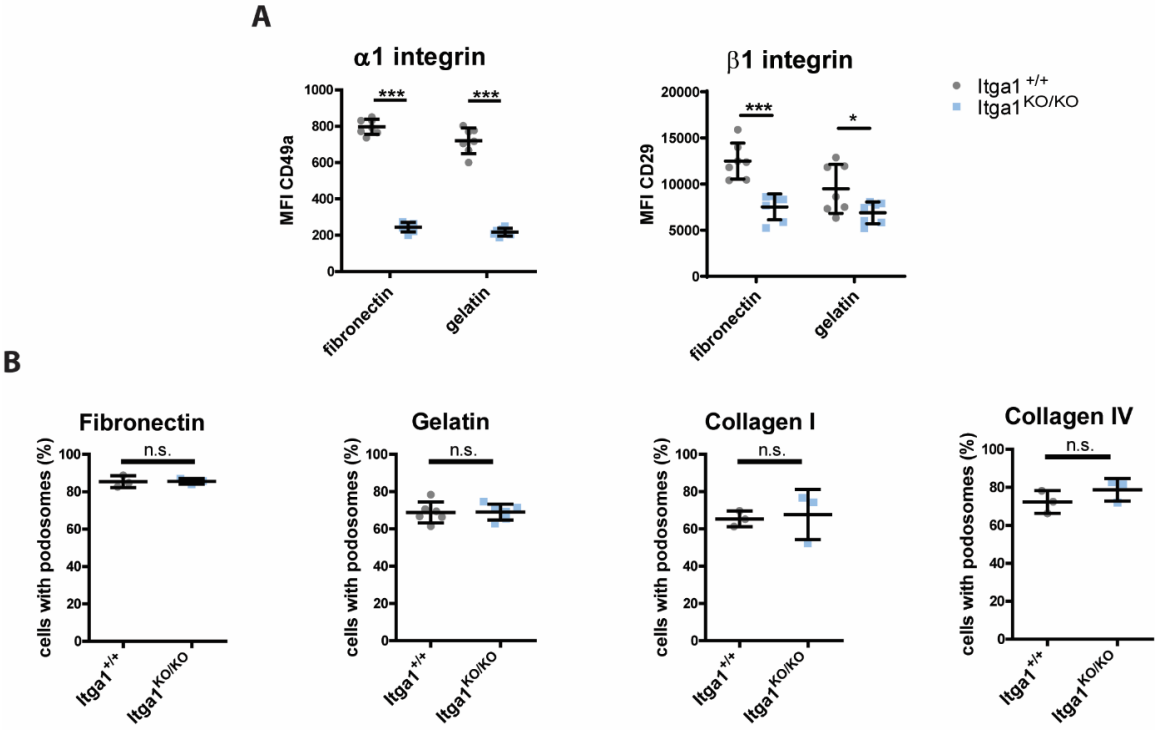

Figure 3.25 – α1 integrins are dispensable for podosome formation in iDCs
iDCs were generated from Itga1 KO mice. (**A**) KO of α1 integrins in iDCs reduces both α1 and β1 integrin levels. (Statistics: 2way ANOVA with Bonferroni's multiple comparison test) (**B**) Podosome formation on FN, gelatin, collagen I or collagen IV is not affected by loss of α1 integrin. (Statistics: Mann –Whitney test; error bars indicate mean +/- SD; n.s. (not significant); *** p<0.001)

To examine whether an interaction of Cyth2 with α1 integrin (signaling) is required for podosome formation, we knocked down Cyth2 in Itga1 KO iDCs using two different siRNAs. Kd efficiency was determined by western blot and yielded almost complete loss of Cyth2 (figure **3.26 A**). Of note, treatment with Cyth2 siRNA #2 also had effects on the very similar Cyth3 protein, but Cyth1 and Cyth4 were not affected and siRNA #1 was entirely specific for Cyth2 (figure **3.26 B**). As illustrated

in figure **3.26 C**, podosome formation on FN was reduced by kd of Cyth2 in wt cells, which is in line with our data from the Cyth2 KO iDCs. Itga1 KO iDCs, however, did not behave differently than wt cells after kd of Cyth2 on FN (figure **3.26 D**). Therefore, α1 integrins are clearly not involved in Cyth2-mediated regulation of podosomes on FN.

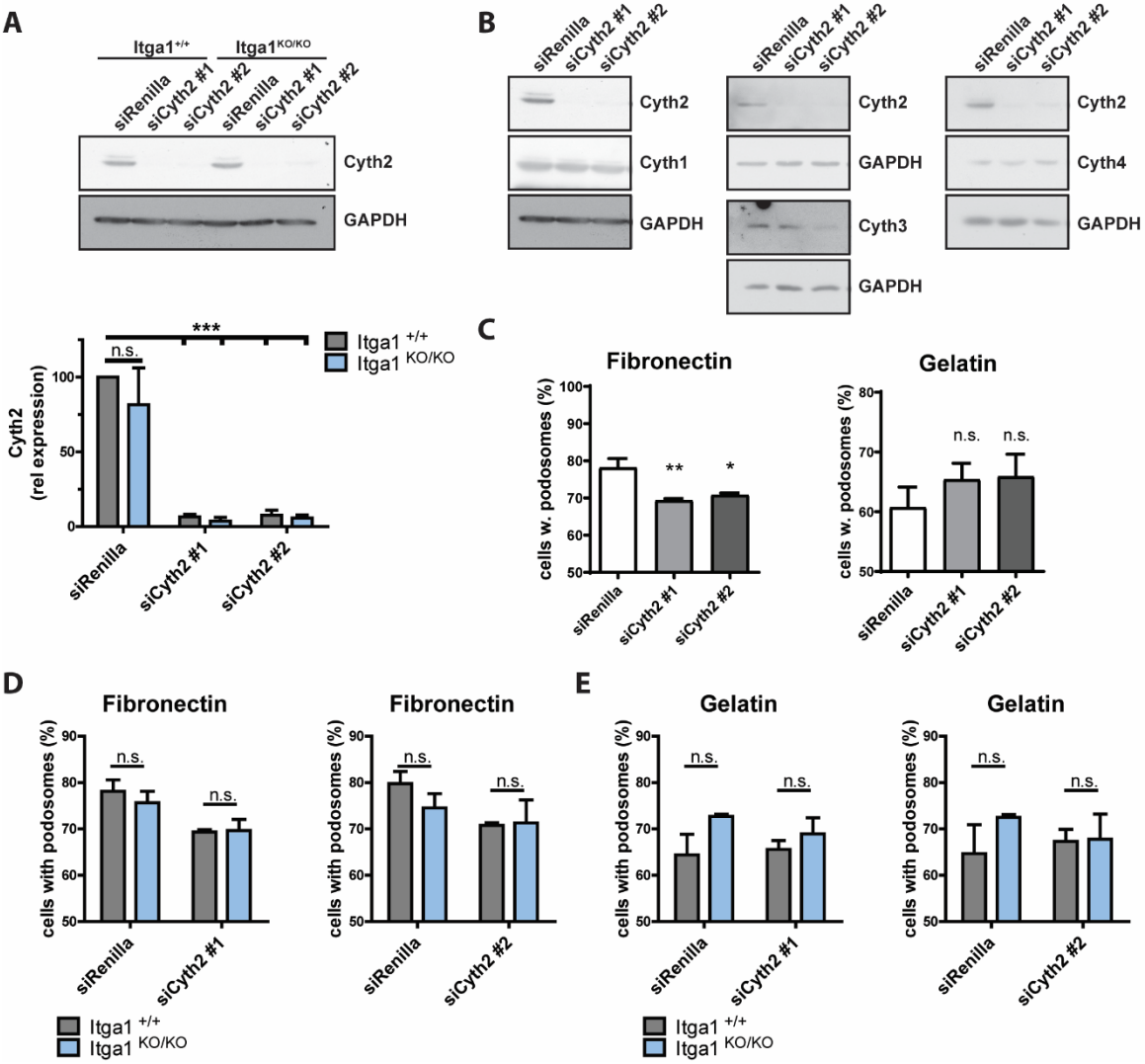

Figure 3.26 – Additional loss of α1 integrin does not alter Cyth2-dependent podosome formation
Kd of Cyth2 results in strong reduction of Cyth2 protein expression in both wt and α1 integrin KO iDCs (Statistics: Mixed-effect analysis with Bonferroni's multiple comparison test) (**A**). The effect of both siCyth2 siRNAs on other cytohesins was assessed (**B**). Quantification of podosome formation by wt iDCs after kd of Cyth2 on either FN or gelatin (statistics: 1way ANOVA with Bonferroni's multiple comparison test) (**C**) Quantification of podosome formation on FN (**D**) or gelatin (**E**) after Cyth2 kd in wt or α1 integrin KO iDCs. (Statistics: 2way ANOVA with Bonferroni's multiple comparison test; Error bars indicate mean +/- SEM; n.s. (not significant) p>0.05; * p<0.05; ** p<0.01; *** p<0.001)

Kd of Cyth2 in wt cells cultured on gelatin resulted in a moderate increase of podosome formation compared to control, which was statistically not significant (figure **3.26 C**) but showed the same tendency as the Cyth2 KO in iDCs. Additional KO of α1 integrin did not change that behavior in

terms of podosome formation (figure **3.26 E**). Therefore, we conclude that α1 integrins are also not involved in formation of podosomes and their regulation via Cyth2 in iDCs on gelatin.

In the end, our analysis of all major integrins in iDCs points to specific matrix receptors that seem to be responsible for the differential regulation of podosome formation on FN and gelatin. While α5β1 integrin is essential for mediating the Cyth2 KO-induced reduction of podosomes on FN, this particular integrin plays a very different role on gelatin. Here, in contrast, loss of α5β1 integrin does not alter the response of Cyth2 KO cells and might even mimic the effects of a Cyth2 KO in wt cells. Moreover, potential influences from additional receptors (e.g. αxβ2 integrin) further hint at fundamental differences in cell adhesion processes on these two substrates.

3.4. Cyth2 affects Rho GTPase activation downstream of integrins

Until now, we have found an integrin ligand-specific regulation of podosome formation by Cyth2 that we can attribute to $\alpha5\beta1$ integrin. However, neither general expression nor trafficking of this integrin is altered in Cyth2 KO iDCs. Therefore, we next analyzed if the integrin-dependent effects on podosome formation could also be mediated via differences in integrin activation and/or signaling events downstream of integrins. As described above, integrin activation affects several signaling pathways, including PI3K/Akt, ERK and JNK signaling as well as regulation of Rho GTPases.

3.4.1. Phosphorylation downstream of integrins is unaltered in Cyth2 KO iDCs

Phosphorylation of key signaling molecules is one of the first events happening upon integrin activation. The FAK homolog Pyk2 is expressed in iDCs and is autophosphorylated at Tyr402 in response to integrin activation, which facilitates further phosphorylation of Pyk2 by Src kinases and recruitment and phosphorylation of other adhesome components, including paxillin.[177] Moreover, Pyk2 has been implicated in podosome biology especially in osteoclasts[178,179].

In a first set of experiments we employed again the controlled integrin adhesion protocol by keeping cells in suspension and then seeding them onto coated surfaces. As figure **3.27** shows, phosphorylation of Pyk2 at Tyr402 indeed increases upon integrin stimulation on both FN and gelatin, but there was no difference between wt and Cyth2 KO iDCs. Also Tyr118-phosphorylation of paxillin, which is a known binding partner of Cyth2[137] and involved in podosome formation[180,181], was induced upon adhesion but not significantly different in the presence or absence of Cyth2. We further looked at localization of paxillin and found it at podosome rings of iDCs, but there were no obvious changes to localization of paxillin on FN vs gelatin or in wt vs Cyth2 KO cells (figure **3.28**).

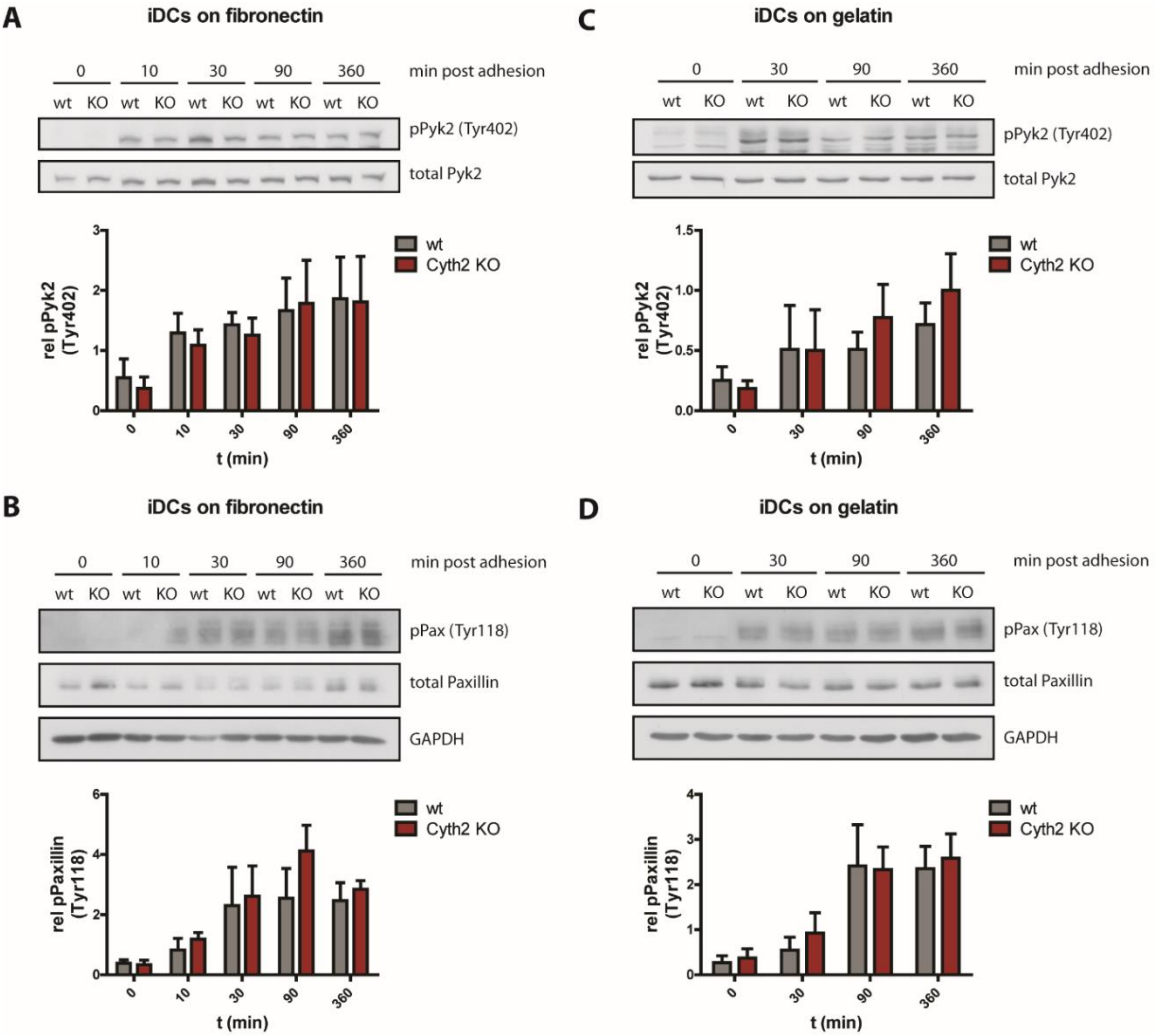

Figure 3.27 – Cyth2 does not influence general activation of integrin signaling upon adhesion

Phosphorylation of Pyk2 and paxillin in wt and Cyth2 KO iDCs upon adhesion onto FN or gelatin was assessed by western blot. (**A**) Phosphorylation of Pyk2 on FN and quantification of 4-6 independent experiments. (**B**) Phosphorylation of paxillin on FN and quantification of 3-4 independent experiments. (**C**) Phosphorylation of Pyk2 on gelatin and quantification of 3-5 independent experiments. (**D**) Phosphorylation of paxillin on gelatin and quantification of 3-5 independent experiments. Error bars indicate mean +/- SEM

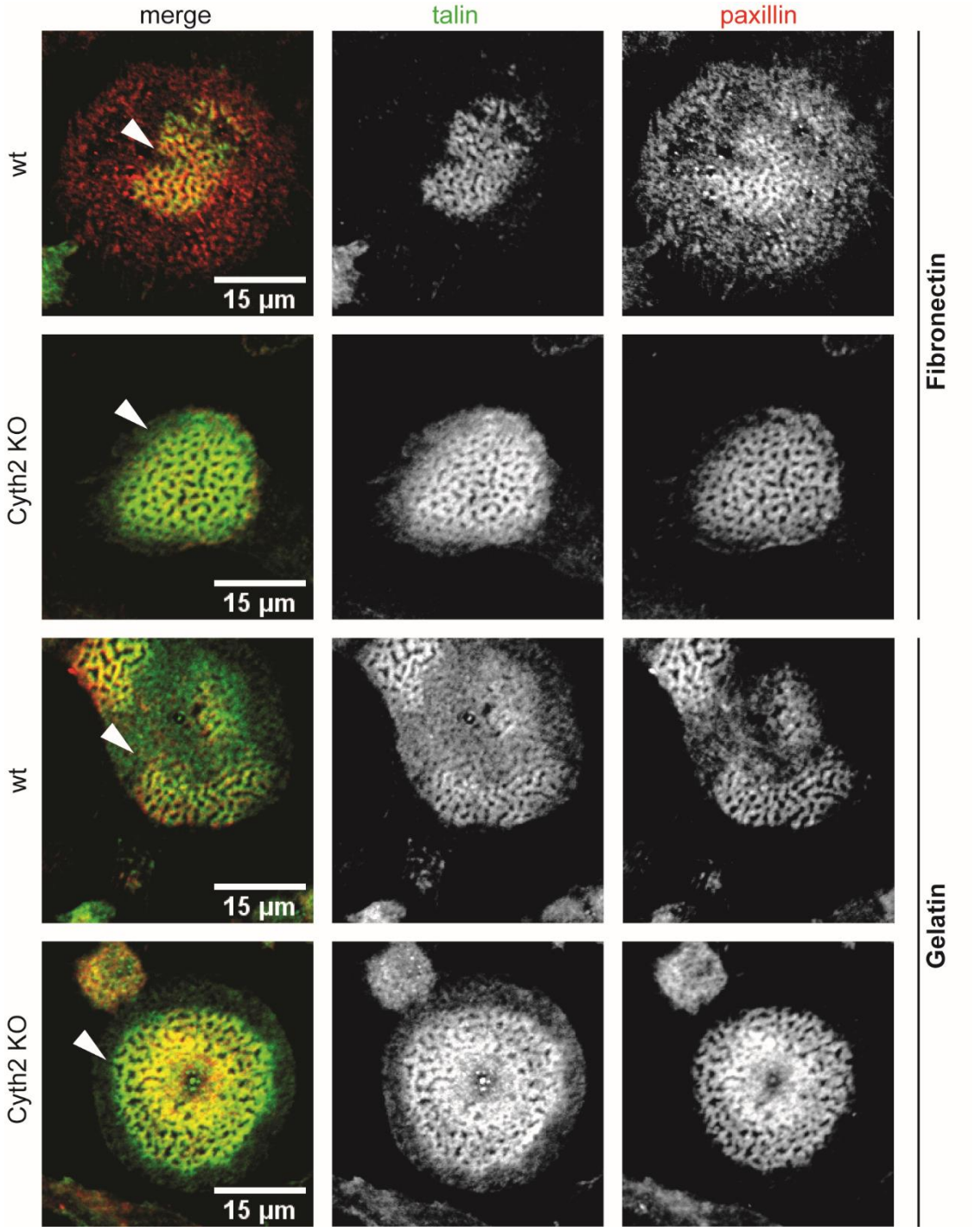

Figure 3.28 – Localization of paxillin to podosome rings

Confocal images of wt and Cyth2 KO iDCs that were cultured on FN or gelatin and stained for talin and paxillin. Arrows indicate podosome clusters. Scale bar represents 15 µm

Further downstream of integrin activation, several signaling pathways are initiated that are characterized by a cascade of phosphorylation events. Therefore, we analyzed phosphorylation of Akt (Ser473) and ERK1/2 (Thr202/Tyr204) upon adhesion to either FN or gelatin (figure **3.29**). Both proteins are increasingly phosphorylated after integrin activation, but again Cyth2 deficient cells did not behave differently compared to control cells. Nevertheless, cells adhering to gelatin

showed again a delayed response especially in terms of paxillin- and ERK-phosphorylation compared to cells on FN.

Considering that quantification of podosome formation usually took place after an o.n. incubation of iDCs on FN or gelatin, we also checked protein phosphorylation at similar, i.e. later, time points (figure **3.30**). However, neither proximal phosphorylation events on Pyk2, Src kinase or paxillin, nor more distal activation of Akt or ERK were altered in iDCs lacking Cyth2 on FN or gelatin.

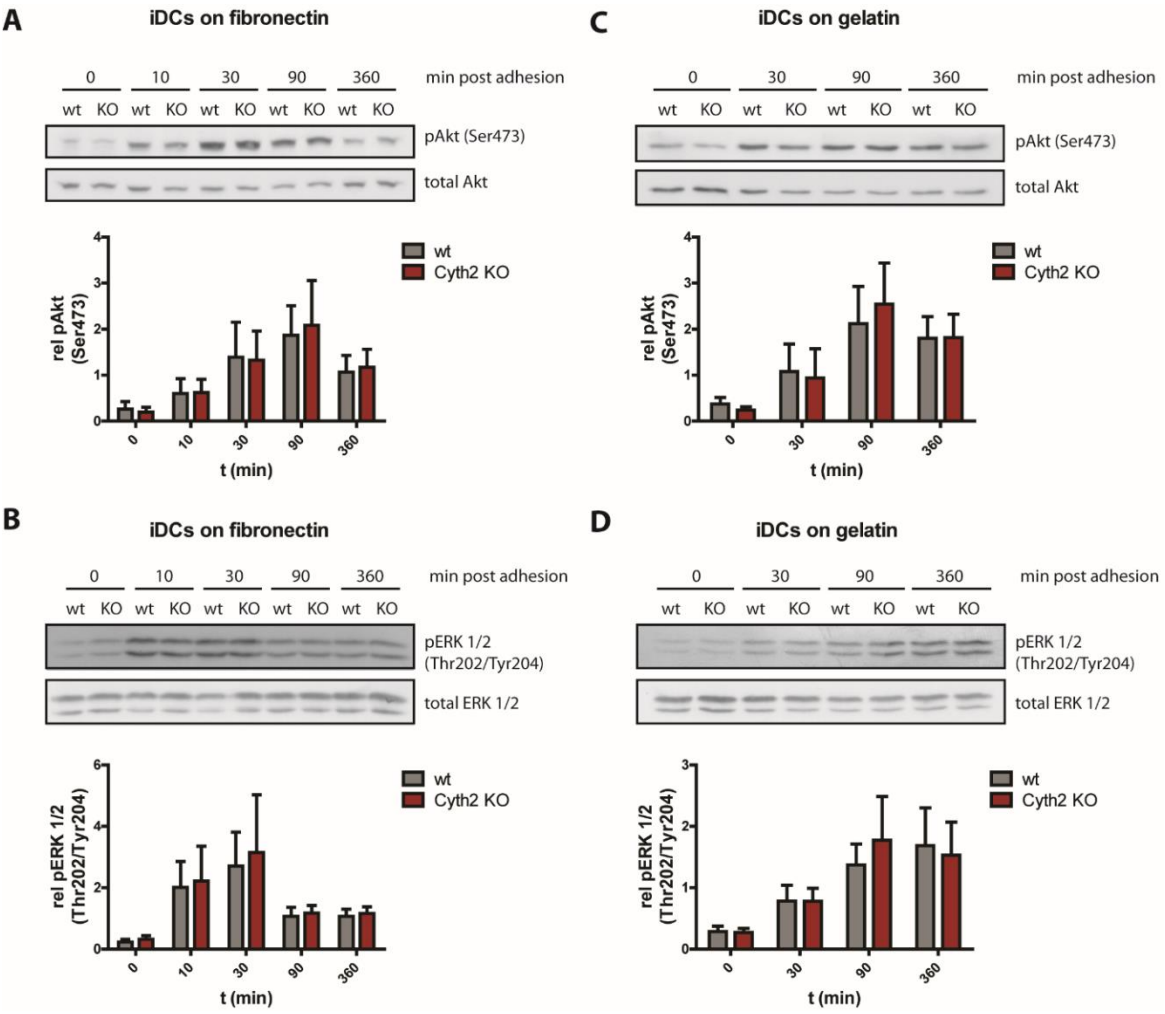

Figure 3.29 – Cyth2 does not influence activation of Akt or ERK signaling pathways upon adhesion

Phosphorylation of Akt and ERK1/2 in wt and Cyth2 KO iDCs upon adhesion onto FN or gelatin was assessed by western blot. (**A**) Phosphorylation of Akt on FN and quantification of 4-6 independent experiments. (**B**) Phosphorylation of ERK1/2 on FN and quantification of 3-4 independent experiments. (**C**) Phosphorylation of Akt on gelatin and quantification of 3-5 independent experiments. (**D**) Phosphorylation of ERK1/2 on gelatin and quantification of 3-5 independent experiments. (Error bars indicate mean +/- SEM)

Taken together, phosphorylation of key signaling components downstream of integrins is not affected by Cyth2 indicating that general integrin activation is not majorly different in Cyth2 KO

iDCs compared to control cells. Furthermore, specific signaling pathways via Akt and ERK do not seem to be involved in regulation of podosome formation by Cyth2.

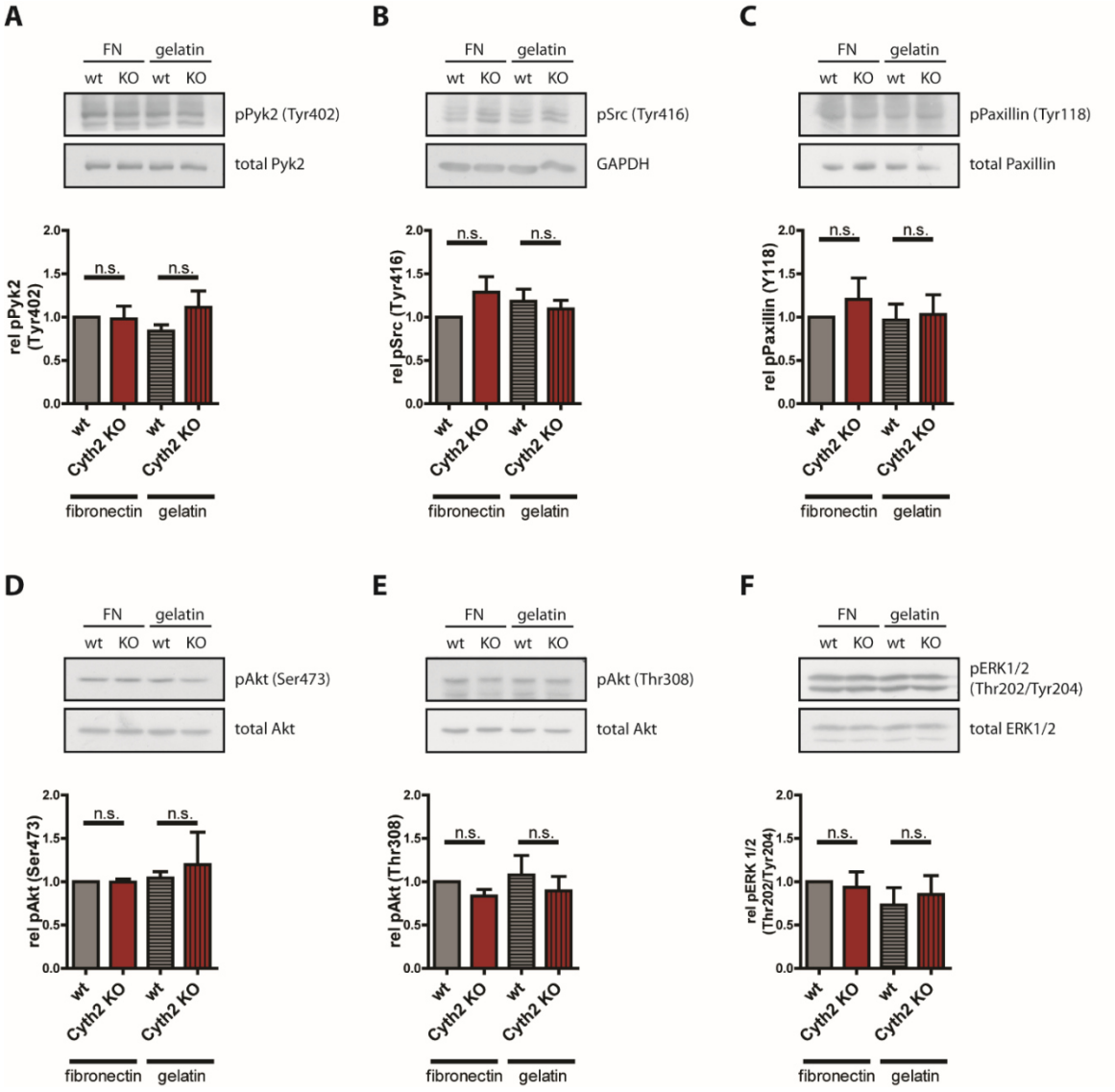

Figure 3.30 – Steady state phosphorylation of integrin signaling components is not affected by Cyth2
Wt and Cyth2 KO iDCs were cultured o.n. on FN or gelatin and analyzed for protein phosphorylation by western blot. (**A, B, C**) Phosphorylation of Pyk2, Src and Paxillin was quantified based on 6 independent experiments. (**D, E, F**) Phosphorylation of Akt and ERK was quantified based on 3 independent experiments. (Statistics: 2way ANOVA with Dunnett's multiple comparison test. Error bars indicate mean +/- SEM; n.s. (not significant) p>0.05)

3.4.2. Activation of RhoA is differentially regulated on different matrices

Apart from activation of general signaling pathways via Akt and ERK, integrin signaling also affects Rho GTPases. These GTPases are major regulators of the actin cytoskeleton and have been implicated in podosome biology in various cell types.[182] Among the different Rho GTPases, especially RhoA has gained a lot of attention in regulation of podosome formation[183–187] and Rafiq and colleagues have placed RhoA downstream of Cyth2 in podosome formation by THP-1 cells[118].

For that reason, we analyzed RhoA activation in iDCs that were cultured on either FN or gelatin. As illustrated in figure **3.31**, RhoA activity was indeed differentially regulated by Cyth2. On FN, loss of Cyth2 led to a significant reduction of RhoA activation compared to wt, whereas this effect was not present on gelatin. On the contrary, levels of active RhoA on gelatin were slightly increased, when Cyth2 was absent. These results indicate, that the differences we observed in podosome formation by Cyth2 KO vs wt cells might be caused by differential activation of RhoA on either FN or gelatin.

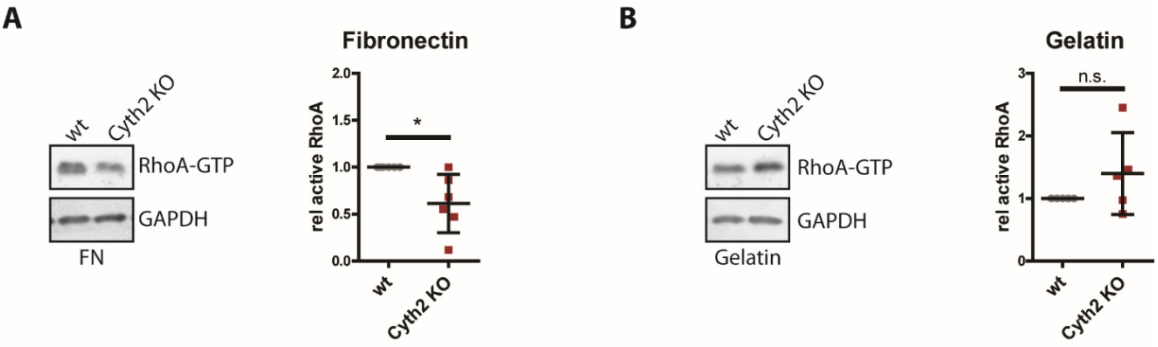

Figure 3.31 – RhoA activity is differentially regulated by Cyth2 on different matrices
RhoA activation on FN (**A**) and gelatin (**B**) was assessed by pulldown assays. (Statistics: paired t-test; Error bars represent mean +/- SD; n.s. (not significant) $p>0.05$; * $p<0.05$)

To verify this hypothesis, we blocked RhoA activity in wt cells with the Rho-specific inhibitor Rhosin[188], which led to a clear reduction of GTP-bound RhoA levels (figure **3.32 A**). This inhibition of Rho significantly decreased podosome frequencies on both FN and gelatin (figure **3.32 B+C**) showing that RhoA is indeed a positive regulator of podosome formation in iDCs.

These results indicate that the Cyth2-dependent effects on podosome formation are mediated via the small GTPase RhoA. As RhoA activity supports podosome formation in iDCs, a reduced activation of RhoA on FN leads to decreased podosome numbers. On gelatin, however, slightly elevated RhoA activation also increases podosome formation. Therefore, the differential regulation of podosome formation on FN and gelatin by Cyth2 seems to be executed via respective modifications of RhoA activity.

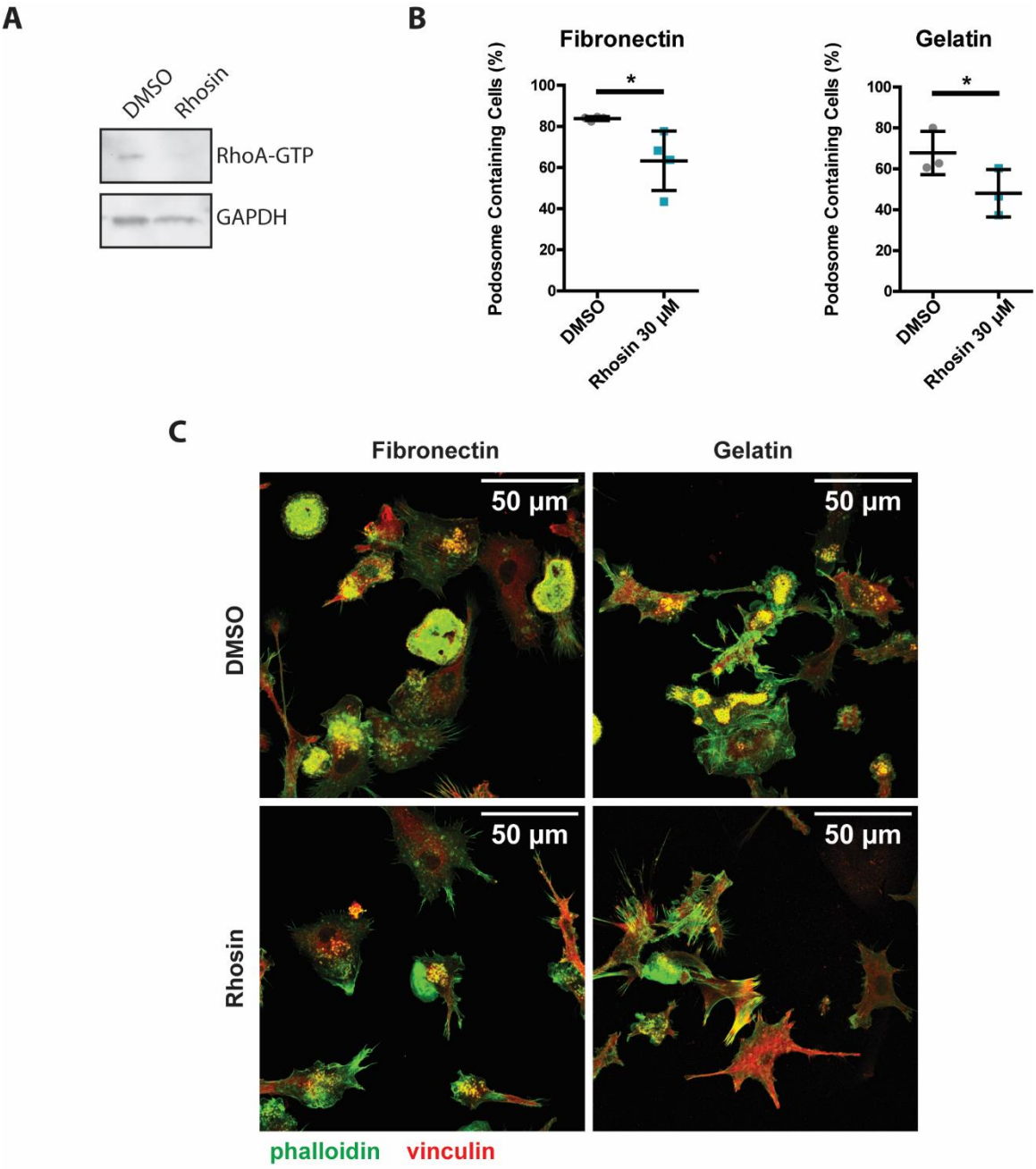

Figure 3.32 – RhoA activation is required for complete podosome formation by iDCs
Inhibition of RhoA activation by Rhosin (30 µM) leads to reduced RhoA activity (**A**) and reduction of podosome formation on FN and gelatin (**B+C**). Scale bar represent 50 µm. (Statistics: t-test; Error bars represent mean +/- SD; * $p<0.05$)

3.4.3. Activity of Arf1 and Arf6 is unaltered in Cyth2 KO iDCs

The main function of cytohesins is the activation of Arf GTPases and podosome formation in THP-1 cells has been shown to be regulated via the Cyth2-Arf1-RhoA axis[118]. In order to study the involvement of Arf GTPases in Cyth2-mediated regulation of podosome formation by iDCs, we assessed activation levels or Arf1 and Arf6 in wt and Cyth2 KO iDCs on different matrices. However, we could not observe any differences in Arf1 or Arf6 activity between wt and KO cells on FN or gelatin (figure **3.33**). These results suggest that neither Arf1 nor Arf6 is involved in Cyth2-dependent podosome formation in iDCs.

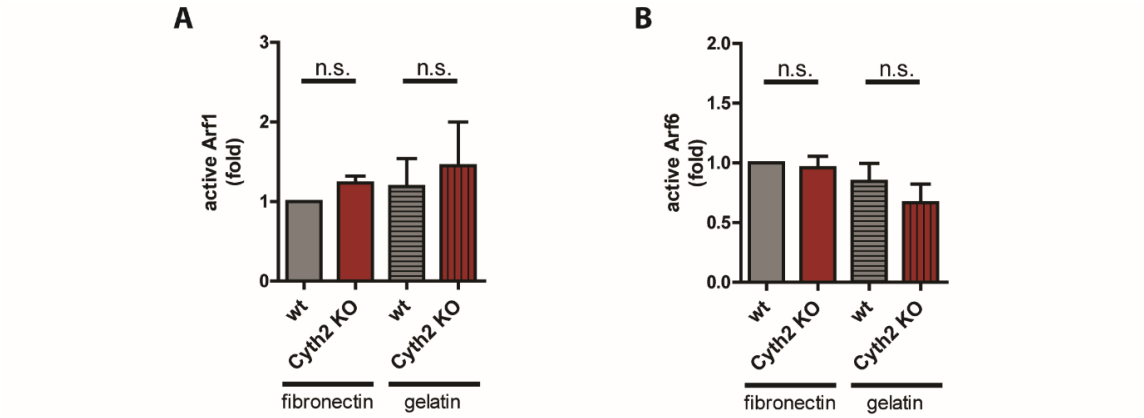

Figure 3.33 – Arf Activation is not different in Cyth2 KO iDCs
Wt and Cyth2 KO iDCs cultured on either FN or gelatin were subjected to G-LISAs for Arf1 (**A**) or Arf6 (**B**). Graphs show mean of 3 independent experiments. (Statistics: 2way ANOVA with Dunnett's multiple comparison test. Error bars represent mean +/- SD; n.s. (not significant) p>0.05)

All in all, our data show that Cyth2 affects podosome formation on specific ECM proteins by altering activation of RhoA. These processes are governed by differential signaling inputs from specific integrins on either FN or gelatin, but do not seem to involve Arf1 or Arf6 GTPases.

3.5. Regulation of podosome formation in iDCs depends on the 2G-isoform of Cyth2

Cytohesins do not only have tissue-specific expression patterns but they can also occur in two distinct isoforms that localize differently within the cell and can have different functional roles[108,189]. As podosomes are locally occurring structures that are in addition known to involve PI3K signaling, we wondered whether the expression of Cyth2 in 2G or 3G isoform has any effect on podosome formation in iDCs.

To answer that question, we first determined the identity of wt Cyth2 in iDCs by sequencing cDNA derived from wt cells. As figure **3.34 A** shows, Cyth2 is expressed predominantly in the 2G isoform, which is known to prefer PIP_3 and might therefore facilitate recruitment and action of Cyth2 at defined cellular locations. To examine whether Cyth2-2G expression is also functionally important for the regulatory role of Cyth2 in podosome formation, we performed rescue experiments in Cyth2 KO cells.

Since iDCs do not tolerate transfection with DNA plasmids, we performed mRNA transfection instead, which results in weaker and rather short-lived protein expression compared to DNA transfections (data not shown). GFP-tagged Cyth2 constructs containing either 2G or 3G stretches in their PH domains were introduced into Cyth2 deficient iDCs. As controls, we transfected both wt and Cyth2 KO cells with a GFP construct. Directly after transfection, cells were seeded onto FN or gelatin and analyzed for Cyth2 expression and podosome formation after 6 h. Transfection of both Cyth2 constructs resulted in robust expression on protein level that was roughly 5fold stronger than endogenous Cyth2 expression (figure **3.34 B**). Podosome frequencies on FN showed the expected difference between wt and Cyth2 KO GFP controls, but re-expression of Cyth2-2G in Cyth2 deficient cells increased podosome formation even above wt levels (figure **3.34 C**). Cyth2-3G, however, was not able to rescue the loss of Cyth2. Similar effects were visible on gelatin: Only Cyth2-2G could reduce podosome frequencies to wt levels, while cells transfected with Cyth2-3G displayed similar values to Cyth2 KO cells transfected with GFP only (figure **3.34 C**). In conclusion, Cyth2 isoforms are functionally different and the regulation of podosome formation on FN and gelatin is only mediated by Cyth2-2G.

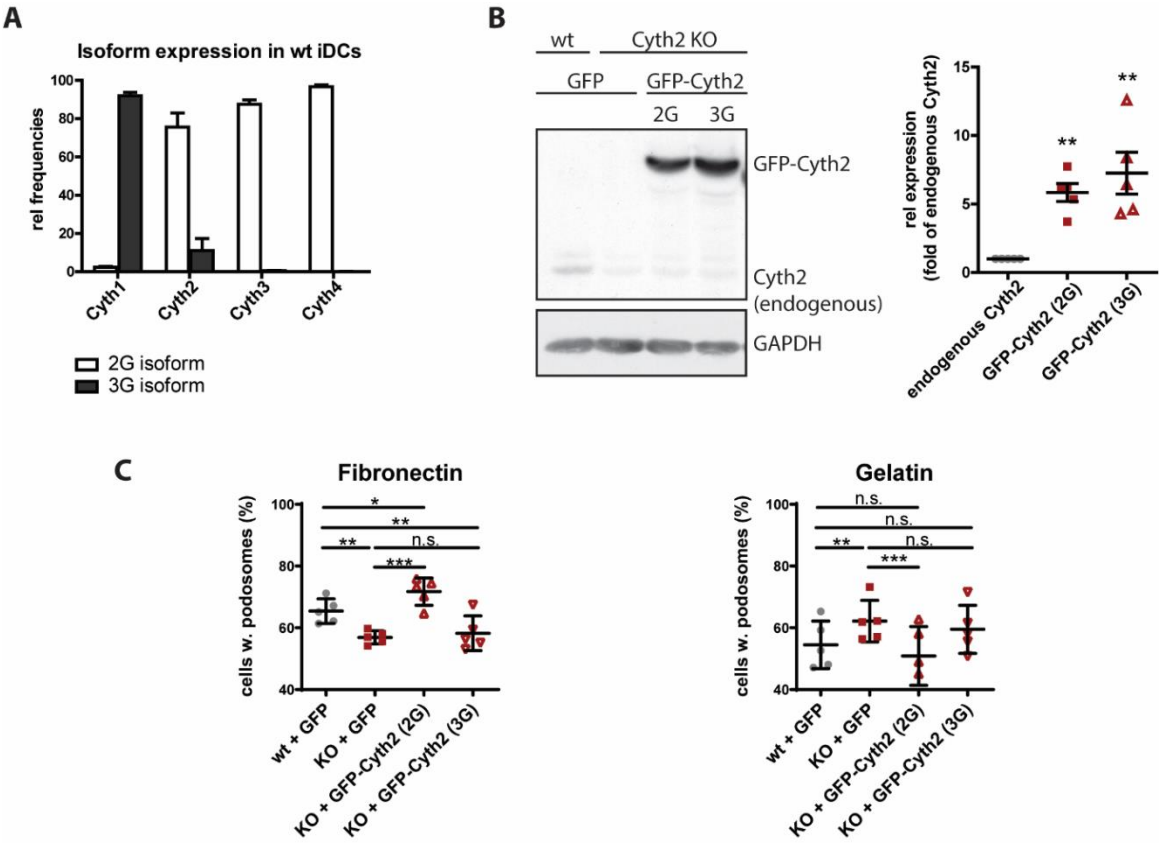

Figure 3.34 – Regulation of podosome formation depends on Cyth2-2G isoform
(**A**) Relative frequencies of 2G and 3G isoforms of Cyth1-4 expressed in wt iDCs. (**B**) Expression of GFP-Cyth2-2G and GFP-Cyth2-3G in Cyth2 KO iDCs was verified and quantified by Western blotting. (**C**) Quantification of podosome formation on FN or gelatin after transfection of iDCs with GFP or GFP-Cyth2-2G/3G constructs. (Statistics: Repeated Measures ANOVA with Bonferroni's multiple comparison test; Error bars represent mean +/- SEM; n.s. (not significant) $p>0.05$; * $p<0.05$; ** $p<0.01$, *** $p<0.001$)

Furthermore, we also studied subcellular localization of the different Cyth2 isoforms, but as figure **3.35** shows, both constructs were distributed mostly uniformly in the cytoplasm sparing only podosome cores irrespective of the underlying coating material. This could be a result of the considerable overexpression or of the time point of analysis. Possibly, choosing earlier time points or studying the dynamics of Cyth2 constructs would make differences more apparent.

We have shown previously that Cyth2 is the only cytohesin that is involved in podosome formation by iDCs (figures **3.2** and **3.4**). As Cyth2 function in that context depends very much on the isoform expression, we wondered whether Cyth2 is the only cytohesin expressed in the 2G isoform and whether that might explain why loss of Cyth1, Cyth3 or Cyth4 does not affect podosomes. However, cDNA sequencing of the other cytohesins revealed that only Cyth1 occurs as 3G version, whereas both Cyth3 and Cyth4 are expressed almost completely in their 2G isoforms (figure **3.34 A**). The effects of Cyth2 on podosome formation are therefore specific for Cyth2 itself and are not

exclusively determined by phosphoinositol-phosphate preference. Nevertheless, expression of Cyth2 in the 2G isoform is necessary to mediate its role in podosome biology.

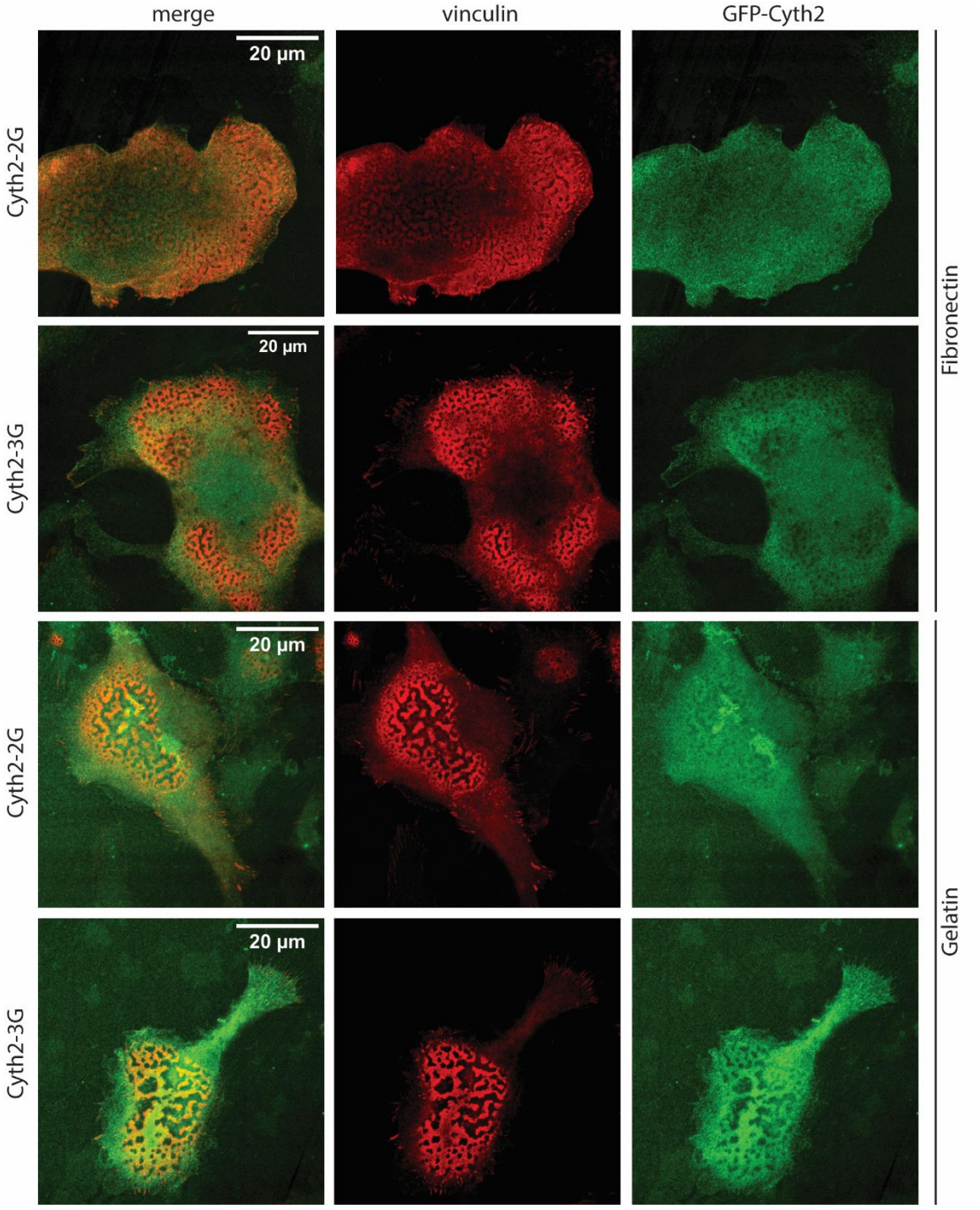

Figure 3.35 – Localization of Cyth2-2G and Cyth2-3G seems not to be different in iDCs
Confocal airyscan images of iDCs on FN and gelatin transfected with GFP-Cyth2-2G/3G and stained with antibodies against vinculin and GFP. Scale bar represent 20 µm.

3.6. The loss of Cyth2 has no immediate effect on myeloid cells *in vivo*

So far, we could show that Cyth2 regulates podosome formation by iDCs in an integrin- and RhoA-dependent manner but these studies have been performed in a simplified *in vitro* setting. It would, of course, be interesting to know whether this regulatory role of Cyth2 also has implications *in vivo*. As we have the LysM-Cre-driven KO mouse at hand, the relevance of Cyth2 for different myeloid cell populations could be analyzed.

3.6.1. Frequencies of myeloid cell populations in different organs is not altered in Cyth2 LysM-Cre mice

Overall, the Cyth2-LysM-Cre mice breed normally and do not show any signs of developmental defects. Since the LysM-driven KO targets myeloid cells, we had a closer look at these immune cell populations in different immunologically relevant organs, focusing especially on DCs. Conventional DCs (cDC) typically occur in two different subtypes, cDC1 and cDC2, which differ in surface marker expression and function. As cDCs in peripheral organs migrate towards draining lymph nodes (LN), these LNs contain both such migratory, as well as resident DC populations.[190]

As figure **3.36** shows, frequencies of neutrophils, monocytes, macrophages and different DC populations in inguinal lymph nodes, mesenteric lymph nodes, spleen or the lungs were not different in Cyth2$^{flox/flox}$ LysM-Cre mice compared to control animals. Also, quantification of neutrophil numbers in the blood or the bone marrow yielded no differences between Cyth2$^{flox/flox}$ LysM-Cre and cre-negative controls (figure **3.37**). Therefore, loss of Cyth2 seems to have no immediate effect on general frequencies of myeloid cells *in vivo*.

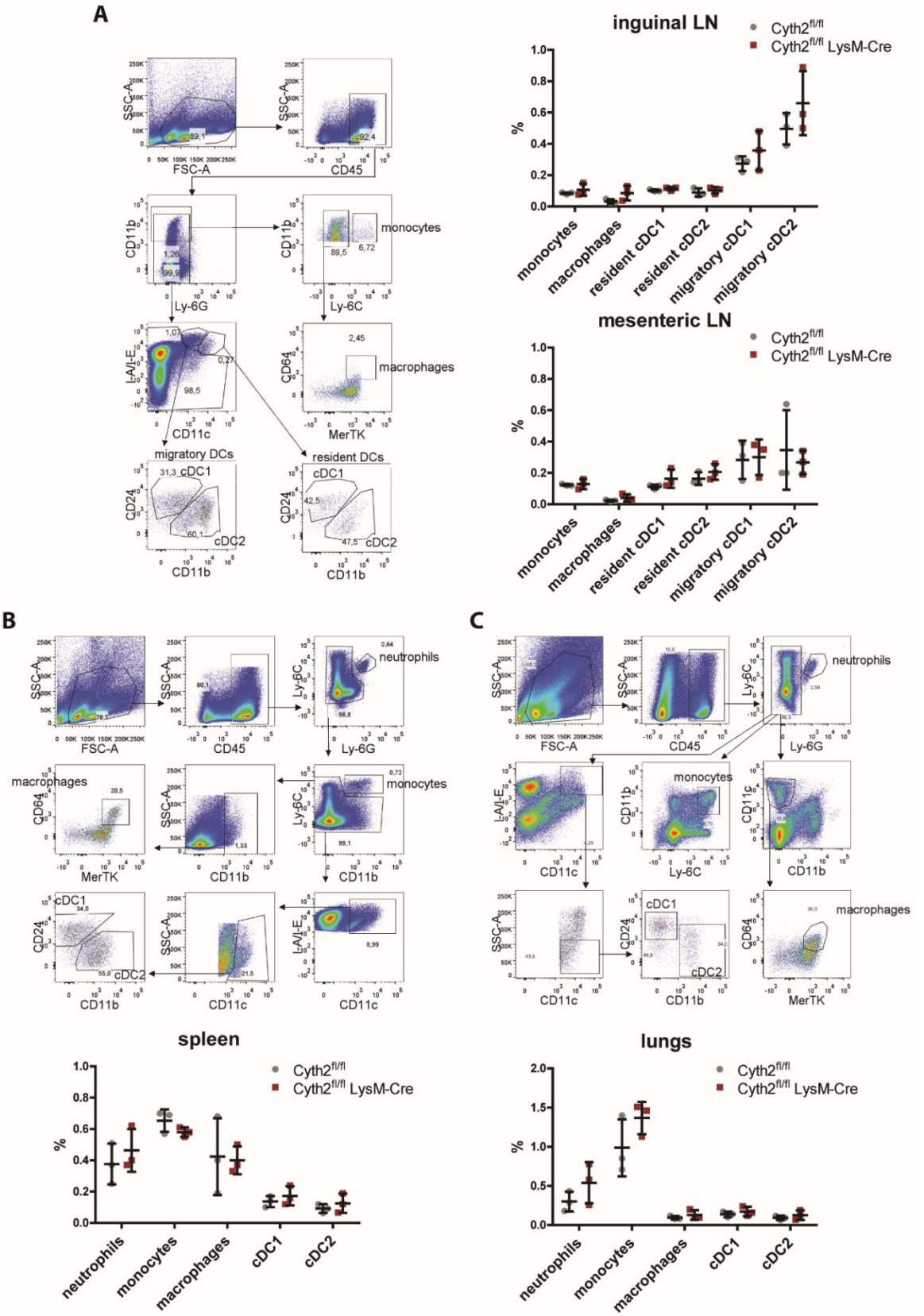

Figure 3.36 – Myeloid cell populations in LN, spleen and lungs are unaltered in Cyth2 KO iDCs

Cyth2flox/flox LysM-Cre and cre-negative control mice were analyzed for frequencies of different myeloid cell populations in inguinal and mesenteric LN (**A**), spleen (**B**) and lungs (**C**) using flow cytometry. Values represent % of live gate. (Error bars indicate mean +/- SD)

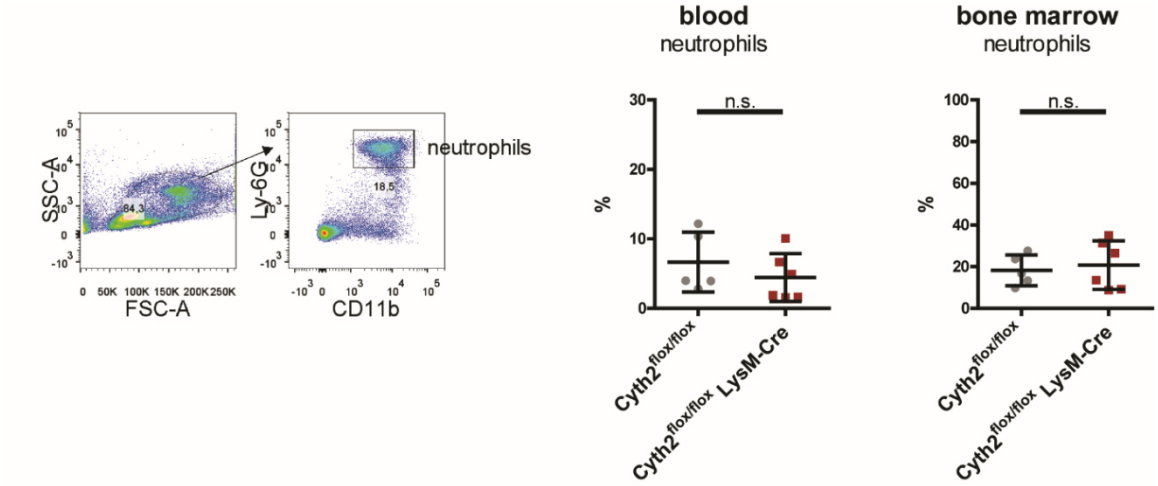

Figure 3.37 – Neutrophil numbers in blood and bone marrow are unchanged in Cyth2 KO iDCs
Cyth2flox/flox LysM-Cre and cre-negative control mice were analyzed for frequencies of neutrophils in blood and bone marrow samples using flow cytometry. Values represent % of live gate. (Statistics: Mann-Whitney test. Error bars indicate mean +/- SD; n.s. (not significant) p>0.05)

3.6.2. Osteoclasts of Cyth2 LysM-Cre mice function normally

While there have been studies dealing with the role of invadopodia during cancer cell metastasis[78,79], a physiological role of podosomes in immune cell function has not been clearly shown *in vivo*. There are reports of leukocytes forming podosome-like protrusion during extravasation[74], but the functional relevance of this observation is not clarified yet. Osteoclasts, however, have long been known to depend on podosomes and the related sealing zone for their degradative activity.[80–82] In contrast to osteoblasts, which synthesize new bone material, osteoclasts are responsible for degradation of bone. Both functions are equally important for bone homeostasis and dysregulation of either osteoblast or osteoclast activity manifests in altered bone structure and density.[191] As osteoclasts are part of the myeloid lineage, they are also targeted by a LysM-Cre-driven KO[192,193] and should be deficient for Cyth2 in our system.

In order to examine if loss of Cyth2 affects osteoclast function, we determined bone mineral density (BMD) of either Cyth2$^{flox/flox}$ LysM-Cre mice or cre-negative control animals (Cyth2$^{flox/flox}$). Together with the group of Prof. Christoph Bourauel at the Dental Clinic of Bonn University we performed µCT measurements and quantified BMD of trabecular bone within the femur (epiphysis and metaphysis) and in the skull (parietal bone and sphenoid bone). However, BMDs of Cyth2$^{flox/flox}$ LysM-Cre mice were not different from control mice (figure **3.38**), indicating that osteoclast function is not affected by loss of Cyth2.

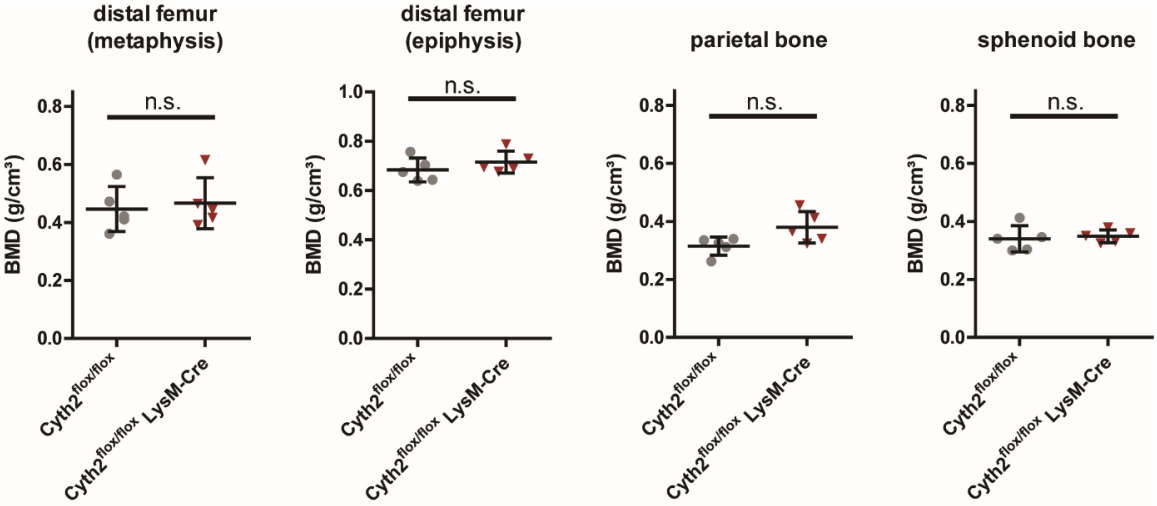

Figure 3.38 – Osteoclast activity is not affected by loss of Cyth2
BMD of femur and skull of Cyth2$^{flox/flox}$ LysM-Cre and cre-negative control mice was quantified using µCT. (Statistics: Mann Whitney Test. Error bars represent mean +/- SD; n.s. (not significant) p>0.05)

Overall, under steady state conditions Cyth2 LysM-Cre mice do not have any obvious phenotype that could be correlated with the effects we see on podosome formation *in vitro*. It is possible, though, that the integrin-specific regulation of podosome formation by Cyth2 becomes more relevant under pathological conditions.

4. Discussion

For this study we asked whether cytohesins are involved in the integrin-related regulation of actin dynamics, specifically podosome formation. Using BMDCs from several cytohesin KO mice, we could show that only Cyth2 plays a role in podosome formation and that this role is relevant, when cells are cultured on FN or gelatin (or collagen IV), but not on Icam-1 or fibrinogen. Interestingly, the effect of Cyth2 on podosomes differs between FN and gelatin. While Cyth2 is required for full podosome formation on FN, it acts inhibitory on podosomes in a gelatin or collagen IV environment. This differential regulation of podosome formation is mediated via RhoA activation and involves specifically $\alpha5\beta1$ integrins.

4.1. Cyth2 action in podosome formation is matrix- and integrin-specific

The importance of Cyth2 for podosome formation has been shown before by Rafiq and colleagues, who knocked down Cyth2 with siRNAs in the human monocyte-like cell line THP-1[118]. They observed a strong reduction of podosome numbers upon kd of Cyth2, which is supported by our data from iDCs cultured on FN. Indeed, Rafiq and colleagues used specifically FN as coating substrate. However, we could extend our understanding of the role of Cyth2 in podosome biology by showing that the positive regulation of podosome formation by Cyth2 is actually restricted to a FN-rich environment. On other substrates, though, Cyth2 deficient cells either behave entirely like wt controls (on fibrinogen or Icam-1) or they respond the opposite way and even increase their podosome numbers (on gelatin or collagen).

The observation that the composition of the ECM influences cellular signaling and behavior is well-known and there are several reports showing that stimulating cells with different matrix proteins induces differences in protein phosphorylation[178,194] or in adhesion behavior[62,195]. We have also observed that adhesion kinetics, cell spreading and general formation of adhesion structures, as well as phosphorylation of key signaling molecules, varies with the underlying coating material. These particular responses are often caused by involvement of specific integrins and the list of publications dealing with binding and signaling variations between different integrin classes is extensive[42–46,196–198].

Our data indicate that the Cyth2-dependent responses to FN and gelatin depend on differential involvement of $\alpha5\beta1$ integrins. While wt cells on FN apparently do not need $\alpha5\beta1$ integrin to form podosomes, the presence of $\alpha5\beta1$ integrins is essential for the reduction of podosome numbers

in Cyth2 KO cells. On gelatin, though, the KO of Cyth2 induces an increased podosome formation, which is not affected by additional loss of α5β1 integrin. In contrast, wt cells lacking β1 integrin even showed similarly elevated podosome levels on gelatin, which was reproducible by tendency using siRNAs targeting Itga5. The role of Cyth2 is therefore diametrically opposed on the two substrates: On FN it seems to act inhibitory on α5β1 integrin signaling to podosomes, whereas Cyth2 on gelatin might be located in the same pathway as α5β1 integrin and removal of either factor has the same effect on podosome formation. Therefore, Cyth2 is not a general regulator of podosome formation but controls subtle differences in integrin signaling.

In general, β1 integrins are found in invadosomes of several cell types[199–201] and they can play very fundamental roles in invadosome formation and stability. While in some studies β1 integrins are required for and promote formation of invadopodia[202–205], these integrins have also been shown to act inhibitory[206]. In other publications using immature monocyte-derived DCs or osteoclasts β1 integrins even appear to be negligible for podosome formation.[83,200] This might indicate intricate differences between podosomes and invadopodia or simply reflect cell type-specific characteristics. Consistent with that, the equipment of a cell with specific integrins might affect how important β1 integrins actually are. In both osteoclasts and DCs, whose podosomes seemed to be independent of β1 integrin signaling, β1 integrin is not the major integrin expressed, but is accompanied by high levels of β3 integrins and/or β2 integrins. These could compensate for a loss of β1 integrin in maintaining podosome structures. In line with this thought, we and others[77] could show that KO of β2 integrins has equally strong effects on podosome formation in iDCs. Similarly, osteoclasts need at least 2 of their 3 major integrin classes to maintain podosomes.[83]

Interestingly, the experiments showing a dependence on β1 integrins for invadopodia formation were conducted on gelatin, whereas the osteoclast and DC data were generated on FCS-coated surfaces and a mixture of FN and gelatin, respectively. However, considering that we observed the opposite (i.e. an inhibition of podosome formation by β1 integrins) on gelatin, these differences are most likely not exclusively explainable by differential matrix sensing. Unfortunately, a direct comparison between our data and the before-mentioned studies using myeloid cells (osteoclasts and DCs) in terms of matrix effects is difficult, because van Helden and colleagues coated with a mixture of FN and gelatin and the FCS used for the experiments with osteoclasts contains numerous proteins, including FN and fibrinogen[207,208]. Nevertheless, the role of β1 integrin in podosome formation seems to be complex and very much dependent on cell type and experimental procedures.

4.2. α5β1 integrins can mediate gelatin-dependent effects

The contribution of α5β1 integrins to podosome formation in a FN-environment is not unexpected, as FN is the classical ligand for α5β1 integrins[11]. Gelatin, however, is not described to be bound by this particular integrin. As gelatin is hydrolyzed collagen[169], it is most likely recognized by cellular collagen receptors. In iDCs, such collagen-specific integrins are either α1β1 or αxβ2 integrins. Moreover, in Cyth2 KO iDCs we also see an increase in podosome frequencies on collagen IV and at least in tendency on collagen I, which is in line with the data on gelatin and further strengthens the idea that gelatin is bound by collagen receptors.

4.2.1. Potential receptors for gelatin in iDCs and their role in podosome formation

α1β1 integrin is a classical collagen receptor, which has a higher affinity for collagen IV than collagen I.[209] Vice versa, collagen I is the preferred ligand of α2β1 integrin[209], which is not found in iDCs. This could explain why general iDC adhesion and spreading on collagen IV is better than on collagen I (figure **3.9**) and might also explain why the effect of Cyth2 on podosome formation is stronger on collagen IV. However, in our experiments even α1 integrin is expressed at relatively low levels and α1 integrin KO cells adhere normally onto both collagen I and collagen IV. Moreover, we have extensively analyzed the potential contribution of α1 integrin to the Cyth2-mediated effect on podosome formation but have not found any sign of a functional involvement. Therefore, α1β1 integrin is most likely not responsible for recognizing gelatin and mediating Cyth2-dependent effects in iDCs.

αxβ2 integrin is the highest expressed integrin in iDCs and the αx integrin chain (also called CD11c) is the prototype of a DC-specific antigen[210]. However, in comparison to αL or αM, the αx integrin is only poorly characterized, especially in terms of collagen-binding. A study by Garnotel and colleagues showed that αx integrin mediates adhesion of monocytes to collagen I[176] and it was published that αx integrin can bind to denatured proteins[211]. Therefore, gelatin could indeed be a ligand of αxβ2 integrin. Our kd experiments of Itgax on gelatin seemed promising, because treatment with one siRNA altered podosome levels of both wt and Cyth2 KO cells to an FN-like state. This would indicate that αx integrin might indeed be responsible for the reverse regulation of podosome formation by Cyth2 on gelatin vs FN. However, the strength of the effect on podosome formation and the kd efficiency of both siRNAs did not correlate well. Possibly, one of them has some off-target effects that influence podosome formation in a different way. In the

future, one would have to use more independent siRNAs or Itgax KO cells to identify a true αx-specific effect.

The two other β2 integrins (αL and αM) did not majorly affect podosomes and might compensate for the potential role of αX integrin in podosome formation on the general β2 integrin ligands fibrinogen and Icam-1. In line with that, gelatin would stimulate specifically αXβ2 integrin leading to the observed Cyth2-dependent effect on podosomes. The common β2 integrin chain is crucial for podosome formation in general and partial reduction of this integrin by RNA interference altered podosome levels only moderately, but still abolished the Cyth2-dependent effect. This could be due to concomitant reductions of αx integrin surface expression or could be caused by a general disturbance of podosome formation pathways leaving the mild effect of Cyth2 dispensable.

Apart from collagen-binding integrins there are also other membrane proteins that can recognize and bind to collagen. These include the discoidin domain receptors DDR1 and DDR2, glycoprotein VI, leukocyte-associated immunoglobulin-like receptor-1 (LAIR-1), certain mannose receptors, and proteoglycans like CD44 or syndecans.[212] Of these receptors, only Mannose receptor 1, some syndecans and CD44 are expressed by iDCs on mRNA levels, but their expression is not affected by loss of Cyth2 or differences in protein coating (data not shown). Both CD44[213] and syndecans[214] have been connected with invadosomes. Still, further experiments would be required to elucidate the potential involvement of these non-integrin collagen receptors in Cyth2-mediated podosome formation.

4.2.2. α5β1 integrin and its role in adhesion to collagens

Despite the number of potential gelatin/collagen receptors expressed by iDCs, our results indicate that even on gelatin α5β1 integrin might be functionally involved. While there are no reports of collagen being a specific ligand for α5 integrins, some researchers have observed a role of α5 integrins in collagen-rich environments. Antibody-based activation of α5β1 integrin, for example, has been shown to inhibit migration of muscle cells on gelatin[215] and mesenchymal stem cells adhered less in a gelatin-hyaluronan gel, when α5 integrin was blocked[216]. Still, there are no indications for α5β1 binding directly to collagens, even though it was reported that partially denatured collagen can expose RGD (arginine-glycin-aspartic acid) motifs[217], which are the prime recognition sequences for α5 integrins in FN[9].

However, it is possible that α5β1 integrins bind to collagen/gelatin indirectly. Glycoproteins like FN do not only link cells to the ECM but also interconnect different components of the ECM with each other[5] and FN contains a collagen (or gelatin)-binding site at its N-terminus[218]. This collagen-binding ability of FN is particularly important for deposition of both FN and collagen in the ECM[219] and supports spreading of CHO cells on a mixture of FN and gelatin[220]. Moreover, specifically α5 integrins have been shown to mediate adhesion of chondrocytes to denatured collagen, but not to native collagen, via a so-called "α5β1-FN bridge".[221]

ECM is constantly synthesized and modified by the cells living within, especially fibroblasts.[5] Also immune cells have been shown to produce FN.[222–224] As iDCs express the FN gene (data not shown), it is possible that they also secrete FN into their environment even when they are seeded onto pure gelatin. These secreted FN fibrils then could potentially link gelatin to α5β1 integrins and modify cellular behavior. Moreover, our observation that iDC adhesion onto gelatin takes considerably longer than onto FN could be explained by deposition of endogenous FN prior to full adhesion of iDCs. In addition, we cultured iDCs in medium containing serum, which includes not only growth factors but also several integrin ligands, like FN[208]. So far, however, we have neither analyzed FN deposition in our assays, nor the role of FN-gelatin interaction for podosome formation. Nevertheless, such an indirect binding to gelatin via FN fibrils could convincingly explain how α5β1 integrins can influence adhesion to gelatin.

4.2.3. Integrin receptor crosstalk or different integrin activation might explain the matrix-dependent changes in podosome formation observed for Cyth2 KO iDCs

Independent of the exact interaction between gelatin and α5β1 integrin, the question still remains how involvement of this particular integrin can affect podosome formation so differently on FN or gelatin. One possible explanation could be that the potential direct interaction between gelatin and α5β1 integrin induces a different conformation of the integrin than binding to FN. Conformation-specific effects have been described for α4β7 integrin in lymphocytes, which has higher affinities for either VCAM or MadCAM depending on its conformation state.[225,226] Such variations in integrin activation might affect downstream signaling cascades resulting ultimately in different podosome formation.

Similarly, the interaction between FN and gelatin might modify the binding between FN and α5β1 integrin leading to a different integrin conformation. This could be mediated by conformational changes of FN itself leading to altered recognition by the integrin, for example by generation of

additional binding sites for the integrin. Apart from the RGD motif α5β1 integrins, for instance, also interact with the synergy site on FN, which is able to further modulate FN binding.[227,228] However, both RGD and synergy sites are bound by slightly different conformational states of α5 integrin.[229,230] Comparable mechanisms in iDCs could then lead to slightly altered integrin activation and intracellular signaling events on gelatin.

In addition to α5β1 integrins being the prime direct or indirect receptor for gelatin, it is also possible that these integrins simply modify activation or signaling of other gelatin receptors. This process is called crosstalk and is a common feature of integrin biology. Cells usually express several integrins simultaneously, as well as other surface receptors, and their signaling cascades influence each other. Many key signaling modules are shared by numerous receptors, e.g. Akt, ERK or Src kinase, but are regulated differently, positively or negatively. Moreover, feedback mechanisms can also modify signaling from other receptors.[231] Such crosstalk has been described between integrins and several growth factor receptors[232–234] or other, non-integrin adhesion receptors[131,195,235], but it also occurs within the group of integrins themselves. For example, in T cell adhesion and extravasation processes the time-controlled activation of αLβ2 and α4β1 integrins is regulated by a complex crosstalk between both integrin classes.[236,237] Moreover, there are several reports on α5β1 integrin regulation by and of other integrins, which modifies integrin activation and ligand binding, integrin recycling or specific functional outcomes of α5 integrin signaling.[236,238–244].

Similar to these data, a scenario, where α5β1 integrin modulates signaling events downstream of gelatin-binding receptors (e.g. αxβ2 integrin or other gelatin receptors) or where α5β1 integrin signals are modified themselves, is a very plausible explanation for the differential effects of Cyth2 KO on podosome formation on different matrices. This is especially intriguing as receptor crosstalk is discussed as an important mechanism during formation of invadosomes, where signals from different integrin classes or other matrix receptors converge on central podosome regulators like Src kinase or protein kinase C.[245]

4.3. Selective regulation of Rho GTPases mediates the effect of Cyth2 on podosomes

Apart from identifying the responsible integrins for Cyth2-mediated effects on podosome formation, we also examined intracellular signaling mechanisms involving Cyth2. Our data showed that neither proximal phosphorylation events downstream of integrin receptors nor more distal effects on the Akt or ERK signaling pathways are altered by loss of Cyth2. This indicates that general activation and signal transduction from integrins is not majorly compromised by Cyth2 KO. The observation that cell spreading and FA formation are also not significantly different in Cyth2 KO cells on FN or gelatin further supports the notion that overall adhesion behavior is not affected. Due to the lack of conformation-specific reporter antibodies for murine integrins, though, we cannot definitely exclude that Cyth2 acts directly at $\alpha5\beta1$ integrin and modifies its activation.

Integrin signaling, however, includes a plethora of pathways and effectors and we could identify RhoA as a potential mediator of the differential effects of Cyth2 on podosome formation on different matrices. The activation state of this GTPase is differentially altered by loss of Cyth2 on either coating substrate. On FN, RhoA activity is reduced by Cyth2 KO, while on gelatin we see a mild increase in RhoA activation. Furthermore, pharmacological inhibition of Rho showed that RhoA indeed is a positive regulator of podosomes in iDCs. Therefore, we conclude that RhoA is differently activated downstream of Cyth2 on either FN or gelatin, which results in altered podosome formation.

4.3.1. RhoA activation promotes podosome formation in iDCs

Rho GTPases in general are critically involved in formation of invadosomes.[246] RhoA in particular is responsible for contractility of the cytoskeleton by regulating the activity of ROCK. ROCK in turn modifies the phosphorylation state of myosin II and thereby the contractility of actin fibres.[60] This myosin-dependent contractibility is an important pre-requisite for dynamic formation and turnover of invadosomes, as well as their mechanosensing function.[85,247–251] Apart from the ROCK-myosin pathway, RhoA also targets formins, especially mDia. These actin-nucleators are key regulators of the actin-rich invadosomes.[68,252–254]

Still, the exact role of RhoA in invadosome formation remains controversial. While active RhoA has been observed at invadosomes[186] and increased RhoA activity can promote invadosome formation and stability[185,255–260], other studies have reported that RhoA activation leads to disassembly of invadosomes[90,118,184,187,200,261,262]. The reason for these differences is not entirely

understood but could in part be due to that fact that RhoA, like any GTPase, constantly cycles between its activation states. RhoA activation, as well as its inactivation, is most likely required at very specific time points and localizations during the invadosome life cycle. In addition, the different roles for RhoA might simply reflect cell type-specific variances. Depending on the intrinsic basal activation levels of RhoA or the expression of certain regulators and effectors in each cell type, alterations in RhoA activity in either direction might have different outcomes for invadosome formation.[263]

Interestingly, Rafiq and colleagues showed that inhibition of cytohesins increases RhoA activity and reduces podosome formation in THP-1 cells.[118] This effect on podosomes depends on myosin II and ROCK. In their system RhoA is therefore a negative regulator of podosome formation, which is in clear contrast to our data. Considering the before-mentioned literature, the seemingly opposing effects of RhoA activation in podosome formation in THP-1 cells and iDCs are probably caused by inherent differences in key regulatory pathways. Even though both THP-1 cells and iDCs are myeloid cells, they still display crucial differences. While iDCs form podosomes spontaneously without any further modification by the experimenter, THP-1 cells have to be treated with TGF-β or PMA in order to induce significant numbers of podosome-like structures. Both substances have been shown to influence RhoA activation[264,265] and could have additional effects on other pathways, which might affect podosome formation – similar to the receptor crosstalk described above. Moreover, the principal route leading to podosome formation in the first place could be different depending on the stimulus and therefore RhoA might be involved at different or additional steps.

THP-1 cells also appear very different in terms of morphology. Being monocyte-like cells, they are relatively small and round and spread only little on a 2D surface.[118] iDCs in contrast form filopodia and broad protrusions and are often polarized in one direction. Differences in RhoA activation state can have very profound effects on cellular morphology and adhesion.[266] Therefore, the different morphology of THP-1 cells and iDCs further supports the notion that general actin organizing mechanisms are regulated differently in both cell types. Still, additional experiments using, for example, FRET (fluorescence resonance energy transfer)-based biosensors for RhoA activity could further confirm and expand our knowledge on the localized and time-specific effects of RhoA in podosome formation by iDCs. Based on our data we also cannot completely exclude that the increased podosome numbers of Cyth2 KO cells on gelatin rely on additional pathways apart from RhoA.

4.3.2. Cyth2 affects RhoA activation independently of Arf GTPases

Our data show that loss of Cyth2 affects both RhoA activity and podosome formation differentially on either FN or gelatin, which indicates that RhoA acts downstream of Cyth2. Nevertheless, loss of Cyth2 seems to affect RhoA activation differently on both coating substrates. Cytohesins in general have been shown to control RhoA activity in other settings before, but again the literature on that topic is ambiguous. The cytohesin homolog in *Drosophila* (Steppke), for instance, inhibits Rho activity at different steps during the development of *Drosophila* embryos[267–269], while our lab could show that Cyth1 is required for full RhoA activation in mature DCs[135]. The proposed pathway by Rafiq and colleagues, however, claims that Cyth2 downregulates RhoA activity in THP-1 cells (on FN)[118], which is contrary to our results from iDCs on FN. Most likely, as discussed above, RhoA-related signaling and effects depend very much on the cell type and the experimental conditions and therefore the role of cytohesins in activation of this GTPase can be diverse as well.

In most publications, including Rafiq and colleagues, cytohesins act via Arf GTPases to influence their downstream effector RhoA[118,267–269]. Since Arf GTPases are the prime targets of cytohesin GEF action[106], this connection is very obvious. RhoA and Arf GTPases often share common regulators[270,271] and effectors[272–274], and can influence each other[275,276]. Our data, however, showed that neither Arf1 nor Arf6 activation is altered by loss of Cyth2 in iDCs, which suggests that the regulation of RhoA in this specific case is not mediated via these GTPases.

It is still possible that Arf activation in iDCs might only be different at very specific subcellular localizations and our analysis of whole-cell lysates simply did not detect these small alterations. Again, an approach using FRET-based biosensors could help to resolve such localized activity patterns. Moreover, there are in total six Arf GTPases, of which Arf1 and Arf6 are by far the best characterized representatives. Both Arf1[118,119] and Arf6[115] have already been implicated in regulation of invadosome formation. It cannot be ruled out, however, that in terms of podosome formation in iDCs Cyth2 acts specifically on Arf2-5. Based on current literature, though, there is little evidence that these Arf proteins are active anywhere else than at the Golgi apparatus.[112]

Another intriguing possibility would be that Cyth2 acts in a GEF-independent manner to regulate podosome formation. With its coiled-coil domain Cyth2 can interact with several other proteins, including the scaffold proteins paxillin[137] and GRASP/Tamalin[143], which have been shown to associate with certain Rho GEFs[143,277]. This way Cyth2 might simply affect the localized recruitment of Rho regulators. Such Arf-independent roles of cytohesins have been described before. In epithelial cells Luong and colleagues described effects of Cyth2 on actin dynamics that relied on its ability to bind to phosphoinositides but not its GEF function.[278] Moreover, an Arf-independent

function of Cyth2 also fits very well with our observations that trafficking of integrins is not altered in Cyth2 KO cells, as regulation of receptor dynamics is a key function of Arf GTPases[112]. Including a GEF-mutant form (E156K) of Cyth2 in rescue experiments of Cyth2 KO cells, could solve the question whether Arf proteins play a role at all in Cyth2-mediated podosome formation.

Considering that we have found evidence for an integrin-dependent regulation of RhoA, it would make sense if Cyth2 were directly involved in integrin-related RhoA activation pathways. RhoA activity is regulated in two stages upon integrin stimulation. Directly after adhesion RhoA is inhibited via a Src-p190RhoGAP axis, only to be reactivated after a few minutes.[279–281] This later re-activation of RhoA can be mediated by several GEFs downstream of integrins: p190RhoGEF[282], LARG and p115RhoGEF[283]. Interestingly, the second phase of RhoA activation can be induced specifically by $\alpha5\beta1$ integrins, but not by $\alpha v\beta3$ integrins.[284] Similar integrin-specific differences in RhoA activation have been reported for $\alpha3$ and $\alpha2$ integrins, which inhibit or promote RhoA activity, respectively.[285]

The easiest explanation for the differential involvement of Cyth2 in RhoA-mediated podosome formation downstream of either FN or gelatin would therefore be alterations in Rho GEF or GAP recruitment or activation downstream of $\alpha5\beta1$ integrins. Given the huge number of potential candidates, identifying the responsible factor and its connection to Cyth2 constitutes a major challenge. An unbiased analysis of the proteome associated with podosomes of wt and Cyth2 deficient cells on several substrates would probably be the best way to go about this issue. The composition of both invadosomes[286,287] and FAs[47,288–290] has been described with similar means. Some studies even found integrin- and matrix-dependent differences, e.g. concerning GTPase recruitment to FAs on FN vs VCAM[291]. Kutys and colleagues approached this question using an active-GEF affinity screen in cells migrating on FN or collagen. They found a specific pair of Rho GEF and GAP (β-Pix and SRGAP1) to be activated in a collagen environment but not on FN.[46] These two factors enhanced activation of Cdc42 and dampened RhoA activity, which enabled efficient cell migration on collagen. Moreover, the authors linked this differential involvement of Rho regulators specifically to $\alpha2\beta1$ integrin but not $\alpha5\beta1$ integrin. Likewise, culturing iDCs on either FN or gelatin could result in slightly altered composition of adhesion complexes in podosomes, where Cyth2 might be differentially involved in recruitment of specific Rho GEFs or GAPs. Such a possible mechanism is illustrated in figure **4.1**.

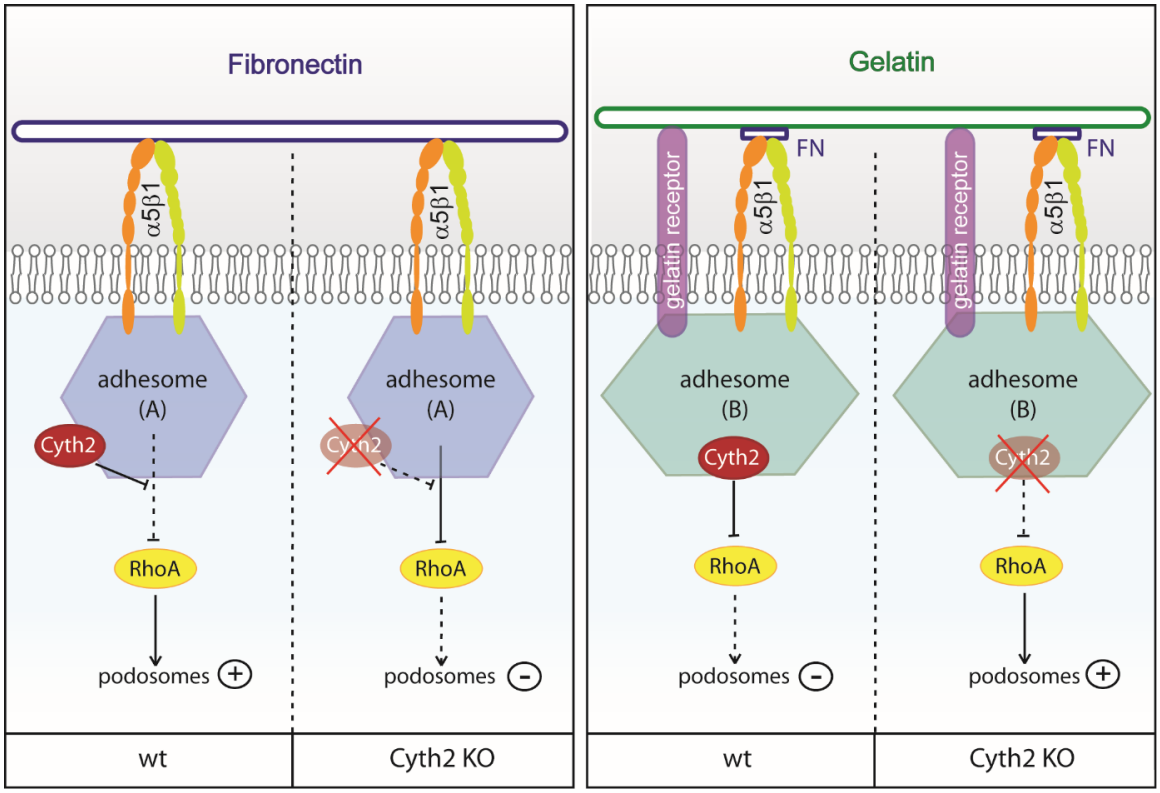

Figure 4.1 – Mechanistic scheme of Cyth2-dependent regulation of podosome formation on FN and gelatin

Culturing iDCs on either FN or gelatin leads to differential regulation of Cyth2-dependent podosome formation. This could be explained by engagement of different matrix receptors leading alterations in adhesome composition.

On FN, activation of α5β1 integrin leads to assembly of a specific adhesome (A), where Cyth2 suppresses RhoA-inhibiting pathways. When Cyth2 is lost, the signals coming from α5β1 integrin lead to a reduction of RhoA activation and therefore decreased podosome formation.

On gelatin, a more complex array of receptors, including potentially α5β1 integrin but also other gelatin receptor(s), induces formation of a differently composed adhesome (B). Here, Cyth2 has a different function and mediates suppression of RhoA activation. In Cyth2 KO cells, this inhibition of RhoA is released and podosome formation is stimulated. Similarly, loss of α5β1 integrin abolishes this inhibitory signaling axis.

4.4. Podosome formation is specifically regulated by Cyth2-2G

In this thesis we aimed at elucidating the role of cytohesins in integrin-dependent podosome formation. However, we could only detect a dependency of iDCs on Cyth2 for differential formation of podosomes on either FN or gelatin. Cyth1, Cyth3 and Cyth4 were not required to maintain podosome numbers in these cells.

4.4.1. Cyth1, Cyth3 and Cyth4 do not affect podosome formation on FN or gelatin

All four cytohesins are very similar in their structure and protein sequence. Cyth4, which is most different from the other cytohesins, still shares ~70 % sequence identity with Cyth1-3.[102] There are numerous publications showing that Cyth2 plays a role in integrin biology and actin dynamics.[129,136,137,140,144,145] Except for Cyth4, whose cell biological function is not described so far, both Cyth1[103,132,135,292,293] and Cyth3[128,129,294,295] have been implicated in integrin-related adhesion and actin remodeling processes as well. Despite reported functional overlap of these proteins with Cyth2[103,104,134,146,189,278,296], none of the other cytohesins affected podosome formation in our experiments. The podosome-related function of Cyth2 is therefore very specific for this particular protein. Still, we cannot rule out that other cytohesins might be involved in podosome formation on different integrin ligands than the ones we tested for this study.

In line with our data, Rafiq and colleagues excluded a role of Cyth1 in the regulation of podosome formation by THP-1 cells.[118] In their system, Cyth1 localizes diffusely throughout the cytoplasm, while Cyth2 accumulates specifically at podosome rings. Our data, however, do not replicate this specific localization of Cyth2 to podosomes. Rather, we observed a more unspecific distribution in the cytoplasm, which was similar to the stainings shown for Cyth1 by Rafiq and colleagues. In many studies Cyth2 is found diffusely distributed throughout the cell, while Cyth1 is often associated more clearly with the cell membrane[108,128,297]. The discrepancy between our observations and Rafiq's data could be due to cell type-specific differences or experimental procedures, as stimulation with PMA or fMLP has been shown to induce translocation of Cyth1 and Cyth2 to the cell membrane.[298] Additionally, the action of Cyth2 at podosomes could be restricted to certain phases of podosome turnover and the recruitment of Cyth2 therefore might be only transient.

4.4.2. Cytohesin isoforms determine their localization and function

In addition to functional differences within the family of cytohesins, also the isoform expression of cytohesins can be an important factor for function as well as subcellular localization. In our experiments we could show that the regulation of podosome formation is exclusively controlled by Cyth2-2G and not by the 3G isoform. Interestingly, Oh and Santy reported that the regulation of β1 integrin recycling by Cyth2 and Cyth3 in HeLa cells is not protein-specific but entirely determined by the isoform expression. Only the 3G isoform of either Cyth2 or Cyth3 affected integrin trafficking, while the 2G isoforms were not involved.[129,189] Considering that in wt iDCs Cyth2 is predominantly expressed in the 2G isoform, this could explain why we did not observe effects on integrin trafficking in Cyth2 KO cells. Moreover, similar isoform-dependent functional differences between cytohesins can be excluded in our system, because also Cyth3 and Cyth4 are expressed as 2G isoforms in iDCs. Apart from the studies by Oh and Santy, also Cyth1 isoforms have been reported to have different roles in cell migration and formation of actin ruffles. Cyth1-2G preferably localizes to the leading edge of migrating cells, while Cyth1-3G is found constitutively at the cell membrane but in an unpolarized fashion.[108]

2G/3G isoforms of cytohesins differ in their affinity for PIP_2 and PIP_3, with 2G isoforms preferring PIP_3, while 3G isoforms bind to both phospholipids equally well.[107] PIP_2 is the most abundant phosphatidylinositol, whereas PIP_3 is almost undetectable in unstimulated cells. Upon stimulation, PIP_2 can be phosphorylated by PI3K to generate PIP_3, which acts as a central signaling hub for several signaling pathways. Vice versa, PTEN dephosphorylates PIP_3 to PIP_2.[299] Podosomes are very locally occurring structures at the plasma membrane and spots of localized signaling events. Therefore, it is not surprising that the membrane composition at podosomes is distinct from other parts of the plasma membrane. Certain phospholipids, including PIP_3, have been found enriched at invadopodia [184,300], while the specific localization of PIP_2 to these structures is controversial[300,301]. Nevertheless, PI3K activity has been shown to be required for podosome formation[184,302], whereas PTEN acts inhibitory[303,304], illustrating the importance of especially PIP_3 for invadosomes.

With this information in mind, the particular role of Cyth2-2G, but not Cyth2-3G, in podosome formation could indeed be explained by recruitment of especially the 2G isoform to podosomes. Yet, we could not observe any accumulation of Cyth2-2G at podosomes, in contrast to the data of Rafiq and colleagues[118]. They do, however, not specify which isoform of Cyth2 they used in their study. As we did not observe a more specific pattern with Cyth2-3G either, these dissimilarities in localization could again be a matter of cell type-specific differences or could be caused by the

experimental setup. Stimulation of THP-1 cells with TGF-β or PMA may alter PIP_3 levels more distinctly compared to the untreated iDCs. Moreover, recruitment of Cyth2 to podosomes could simply be dependent on the kinetics of sequential signaling events during podosome assembly or disassembly[73]. These questions could be addressed by monitoring the dynamics of Cyth-2G and Cyth2-3G starting with initiation of adhesion – ideally using live cell imaging techniques. Furthermore, the lipid composition at podosome membranes of iDCs could be examined with reporter constructs for different phosphatidylinositols.

4.5. Physiological relevance of Cyth2-mediated podosome formation

The major part of this thesis deals with the elucidation of the cell biological and mechanistic role of Cyth2 in iDC podosome formation and is therefore performed in an *in vitro* setting. The *in vivo* relevance of this effect, however, is still not clear. The importance of invadopodia for cancer cell metastasis is well established in the literature and there are several publications showing a clear correlation between the presence of invadopodia and the ability of tumor cells to form metastases[78,79]. Yet, this is not the case for immune cell podosomes. While these structures are known to play a role in migration and adhesion processes *in vitro*[75–77] and have been identified in extravasating leukocytes *in vivo*[74], there are no functional data on the involvement of podosomes during an actual immune reaction *in vivo*. Based on our (*in vitro)* knowledge about podosomes, though, they are most likely involved in general migration and invasion processes of immune cells.

4.5.1. Myeloid cell populations in vivo are not affected by Cyth2 KO

In the context of DC biology, there are two major steps of cell migration. cDCs develop from hematopoietic stem cells in the bone marrow and enter the blood as precursors (pre-DCs). When these pre-DCs arrive in the periphery, they extravasate from the blood and finally differentiate within the respective organ. The second phase of DC migration happens after an immunological stimulus. Upon pathogen encounter DCs in the periphery mature and start migrating towards draining lymph nodes, where they initiate the adaptive immune response.[305] Given that podosomes occur only in immature BMDCs and disappear upon maturation[200], it is more likely that the first wave of migration of pre-DCs or the positioning of immature DCs within organs is affected by a Cyth2-dependent deregulation of podosomes.

Using myeloid cell-specific Cyth2 KO mice we analyzed steady state frequencies of different myeloid populations in several immunologically relevant organs (blood, spleen, lymph nodes and lungs) and focused especially on DCs. However, we could not detect any differences between Cyth2$^{flox/flox}$ LysM-Cre mice and controls. This could be due to the fact that the penetration of the LysM-Cre driven KO is not complete in all myeloid cell types and targets especially DCs only partially[306], which might mask small effects on subpopulations.

Furthermore, the absence of an *in vivo* phenotype suggests that either the observed effect *in vitro* is not strong enough to manifest in a systemic phenotype or that the matrix-specific mechanisms are indeed too specific and are not functionally relevant in the mixed matrix environment *in vivo*. Both FN and collagen are major components of ECM, although their exact contribution varies between different tissues. Soft organs, (e.g. the brain) contain less collagen than stiffer tissue, like ligaments[307], and tumors are known to alter their microenvironment by depositing more collagen[308]. Conversely, provisional matrix, with is formed during wound healing, is especially rich in FN, while collagen is deposited later, when the provisional matrix is replaced by normal ECM.[309] The matrix- and integrin-dependent regulation of podosome formation might therefore be relevant only in very specific locations and situations.

In addition to the two major DC subtypes that we analyzed (cDC1 and cDC2), DCs have been shown to differentiate into more specialized subpopulations, especially in non-lymphoid organs such as skin, lungs or intestine.[310,311] A more complex staining panel and the inclusion of other organs would be required to rule out an effect of the Cyth2 KO on minor DC subpopulations.

Apart from cell frequencies, it is possible that sub-organ localization of Cyth2 KO DCs is altered compared to wt DCs, which would not be detectable by flow cytometry. In the spleen, immature DCs are found especially at the bridging channels between red pulp and T cell zones and locate to T cell zones only upon stimulation[312]. Interfering with different migration-associated receptors can substantially alter positioning of DC populations, which also has consequences for immune reactions.[313–315] Similar effects in Cyth2$^{flox/flox}$ LysM-Cre mice would have to be further analyzed by immunohistochemistry stainings for different DC populations.

Finally, it is still possible that Cyth2-mediated podosome formation becomes only relevant upon an immunological challenge and experiments in our lab have already indicated that DC recruitment is mildly affected by Cyth2 KO in a legionella infection model (Anastasia Solomatina, unpublished data). Further studies in that direction might shed some light on the role of Cyth2 and podosomes during immune reactions.

4.5.2. Integrin expression of osteoclasts differs substantially from iDCs

Besides the analysis of myeloid immune cells, we also examined the functionality of osteoclasts, because their sealing zone is the best characterized physiological context for podosome function *in vivo*[80–82]. However, we could not detect any differences in BMD of Cyth2$^{flox/flox}$ LysM-Cre mice compared to controls indicating that osteoclasts are also not affected by loss of Cyth2.

Although both DCs and osteoclasts are derived from the myeloid lineage and form podosomes constitutively, they differ not only functionally but also in terms of integrin expression. $\alpha v\beta 3$ integrins, which are mostly absent in iDCs, are the major integrin in osteoclasts and constitute a key component of the sealing zone[316]. $\beta 1$ and $\beta 2$ integrins are also expressed by osteoclasts and relevant for their degradative function[83,317,318]. The presence of especially $\alpha 5\beta 1$ integrin, though, is controversially discussed[316,319,320] and there are no functional data on the involvement of this particular $\beta 1$ integrin in osteoclast function. Even if $\alpha 5\beta 1$ integrins were expressed in osteoclasts at low levels, this would probably not be sufficient to induce a significant, Cyth2-dependent effect on podosome formation or degradation of bone. Nevertheless, we have not studied osteoclasts themselves but only analyzed a functional read-out of their activity. In order to make a definite statement on the role of Cyth2 in osteoclast sealing zone formation, one would have to examine these structures on a cellular level.

4.6. Conclusion and outlook

Taken together, our results show that Cyth2 acts as a fine-tuning regulator of podosome formation. Depending on the composition of the environmental matrix Cyth2 differentially modulates integrin signaling pathways leading to alterations in RhoA activation and, ultimately, podosome formation. This effect is not a general function of the cytohesin family, but specific for Cyth2 and its 2G isoform.

We have been able to elucidate intricate modifications of intracellular signaling pathways in response to different matrix proteins. Our data illustrate how precisely integrin-dependent pathways are controlled and that already small alterations in extracellular stimuli can have significant effects on intracellular signaling cascades and functional outcomes. Cyth2 is a distinct player in this context as it changes its role from an inhibitory element of $\alpha5\beta1$ integrin-dependent podosome regulation to a positive factor of the same axis. This mechanism might enable functional adaptations to specific ECM microenvironments.

In the future, the exact pathways connecting $\alpha5\beta1$ integrins with Cyth2 and RhoA activation need to be clarified. As discussed above, a proteomics approach on podosome structures is most likely to detect variations in integrin complex composition on FN and gelatin. Moreover, identifying the suspected receptor for gelatin or the differences in $\alpha5\beta1$ integrin binding and activation on gelatin vs FN is crucial to fully understand the underlying mechanism of differential podosome formation. Even though we have not been able to detect a physiological relevance of this integrin-specific regulation, further experiments – not only on immune cells, but also using, for example, invadopodia-forming cancer cells – will determine if these mechanisms also affect invasion and/or migration processes *in vivo*.

5. Summary

The interaction of a cell with the surrounding tissue is crucial not only to provide mechanical stability but also to enable adaptation of cellular responses to the environment. Recognition of extracellular matrix (ECM) is primarily exerted by integrin receptors, which consist of an α and a β chain. The high diversity of these integrin dimers allows for a variety of ligand specificities but differences in intracellular signaling cascades are only partially understood.

Within the cell, integrin-mediated adhesions are organized in specific adhesion structures. Among these, podosomes are characterized by their typical organization in an actin-rich core and an adhesive ring structure, which contains integrins and adhesion-related adaptor and signaling molecules. Apart from mediating adhesion, podosomes also are important during cell migration and invasion. Their formation is induced by growth factor or integrin signaling and depends very much on actin remodeling factors.

Both actin dynamics and integrin signaling are regulated by numerous factors, including the cytohesin protein family. Cytohesins primarily act as guanine nucleotide exchange factors (GEFs) for Arf GTPases, but they are also involved in activation and recycling of integrins, as well as actin remodeling processes. One member of the cytohesin family, Cyth2, has recently been shown to be important for podosome formation in THP-1 cells. So far, though, it is unclear whether integrin-related functions of cytohesins also affect podosome formation. Therefore, this study aimed at identifying the role of different cytohesins in integrin-dependent podosome formation.

Using bone marrow-derived dendritic cells (BMDCs) from several cytohesin KO mice, we found that only Cyth2, but not Cyth1, Cyth3 or Cyth4, regulates podosome formation in a matrix-depending manner. Loss of Cyth2 impaired podosome formation on a fibronectin (FN) matrix, while Cyth2 KO BMDCs on fibrinogen or Icam-1 remained unaffected. Moreover, Cyth2 KO cells cultured on gelatin or collagen even increased their podosome numbers compared to wildtype cells. These effects were dependent on a differential involvement of $\alpha5\beta1$ integrin and were mediated via the small GTPase RhoA.

Thus, our results show that Cyth2 is involved in regulation of integrin-dependent responses to environmental cues leading to differential formation of podosomes. Such specific adaptations of signaling pathways downstream of different integrins might affect invasion and migration processes of immune cells in certain ECM microenvironments *in vivo*.

References

1. Bianconi, E. *et al.* An estimation of the number of cells in the human body. *Ann. Hum. Biol.* **40**, 463–471 (2013).

2. Gumbiner, B. M. Cell adhesion: the molecular basis of tissue architecture and morphogenesis. *Cell* **84**, 345–57 (1996).

3. Bonnans, C., Chou, J. & Werb, Z. Remodelling the extracellular matrix in development and disease. *Nat. Rev. Mol. Cell Biol.* **15**, 786–801 (2014).

4. Pozzi, A., Yurchenco, P. D. & Iozzo, R. V. The nature and biology of basement membranes. *Matrix Biol.* **57**–**58**, 1–11 (2017).

5. Kumar, V., Abbas, A. K., Fausto, N. & Mitchell, R. N. *Robbins Basic Pathology*. (Saunders, 2007).

6. Wang, Y., Gallant, R. C. & Ni, H. Extracellular matrix proteins in the regulation of thrombus formation. *Curr. Opin. Hematol.* **23**, 280–287 (2016).

7. Leckband, D. E. & de Rooij, J. Cadherin Adhesion and Mechanotransduction. *Annu. Rev. Cell Dev. Biol.* **30**, 291–315 (2014).

8. McEver, R. P. Selectins: initiators of leucocyte adhesion and signalling at the vascular wall. *Cardiovasc. Res.* **107**, 331–339 (2015).

9. Makrilia, N., Kollias, A., Manolopoulos, L. & Syrigos, K. Cell Adhesion Molecules: Role and Clinical Significance in Cancer. *Cancer Invest.* **27**, 1023–1037 (2009).

10. Hynes, R. O. Integrins: Versatility, modulation, and signaling in cell adhesion. *Cell* **69**, 11–25 (1992).

11. Humphries, J. D. Integrin ligands at a glance. *J. Cell Sci.* **119**, 3901–3903 (2006).

12. Kling, D., Fingerle, J. & Harlan, J. M. Inhibition of leukocyte extravasation with a monoclonal antibody to CD18 during formation of experimental intimal thickening in rabbit carotid arteries. *Arterioscler. Thromb. A J. Vasc. Biol.* **12**, 997–1007 (1992).

13. Walzog, B., Scharffetter-Kochanek, K. & Gaehtgens, P. Impairment of neutrophil emigration in CD18-null mice. *Am. J. Physiol. Liver Physiol.* **276**, G1125–G1130 (1999).

14. Tronik-Le Roux, D. *et al.* Thrombasthenic mice generated by replacement of the integrin alpha(IIb) gene: demonstration that transcriptional activation of this megakaryocytic locus precedes lineage commitment. *Blood* **96**, 1399–408 (2000).

15. Yang, J. T., Rayburn, H. & Hynes, R. O. Cell adhesion events mediated by alpha 4 integrins are essential in placental and cardiac development. *Development* **121**, 549–60 (1995).

16. Yang, J. T., Rayburn, H. & Hynes, R. O. Embryonic mesodermal defects in alpha 5 integrin-deficient mice. *Development* **119**, 1093–105 (1993).

17. Stephens, L. E. *et al.* Deletion of beta 1 integrins in mice results in inner cell mass failure and peri-implantation lethality. *Genes Dev.* **9**, 1883–1895 (1995).

18. Bader, B. L., Rayburn, H., Crowley, D. & Hynes, R. O. Extensive Vasculogenesis, Angiogenesis, and Organogenesis Precede Lethality in Mice Lacking All αv Integrins. *Cell* **95**, 507–519 (1998).

19. Kreidberg, J. A. *et al.* Alpha 3 beta 1 integrin has a crucial role in kidney and lung organogenesis. *Development* **122**, 3537–47 (1996).

20. Georges-Labouesse, E., Mark, M., Messaddeq, N. & Gansmüller, A. Essential role of α6 integrins in cortical and retinal lamination. *Curr. Biol.* **8**, 983-S1 (1998).

21. Müller, U. *et al.* Integrin alpha8beta1 is critically important for epithelial-mesenchymal interactions during kidney morphogenesis. *Cell* **88**, 603–13 (1997).

22. Schmits, R. *et al.* LFA-1-deficient mice show normal CTL responses to virus but fail to reject immunogenic tumor. *J. Exp. Med.* **183**, 1415–26 (1996).

23. Wu, H. *et al.* Functional Role of CD11c + Monocytes in Atherogenesis Associated With Hypercholesterolemia. *Circulation* **119**, 2708–2717 (2009).

24. Scharffetter-Kochanek, K. *et al.* Spontaneous Skin Ulceration and Defective T Cell Function in CD18 Null Mice. *J. Exp. Med.* **188**, 119–131 (1998).

25. Wu, H. *et al.* Deficiency of CD11b or CD11d Results in Reduced Staphylococcal Enterotoxin-Induced T Cell Response and T Cell Phenotypic Changes. *J. Immunol.* **173**, 297–306 (2004).

26. Mayer, U. *et al.* Absence of integrin α7 causes a novel form of muscular dystrophy. *Nat. Genet.* **17**, 318–323 (1997).

27. Dupuy, A. G. & Caron, E. Integrin-dependent phagocytosis - spreading from microadhesion to new concepts. *J. Cell Sci.* **121**, 1773–1783 (2008).

28. Sun, Z., Costell, M. & Fässler, R. Integrin activation by talin, kindlin and mechanical forces. *Nat. Cell Biol.* **21**, 25–31 (2019).

29. Monkley, S. J. *et al.* Disruption of the talin gene arrests mouse development at the gastrulation stage. *Dev. Dyn.* **219**, 560–74 (2000).

30. Calderwood, D. A., Campbell, I. D. & Critchley, D. R. Talins and kindlins: partners in integrin-mediated adhesion. *Nat. Rev. Mol. Cell Biol.* **14**, 503–517 (2013).

31. Raaijmakers, J. H. & Bos, J. L. Specificity in Ras and Rap Signaling. *J. Biol. Chem.* **284**, 10995–10999 (2009).

32. Fagerholm, S. C., Lek, H. S. & Morrison, V. L. Kindlin-3 in the immune system. *Am. J. Clin. Exp. Immunol.* **3**, 37–42 (2014).

33. Montanez, E. *et al.* Kindlin-2 controls bidirectional signaling of integrins. *Genes Dev.* **22**, 1325–1330 (2008).

34. Ussar, S. *et al.* Loss of Kindlin-1 Causes Skin Atrophy and Lethal Neonatal Intestinal Epithelial Dysfunction. *PLoS Genet.* **4**, e1000289 (2008).

35. Moser, M., Nieswandt, B., Ussar, S., Pozgajova, M. & Fässler, R. Kindlin-3 is essential for integrin activation and platelet aggregation. *Nat. Med.* **14**, 325–330 (2008).

36. Li, H. *et al.* Structural basis of kindlin-mediated integrin recognition and activation. *Proc. Natl. Acad. Sci.* **114**, 9349–9354 (2017).

37. Jahed, Z., Haydari, Z., Rathish, A. & Mofrad, M. R. K. Kindlin Is Mechanosensitive: Force-Induced Conformational Switch Mediates Cross-Talk among Integrins. *Biophys. J.* (2019). doi:10.1016/j.bpj.2019.01.038

38. Zaidel-Bar, R., Itzkovitz, S., Ma'ayan, A., Iyengar, R. & Geiger, B. Functional atlas of the integrin adhesome. *Nat. Cell Biol.* **9**, 858–867 (2007).

39. Harburger, D. S. & Calderwood, D. A. Integrin signalling at a glance. *J. Cell Sci.* **122**, 159–163 (2009).

40. Moreno-Layseca, P. & Streuli, C. H. Signalling pathways linking integrins with cell cycle progression. *Matrix Biol.* **34**, 144–153 (2014).

41. Huveneers, S. & Danen, E. H. J. Adhesion signaling - crosstalk between integrins, Src and Rho. *J. Cell Sci.* **122**, 1059–1069 (2009).

42. Langholz, O. *et al.* Collagen and collagenase gene expression in three-dimensional collagen lattices are differentially regulated by alpha 1 beta 1 and alpha 2 beta 1 integrins. *J. Cell Biol.* **131**, 1903–15 (1995).

43. Huveneers, S., Truong, H., Fassler, R., Sonnenberg, A. & Danen, E. H. J. Binding of soluble fibronectin to integrin 5 1 - link to focal adhesion redistribution and contractile shape. *J. Cell Sci.* **121**, 2452–2462 (2008).

44. Miao, H. *et al.* Differential regulation of Rho GTPases by beta1 and beta3 integrins: the role of an extracellular domain of integrin in intracellular signaling. *J. Cell Sci.* **115**, 2199–206 (2002).

45. Lishko, V. K., Yakubenko, V. P. & Ugarova, T. P. The interplay between integrins αmβ2 and α5β1 during cell migration to fibronectin. *Exp. Cell Res.* **283**, 116–126 (2003).

46. Kutys, M. L. & Yamada, K. M. An extracellular-matrix-specific GEF–GAP interaction regulates Rho GTPase crosstalk for 3D collagen migration. *Nat. Cell Biol.* **16**, 909–917 (2014).

47. Horton, E. R. *et al.* Definition of a consensus integrin adhesome and its dynamics during adhesion complex assembly and disassembly. *Nat. Cell Biol.* **17**, 1577–1587 (2015).

48. Paul, N. R., Jacquemet, G. & Caswell, P. T. Endocytic Trafficking of Integrins in Cell Migration. *Curr. Biol.* **25**, R1092–R1105 (2015).

49. Moreno-Layseca, P., Icha, J., Hamidi, H. & Ivaska, J. Integrin trafficking in cells and tissues. *Nat. Cell Biol.* **21**, 122–132 (2019).

50. Pollard, T. D. Actin and Actin-Binding Proteins. *Cold Spring Harb. Perspect. Biol.* **8**, a018226 (2016).

51. Rottner, K., Faix, J., Bogdan, S., Linder, S. & Kerkhoff, E. Actin assembly mechanisms at a glance. *J. Cell Sci.* **130**, 3427–3435 (2017).

52. Snapper, S. B. *et al.* N-WASP deficiency reveals distinct pathways for cell surface projections and microbial actin-based motility. *Nat. Cell Biol.* **3**, 897–904 (2001).

53. Takenawa, T. & Suetsugu, S. The WASP–WAVE protein network: connecting the membrane to the cytoskeleton. *Nat. Rev. Mol. Cell Biol.* **8**, 37–48 (2007).

54. Pollitt, A. Y. & Insall, R. H. WASP and SCAR/WAVE proteins: the drivers of actin assembly. *J. Cell Sci.* **122**, 2575–2578 (2009).

55. Mayor, R. & Carmona-Fontaine, C. Keeping in touch with contact inhibition of locomotion. *Trends Cell Biol.* **20**, 319–328 (2010).

56. Lawson, C. D. & Ridley, A. J. Rho GTPase signaling complexes in cell migration and invasion. *J. Cell Biol.* **217**, 447–457 (2018).

57. Hodge, R. G. & Ridley, A. J. Regulating Rho GTPases and their regulators. *Nat. Rev. Mol. Cell Biol.* **17**, 496–510 (2016).

58. Edwards, D. C., Sanders, L. C., Bokoch, G. M. & Gill, G. N. Activation of LIM-kinase by Pak1 couples Rac/Cdc42 GTPase signalling to actin cytoskeletal dynamics. *Nat. Cell Biol.* **1**, 253–259 (1999).

59. Sanders, L. C., Matsumura, F., Bokoch, G. M. & de Lanerolle, P. Inhibition of Myosin Light Chain Kinase by p21-Activated Kinase. *Science (80-.).* **283**, 2083–2085 (1999).

60. Jaffe, A. B. & Hall, A. RHO GTPASES: Biochemistry and Biology. *Annu. Rev. Cell Dev. Biol.* **21**, 247–269 (2005).

61. Fogh, B. S., Multhaupt, H. A. B. & Couchman, J. R. Protein Kinase C, Focal Adhesions and the Regulation of Cell Migration. *J. Histochem. Cytochem.* **62**, 172–184 (2014).

62. Geiger, B. & Yamada, K. M. Molecular Architecture and Function of Matrix Adhesions. *Cold Spring Harb. Perspect. Biol.* **3**, a005033–a005033 (2011).

63. Linder, S. & Wiesner, C. Tools of the trade: podosomes as multipurpose organelles of monocytic cells. *Cell. Mol. Life Sci.* **72**, 121–135 (2015).

64. Paterson, E. K. & Courtneidge, S. A. Invadosomes are coming: new insights into function and disease relevance. *FEBS J.* **285**, 8–27 (2018).

65. Murphy, D. A. & Courtneidge, S. A. The 'ins' and 'outs' of podosomes and invadopodia: characteristics, formation and function. *Nat. Rev. Mol. Cell Biol.* **12**, 413–426 (2011).

66. Paz, H., Pathak, N. & Yang, J. Invading one step at a time: the role of invadopodia in tumor metastasis. *Oncogene* **33**, 4193–4202 (2014).

67. Chen, W.-T. Proteolytic activity of specialized surface protrusions formed at rosette contact sites of transformed cells. *J. Exp. Zool.* **251**, 167–185 (1989).

68. Panzer, L. *et al.* The formins FHOD1 and INF2 regulate inter- and intra-structural contractility of podosomes. *J. Cell Sci.* **129**, 298–313 (2016).

69. Abram, C. L. *et al.* The Adaptor Protein Fish Associates with Members of the ADAMs Family and Localizes to Podosomes of Src-transformed Cells. *J. Biol. Chem.* **278**, 16844–16851 (2003).

70. Seals, D. F. *et al.* The adaptor protein Tks5/Fish is required for podosome formation and function, and for the protease-driven invasion of cancer cells. *Cancer Cell* **7**, 155–165 (2005).

71. Di Martino, J. *et al.* Cdc42 and Tks5. *Cell Adh. Migr.* **8**, 280–292 (2014).

72. van den Dries, K. *et al.* Dual-color superresolution microscopy reveals nanoscale organization of mechanosensory podosomes. *Mol. Biol. Cell* **24**, 2112–2123 (2013).

73. Hoshino, D., Branch, K. M. & Weaver, A. M. Signaling inputs to invadopodia and podosomes. *J. Cell Sci.* **126**, 2979–2989 (2013).

74. Carman, C. V. *et al.* Transcellular Diapedesis Is Initiated by Invasive Podosomes. *Immunity* **26**, 784–797 (2007).

75. Van Goethem, E., Poincloux, R., Gauffre, F., Maridonneau-Parini, I. & Le Cabec, V. Matrix Architecture Dictates Three-Dimensional Migration Modes of Human Macrophages: Differential Involvement of Proteases and Podosome-Like Structures. *J. Immunol.* **184**, 1049–1061 (2010).

76. Linder, S., Nelson, D., Weiss, M. & Aepfelbacher, M. Wiskott-Aldrich syndrome protein regulates podosomes in primary human macrophages. *Proc. Natl. Acad. Sci.* **96**, 9648–9653 (1999).

77. Gawden-Bone, C. *et al.* A crucial role for β2 integrins in podosome formation, dynamics and Toll-like-receptor-signaled disassembly in dendritic cells. *J. Cell Sci.* **127**, 4213–24 (2014).

78. Leong, H. S. *et al.* Invadopodia Are Required for Cancer Cell Extravasation and Are a Therapeutic Target for Metastasis. *Cell Rep.* **8**, 1558–1570 (2014).

79. Ngan, E. *et al.* LPP is a Src substrate required for invadopodia formation & efficient breast cancer lung metastasis. *Nat. Commun.* **8**, 1–15 (2017).

80. Kanehisa, J. *et al.* A band of F-actin containing podosomes is involved in bone resorption by osteoclasts. *Bone* **11**, 287–293 (1990).

81. Miyauchi, A. *et al.* Osteoclast cytosolic calcium, regulated by voltage-gated calcium channels and extracellular calcium, controls podosome assembly and bone resorption. *J. Cell Biol.* **111**, 2543–2552 (1990).

82. Georgess, D., Machuca-Gayet, I., Blangy, A. & Jurdic, P. Podosome organization drives osteoclast-mediated bone resorption. *Cell Adh. Migr.* **8**, 192–204 (2014).

83. Schmidt, S. *et al.* Kindlin-3–mediated signaling from multiple integrin classes is required for osteoclast-mediated bone resorption. *J. Cell Biol.* **192**, 883–897 (2011).

84. Malinin, N. L. *et al.* A point mutation in KINDLIN3 ablates activation of three integrin subfamilies in humans. *Nat. Med.* **15**, 313–318 (2009).

85. van den Dries, K. *et al.* Interplay between myosin IIA-mediated contractility and actin network integrity orchestrates podosome composition and oscillations. *Nat. Commun.* **4**, 1412 (2013).

86. Gasparski, A. N., Ozarkar, S. & Beningo, K. A. Transient mechanical strain promotes the maturation of invadopodia and enhances cancer cell invasion in vitro. *J. Cell Sci.* **130**, 1965–1978 (2017).

87. Proag, A., Bouissou, A., Vieu, C., Maridonneau-Parini, I. & Poincloux, R. Evaluation of the force and spatial dynamics of macrophage podosomes by multi-particle tracking.

Methods **94**, 75–84 (2016).

88. DuFort, C. C., Paszek, M. J. & Weaver, V. M. Balancing forces: architectural control of mechanotransduction. *Nat. Rev. Mol. Cell Biol.* **12**, 308–319 (2011).

89. Zhou, S., Webb, B. A., Eves, R. & Mak, A. S. Effects of tyrosine phosphorylation of cortactin on podosome formation in A7r5 vascular smooth muscle cells. *Am. J. Physiol. Cell Physiol.* **290**, C463-71 (2006).

90. Moreau, V., Tatin, F., Varon, C. & Génot, E. Actin can reorganize into podosomes in aortic endothelial cells, a process controlled by Cdc42 and RhoA. *Mol. Cell. Biol.* **23**, 6809–22 (2003).

91. Rottiers, P. *et al.* TGFbeta-induced endothelial podosomes mediate basement membrane collagen degradation in arterial vessels. *J. Cell Sci.* **122**, 4311–8 (2009).

92. Seano, G. *et al.* Endothelial podosome rosettes regulate vascular branching in tumour angiogenesis. *Nat. Cell Biol.* **16**, 931–41, 1–8 (2014).

93. Spuul, P. *et al.* VEGF-A/Notch-Induced Podosomes Proteolyse Basement Membrane Collagen-IV during Retinal Sprouting Angiogenesis. *Cell Rep.* **17**, 484–500 (2016).

94. Santiago-Medina, M., Gregus, K. A., Nichol, R. H., O'Toole, S. M. & Gomez, T. M. Regulation of ECM degradation and axon guidance by growth cone invadosomes. *Development* **142**, 486–96 (2015).

95. Proszynski, T. J., Gingras, J., Valdez, G., Krzewski, K. & Sanes, J. R. Podosomes are present in a postsynaptic apparatus and participate in its maturation. *Proc. Natl. Acad. Sci. U. S. A.* **106**, 18373–8 (2009).

96. Oikawa, T. *et al.* Tks5-dependent formation of circumferential podosomes/invadopodia mediates cell-cell fusion. *J. Cell Biol.* **197**, 553–68 (2012).

97. Chuang, M.-C. *et al.* Tks5 and Dynamin-2 enhance actin bundle rigidity in invadosomes to promote myoblast fusion. *J. Cell Biol.* **218**, 1670–1685 (2019).

98. Gawden-Bone, C. *et al.* Dendritic cell podosomes are protrusive and invade the extracellular matrix using metalloproteinase MMP-14. *J. Cell Sci.* **123**, 1427–37 (2010).

99. Baranov, M. V. *et al.* Podosomes of dendritic cells facilitate antigen sampling. *J. Cell Sci.* **127**, 1052–1064 (2014).

100. Sage, P. T. *et al.* Antigen recognition is facilitated by invadosome-like protrusions formed by memory/effector T cells. *J. Immunol.* **188**, 3686–99 (2012).

101. Fuss, B., Becker, T., Zinke, I. & Hoch, M. The cytohesin Steppke is essential for insulin signalling in Drosophila. *Nature* **444**, 945–948 (2006).

102. Ogasawara, M. *et al.* Similarities in Function and Gene Structure of Cytohesin-4 and Cytohesin-1, Guanine Nucleotide-exchange Proteins for ADP-ribosylation Factors. *J. Biol. Chem.* **275**, 3221–3230 (2000).

103. Kolanus, W. *et al.* Alpha L beta 2 integrin/LFA-1 binding to ICAM-1 induced by cytohesin-1, a cytoplasmic regulatory molecule. *Cell* **86**, 233–42 (1996).

104. Yamauchi, J. *et al.* Phosphorylation of Cytohesin-1 by Fyn Is Required for Initiation of

Myelination and the Extent of Myelination During Development. *Sci. Signal.* **5**, ra69–ra69 (2012).

105. Liu, L. & Pohajdak, B. Cloning and sequencing of a human cDNA from cytolytic NK/T cells with homology to yeast SEC7. *Biochim. Biophys. Acta - Gene Struct. Expr.* **1132**, 75–78 (1992).

106. Kolanus, W. Guanine nucleotide exchange factors of the cytohesin family and their roles in signal transduction. *Immunol. Rev.* **218**, 102–113 (2007).

107. Klarlund, J. K., Tsiaras, W., Holik, J. J., Chawla, A. & Czech, M. P. Distinct Polyphosphoinositide Binding Selectivities for Pleckstrin Homology Domains of GRP1-like Proteins Based on Diglycine Versus Triglycine Motifs. *J. Biol. Chem.* **275**, 32816–32821 (2000).

108. Ratcliffe, C. D. H. *et al.* HGF-induced migration depends on the PI(3,4,5)P3-binding microexon-spliced variant of the Arf6 exchange factor cytohesin-1. *J. Cell Biol.* **218**, 285–298 (2019).

109. Stephens, L. R., Hughes, K. T. & Irvine, R. F. Pathway of phosphatidylinositol(3,4,5)-trisphosphate synthesis in activated neutrophils. *Nature* **351**, 33–39 (1991).

110. Donaldson, J. G. & Jackson, C. L. ARF family G proteins and their regulators: roles in membrane transport, development and disease. *Nat. Rev. Mol. Cell Biol.* **12**, 362–375 (2011).

111. Gamara, J., Chouinard, F., Davis, L., Aoudjit, F. & Bourgoin, S. G. Regulators and Effectors of Arf GTPases in Neutrophils. *J. Immunol. Res.* **2015**, 1–15 (2015).

112. D'Souza-Schorey, C. & Chavrier, P. ARF proteins: roles in membrane traffic and beyond. *Nat. Rev. Mol. Cell Biol.* **7**, 347–358 (2006).

113. Donaldson, J. G. Multiple Roles for Arf6: Sorting, Structuring, and Signaling at the Plasma Membrane. *J. Biol. Chem.* **278**, 41573–41576 (2003).

114. Sabe, H. Requirement for Arf6 in Cell Adhesion, Migration, and Cancer Cell Invasion. *J. Biochem.* **134**, 485–489 (2003).

115. Heckel, T. *et al.* Src-dependent repression of ARF6 is required to maintain podosome-rich sealing zones in bone-digesting osteoclasts. *Proc. Natl. Acad. Sci.* **106**, 1451–1456 (2009).

116. Segeletz, S., Danglot, L., Galli, T. & Hoflack, B. ARAP1 Bridges Actin Dynamics and AP-3-Dependent Membrane Traffic in Bone-Digesting Osteoclasts. *iScience* **6**, 199–211 (2018).

117. Donnelly, S. K. *et al.* Rac3 regulates breast cancer invasion and metastasis by controlling adhesion and matrix degradation. *J. Cell Biol.* **216**, 4331–4349 (2017).

118. Rafiq, N. B. M. *et al.* Podosome assembly is controlled by the GTPase ARF1 and its nucleotide exchange factor ARNO. *J. Cell Biol.* **216**, 181–197 (2017).

119. Schlienger, S., Ramirez, R. A. M. & Claing, A. ARF1 regulates adhesion of MDA-MB-231 invasive breast cancer cells through formation of focal adhesions. *Cell. Signal.* **27**, 403–415 (2015).

120. Humphreys, D., Davidson, A. C., Hume, P. J., Makin, L. E. & Koronakis, V. Arf6 coordinates actin assembly through the WAVE complex, a mechanism usurped by Salmonella to

invade host cells. *Proc. Natl. Acad. Sci.* **110**, 16880–16885 (2013).

121. Bill, A. *et al.* RETRACTED: Cytohesins Are Cytoplasmic ErbB Receptor Activators. *Cell* **143**, 201–211 (2010).

122. Mannell, H. K. *et al.* ARNO regulates VEGF-dependent tissue responses by stabilizing endothelial VEGFR-2 surface expression. *Cardiovasc. Res.* **93**, 111–119 (2012).

123. Kanamarlapudi, V., Thompson, A., Kelly, E. & López Bernal, A. ARF6 Activated by the LHCG Receptor through the Cytohesin Family of Guanine Nucleotide Exchange Factors Mediates the Receptor Internalization and Signaling. *J. Biol. Chem.* **287**, 20443–20455 (2012).

124. Li, J. *et al.* Grp1 Plays a Key Role in Linking Insulin Signaling to Glut4 Recycling. *Dev. Cell* **22**, 1286–1298 (2012).

125. Lim, J., Zhou, M., Veenstra, T. D. & Morrison, D. K. The CNK1 scaffold binds cytohesins and promotes insulin pathway signaling. *Genes Dev.* **24**, 1496–1506 (2010).

126. Jux, B. *et al.* Cytohesin-3 is required for full insulin receptor signaling and controls body weight via lipid excretion. *Sci. Rep.* **9**, 3442 (2019).

127. Hafner, M. *et al.* Inhibition of cytohesins by SecinH3 leads to hepatic insulin resistance. *Nature* **444**, 941–944 (2006).

128. Korthauer, U. *et al.* Anergic T Lymphocytes Selectively Express an Integrin Regulatory Protein of the Cytohesin Family. *J. Immunol.* **164**, 308–318 (2000).

129. Oh, S. J. & Santy, L. C. Differential effects of cytohesins 2 and 3 on β1 integrin recycling. *J. Biol. Chem.* **285**, 14610–14616 (2010).

130. El Azreq, M.-A., Garceau, V. & Bourgoin, S. G. Cytohesin-1 regulates fMLF-mediated activation and functions of the β 2 integrin Mac-1 in human neutrophils. *J. Leukoc. Biol.* **89**, 823–836 (2011).

131. Sendide, K. *et al.* Cross-Talk between CD14 and Complement Receptor 3 Promotes Phagocytosis of Mycobacteria: Regulation by Phosphatidylinositol 3-Kinase and Cytohesin-1. *J. Immunol.* **174**, 4210–4219 (2005).

132. El Azreq, M.-A. & Bourgoin, S. G. Cytohesin-1 regulates human blood neutrophil adhesion to endothelial cells through β2 integrin activation. *Mol. Immunol.* **48**, 1408–1416 (2011).

133. Rak, J. *et al.* Cytohesin 1 regulates homing and engraftment of human hematopoietic stem and progenitor cells. *Blood* **129**, 950–958 (2017).

134. Mohanan, V. *et al.* C1orf106 is a colitis risk gene that regulates stability of epithelial adherens junctions. *Science (80-.).* **359**, 1161–1166 (2018).

135. Quast, T. *et al.* Cytohesin-1 controls the activation of RhoA and modulates integrin-dependent adhesion and migration of dendritic cells. *Blood* **113**, 5801–5810 (2009).

136. Salem, J. C., Reviriego-Mendoza, M. M. & Santy, L. C. ARF-GEF cytohesin-2/ARNO regulates R-Ras and α5-integrin recycling through an EHD1-positive compartment. *Mol. Biol. Cell* **26**, 4265–4279 (2015).

137. Torii, T. *et al.* Cytohesin-2/ARNO, through Its Interaction with Focal Adhesion Adaptor

Protein Paxillin, Regulates Preadipocyte Migration via the Downstream Activation of Arf6. *J. Biol. Chem.* **285**, 24270–24281 (2010).

138. Santy, L. C. & Casanova, J. E. Activation of ARF6 by ARNO stimulates epithelial cell migration through downstream activation of both Rac1 and phospholipase D. *J. Cell Biol.* **154**, 599–610 (2001).

139. White, D. T., McShea, K. M., Attar, M. A. & Santy, L. C. GRASP and IPCEF promote ARF-to-Rac signaling and cell migration by coordinating the association of ARNO/cytohesin 2 with Dock180. *Mol. Biol. Cell* **21**, 562–71 (2010).

140. Wurtzel, J. G. T. *et al.* RLIP76 regulates Arf6-dependent cell spreading and migration by linking ARNO with activated R-Ras at recycling endosomes. *Biochem. Biophys. Res. Commun.* **467**, 785–791 (2015).

141. Davies, J. C. B., Tamaddon-Jahromi, S., Jannoo, R. & Kanamarlapudi, V. Cytohesin 2/ARF6 regulates preadipocyte migration through the activation of ERK1/2. *Biochem. Pharmacol.* **92**, 651–660 (2014).

142. Santy, L. C., Ravichandran, K. S. & Casanova, J. E. The DOCK180/Elmo Complex Couples ARNO-Mediated Arf6 Activation to the Downstream Activation of Rac1. *Curr. Biol.* **15**, 1749–1754 (2005).

143. Attar, M. A. & Santy, L. C. The scaffolding protein GRASP/Tamalin directly binds to Dock180 as well as to cytohesins facilitating GTPase crosstalk in epithelial cell migration. *BMC Cell Biol.* **14**, 1 (2013).

144. Li, C.-C. *et al.* ARL4D Recruits Cytohesin-2/ARNO to Modulate Actin Remodeling. *Mol. Biol. Cell* **18**, 4420–4437 (2007).

145. Frank, S. R., Hatfield, J. C. & Casanova, J. E. Remodeling of the Actin Cytoskeleton Is Coordinately Regulated by Protein Kinase C and the ADP-Ribosylation Factor Nucleotide Exchange Factor ARNO. *Mol. Biol. Cell* **9**, 3133–3146 (1998).

146. Torii, T. *et al.* Arf6 guanine-nucleotide exchange factor cytohesin-2 regulates myelination in nerves. *Biochem. Biophys. Res. Commun.* **460**, 819–825 (2015).

147. Zhai, J. *et al.* Inhibition of Cytohesins Protects against Genetic Models of Motor Neuron Disease. *J. Neurosci.* **35**, 9088–105 (2015).

148. Yan, X. *et al.* FRMD4A–cytohesin signaling modulates the cellular release of tau. *J. Cell Sci.* **129**, 2003–2015 (2016).

149. Hu, W. *et al.* SecinH3 Attenuates TDP-43 p.Q331K-Induced Neuronal Toxicity by Suppressing Endoplasmic Reticulum Stress and Enhancing Autophagic Flux. *IUBMB Life* **71**, 192–199 (2019).

150. Torii, T. *et al.* Arf6 guanine-nucleotide exchange factor, cytohesin-2, interacts with actinin-1 to regulate neurite extension. *Cell. Signal.* **24**, 1872–1882 (2012).

151. Ito, A. *et al.* Pallidin is a novel interacting protein for cytohesin-2 and regulates the early endosomal pathway and dendritic formation in neurons. *J. Neurochem.* **147**, 153–177 (2018).

152. Speicher, T. *et al.* Knockdown and knockout of β1-integrin in hepatocytes impairs liver

regeneration through inhibition of growth factor signalling. *Nat. Commun.* **5**, 3862 (2014).

153. Bogorad, R. L. *et al.* Nanoparticle-formulated siRNA targeting integrins inhibits hepatocellular carcinoma progression in mice. *Nat. Commun.* **5**, 3869 (2014).

154. Benedicto, A. *et al.* Decreased expression of the β2 integrin on tumor cells is associated with a reduction in liver metastasis of colorectal cancer in mice. *BMC Cancer* **17**, 827 (2017).

155. Gardner, H., Kreidberg, J., Koteliansky, V. & Jaenisch, R. Deletion of Integrin α1 by Homologous Recombination Permits Normal Murine Development but Gives Rise to a Specific Deficit in Cell Adhesion. *Dev. Biol.* **175**, 301–313 (1996).

156. Clausen, B. E., Burkhardt, C., Reith, W., Renkawitz, R. & Förster, I. Conditional gene targeting in macrophages and granulocytes using LysMcre mice. *Transgenic Res.* **8**, 265–77 (1999).

157. Scott, L. M., Priestley, G. V & Papayannopoulou, T. Deletion of alpha4 integrins from adult hematopoietic cells reveals roles in homeostasis, regeneration, and homing. *Mol. Cell. Biol.* **23**, 9349–60 (2003).

158. Stadtfeld, M. & Graf, T. Assessing the role of hematopoietic plasticity for endothelial and hepatocyte development by non-invasive lineage tracing. *Development* **132**, 203–13 (2005).

159. Fire, A. *et al.* Potent and specific genetic interference by double-stranded RNA in Caenorhabditis elegans. *Nature* **391**, 806–811 (1998).

160. Chen, W. T., Olden, K., Bernard, B. A. & Chu, F. F. Expression of transformation-associated protease(s) that degrade fibronectin at cell contact sites. *J. Cell Biol.* **98**, 1546–1555 (1984).

161. Iscove, N. N., Sieber, F. & Winterhalter, K. H. Erythroid colony formation in cultures of mouse and human bone marrow: Analysis of the requirement for erythropoietin by gel filtration and affinity chromatography on agarose-concanavalin A. *J. Cell. Physiol.* **83**, 309–320 (1974).

162. Stewart, G. J., Wang, Y. & Niewiarowski, S. Methylcellulose protects the ability of anchorage-dependent cells to adhere following isolation and holding in suspension. *Biotechniques* **19**, 598–604 (1995).

163. Glisin, V., Crkvenjakov, R. & Byus, C. Ribonucleic acid isolated by cesium chloride centrifugation. *Biochemistry* **13**, 2633–7 (1974).

164. Brinkman, E. K., Chen, T., Amendola, M. & van Steensel, B. Easy quantitative assessment of genome editing by sequence trace decomposition. *Nucleic Acids Res.* **42**, e168–e168 (2014).

165. Love, M. I., Huber, W. & Anders, S. Moderated estimation of fold change and dispersion for RNA-seq data with DESeq2. *Genome Biol.* **15**, 550 (2014).

166. Kim, D. & Herr, A. E. Protein immobilization techniques for microfluidic assays. *Biomicrofluidics* **7**, 041501 (2013).

167. Smith, P. K. *et al.* Measurement of protein using bicinchoninic acid. *Anal. Biochem.* **150**,

76–85 (1985).

168. Towbin, H., Staehelin, T. & Gordon, J. Electrophoretic transfer of proteins from polyacrylamide gels to nitrocellulose sheets: procedure and some applications. *Proc. Natl. Acad. Sci.* **76**, 4350–4354 (1979).

169. Moskowitz, R. W. Role of collagen hydrolysate in bone and joint disease. *Semin. Arthritis Rheum.* **30**, 87–99 (2000).

170. Paszek, M. J. *et al.* Tensional homeostasis and the malignant phenotype. *Cancer Cell* **8**, 241–254 (2005).

171. Levental, I., Georges, P. C. & Janmey, P. A. Soft biological materials and their impact on cell function. *Soft Matter* **3**, 299–306 (2007).

172. Moyle, M., Napier, M. A. & McLean, J. W. Cloning and expression of a divergent integrin subunit β8. *J. Biol. Chem.* **266**, 19650–19658 (1991).

173. Jackson, C. L. *et al.* The Sec7 Family of Arf Guanine Nucleotide Exchange Factors. in *ARF Family GTPases* **132**, 71–99 (Kluwer Academic Publishers, 2004).

174. Burns, S. *et al.* Maturation of DC is associated with changes in motile characteristics and adherence. *Cell Motil. Cytoskeleton* **57**, 118–132 (2004).

175. Lukácsi, S., Nagy-Baló, Z., Erdei, A., Sándor, N. & Bajtay, Z. The role of CR3 (CD11b/CD18) and CR4 (CD11c/CD18) in complement-mediated phagocytosis and podosome formation by human phagocytes. *Immunol. Lett.* **189**, 64–72 (2017).

176. Garnotel, R. *et al.* Human Blood Monocytes Interact with Type I Collagen Through x 2 Integrin (CD11c-CD18, gp150-95). *J. Immunol.* **164**, 5928–5934 (2000).

177. Avraham, H., Park, S.-Y., Schinkmann, K. & Avraham, S. RAFTK/Pyk2-mediated cellular signalling. *Cell. Signal.* **12**, 123–133 (2000).

178. Duong, L. T. *et al.* PYK2 in osteoclasts is an adhesion kinase, localized in the sealing zone, activated by ligation of alpha(v)beta3 integrin, and phosphorylated by src kinase. *J. Clin. Invest.* **102**, 881–892 (1998).

179. Duong, L. T. *et al.* Inhibition of Osteoclast Function by Adenovirus Expressing Antisense Protein-tyrosine Kinase 2. *J. Biol. Chem.* **276**, 7484–7492 (2001).

180. Badowski, C. *et al.* Paxillin Phosphorylation Controls Invadopodia/Podosomes Spatiotemporal Organization. *Mol. Biol. Cell* **19**, 633–645 (2008).

181. Petropoulos, C. *et al.* Roles of paxillin family members in adhesion and ECM degradation coupling at invadosomes. *J. Cell Biol.* **213**, 585–599 (2016).

182. Dovas, A. & Cox, D. Signaling networks regulating leukocyte podosome dynamics and function. *Cell. Signal.* **23**, 1225–1234 (2011).

183. van den Dries, K. *et al.* Geometry sensing by dendritic cells dictates spatial organization and PGE2-induced dissolution of podosomes. *Cell. Mol. Life Sci.* **69**, 1889–1901 (2012).

184. Yu, C. *et al.* Integrin-Matrix Clusters Form Podosome-like Adhesions in the Absence of Traction Forces. *Cell Rep.* **5**, 1456–1468 (2013).

185. Gelman, I. H. & Gao, L. SSeCKS/Gravin/AKAP12 Metastasis Suppressor Inhibits Podosome Formation via RhoA- and Cdc42-Dependent Pathways. *Mol. Cancer Res.* **4**, 151–158 (2006).

186. Berdeaux, R. L., Díaz, B., Kim, L. & Martin, G. S. Active Rho is localized to podosomes induced by oncogenic Src and is required for their assembly and function. *J. Cell Biol.* **166**, 317–323 (2004).

187. Mizoguchi, F., Murakami, Y., Saito, T., Miyasaka, N. & Kohsaka, H. miR-31 controls osteoclast formation and bone resorption by targeting RhoA. *Arthritis Res. Ther.* **15**, R102 (2013).

188. Shang, X. *et al.* Rational Design of Small Molecule Inhibitors Targeting RhoA Subfamily Rho GTPases. *Chem. Biol.* **19**, 699–710 (2012).

189. Oh, S. J. & Santy, L. C. Phosphoinositide specificity determines which cytohesins regulate β1 integrin recycling. *J. Cell Sci.* **125**, 3195–3201 (2012).

190. Durai, V. & Murphy, K. M. Functions of Murine Dendritic Cells. *Immunity* **45**, 719–736 (2016).

191. Raggatt, L. J. & Partridge, N. C. Cellular and Molecular Mechanisms of Bone Remodeling. *J. Biol. Chem.* **285**, 25103–25108 (2010).

192. Zou, W. *et al.* Talin1 and Rap1 Are Critical for Osteoclast Function. *Mol. Cell. Biol.* **33**, 830–844 (2013).

193. Yokota, K. *et al.* Combination of Tumor Necrosis Factor α and Interleukin-6 Induces Mouse Osteoclast-like Cells With Bone Resorption Activity Both In Vitro and In Vivo. *Arthritis Rheumatol.* **66**, 121–129 (2014).

194. Yang, T.-L. *et al.* Differential regulations of fibronectin and laminin in Smad2 activation in vascular endothelial cells in response to disturbed flow. *J. Biomed. Sci.* **25**, 1 (2018).

195. Yu, M., Wang, J., Muller, D. J. & Helenius, J. In PC3 prostate cancer cells ephrin receptors crosstalk to β1-integrins to strengthen adhesion to collagen type I. *Sci. Rep.* **5**, 8206 (2015).

196. Schaufler, V. *et al.* Selective binding and lateral clustering of α 5 β 1 and α v β 3 integrins: Unraveling the spatial requirements for cell spreading and focal adhesion assembly. *Cell Adh. Migr.* **10**, 505–515 (2016).

197. Wu, L. *et al.* Distinct FAK-Src activation events promote α5β1 and α4β1 integrin-stimulated neuroblastoma cell motility. *Oncogene* **27**, 1439–1448 (2008).

198. Reyes-Reyes, M., Mora, N., Gonzalez, G. & Rosales, C. beta1 and beta2 integrins activate different signalling pathways in monocytes. *Biochem. J.* **363**, 273–80 (2002).

199. Hauck, C. R., Hsia, D. A., Ilic, D. & Schlaepfer, D. D. v-Src SH3-enhanced Interaction with Focal Adhesion Kinase at β 1 Integrin-containing Invadopodia Promotes Cell Invasion. *J. Biol. Chem.* **277**, 12487–12490 (2002).

200. van Helden, S. F. G. *et al.* A Critical Role for Prostaglandin E2 in Podosome Dissolution and Induction of High-Speed Migration during Dendritic Cell Maturation. *J. Immunol.* **177**, 1567–1574 (2006).

201. Mueller, S. C. & Chen, W. T. Cellular invasion into matrix beads: localization of beta 1 integrins and fibronectin to the invadopodia. *J. Cell Sci.* **99 (Pt 2)**, 213–25 (1991).

202. Beaty, B. T. *et al.* β1 integrin regulates Arg to promote invadopodial maturation and matrix degradation. *Mol. Biol. Cell* **24**, 1661–1675 (2013).

203. Williams, K. C. & Coppolino, M. G. SNARE-dependent interaction of Src, EGFR and 1 integrin regulates invadopodia formation and tumor cell invasion. *J. Cell Sci.* **127**, 1712–1725 (2014).

204. Destaing, O. *et al.* β1A Integrin Is a Master Regulator of Invadosome Organization and Function. *Mol. Biol. Cell* **21**, 4108–4119 (2010).

205. Nakahara, H. *et al.* Activation of β1 Integrin Signaling Stimulates Tyrosine Phosphorylation of p190 RhoGAP and Membrane-protrusive Activities at Invadopodia. *J. Biol. Chem.* **273**, 9–12 (1998).

206. Liu, S., Yamashita, H., Weidow, B., Weaver, A. M. & Quaranta, V. Laminin-332â€“Î²1 integrin interactions negatively regulate invadopodia. *J. Cell. Physiol.* **132**, n/a-n/a (2009).

207. Adkins, J. N. *et al.* Toward a Human Blood Serum Proteome. *Mol. Cell. Proteomics* **1**, 947–955 (2002).

208. Grinnell, F. & Feld, M. K. Fibronectin adsorption on hydrophilic and hydrophobic surfaces detected by antibody binding and analyzed during cell adhesion in serum-containing medium. *J. Biol. Chem.* **257**, 4888–93 (1982).

209. Leitinger, B. Transmembrane Collagen Receptors. *Annu. Rev. Cell Dev. Biol.* **27**, 265–290 (2011).

210. Poltorak, M. P. & Schraml, B. U. Fate Mapping of Dendritic Cells. *Front. Immunol.* **6**, 203–213 (2015).

211. Davis, G. E. The Mac-1 and p150,95 β2 integrins bind denatured proteins to mediate leukocyte cell-substrate adhesion. *Exp. Cell Res.* **200**, 242–252 (1992).

212. Heino, J. The collagen family members as cell adhesion proteins. *BioEssays* **29**, 1001–1010 (2007).

213. Di Martino, J. *et al.* The microenvironment controls invadosome plasticity. *J. Cell Sci.* **129**, 1759–1768 (2016).

214. Bühligen, J. *et al.* Lysophosphatidylcholine-mediated functional inactivation of syndecan-4 results in decreased adhesion and motility of dendritic cells. *J. Cell. Physiol.* **225**, 905–914 (2010).

215. Boettiger, D. *et al.* Regulation of Integrin α5β1 Affinity during Myogenic Differentiation. *Dev. Biol.* **169**, 261–272 (1995).

216. Angele, P. *et al.* Characterization of esterified hyaluronan-gelatin polymer composites suitable for chondrogenic differentiation of mesenchymal stem cells. *J. Biomed. Mater. Res. Part A* **91A**, 416–427 (2009).

217. Taubenberger, A. V., Woodruff, M. A., Bai, H., Muller, D. J. & Hutmacher, D. W. The effect of unlocking RGD-motifs in collagen I on pre-osteoblast adhesion and differentiation.

Biomaterials **31**, 2827–2835 (2010).

218. Owens, R. J. & Baralle, F. E. Mapping the collagen-binding site of human fibronectin by expression in Escherichia coli. *EMBO J.* **5**, 2825–30 (1986).

219. McDonald, J. A., Kelley, D. G. & Broekelmann, T. J. Role of fibronectin in collagen deposition: Fab' to the gelatin-binding domain of fibronectin inhibits both fibronectin and collagen organization in fibroblast extracellular matrix. *J. Cell Biol.* **92**, 485–92 (1982).

220. McDonald, J. A., Broekelmann, T. J., Kelley, D. G. & Villiger, B. Gelatin-binding domain-specific anti-human plasma fibronectin Fab' inhibits fibronectin-mediated gelatin binding but not cell spreading. *J. Biol. Chem.* **256**, 5583–7 (1981).

221. Tuckwell, D. S., Ayad, S., Grant, M. E., Takigawa, M. & Humphries, M. J. Conformation dependence of integrin-type II collagen binding. Inability of collagen peptides to support alpha 2 beta 1 binding, and mediation of adhesion to denatured collagen by a novel alpha 5 beta 1-fibronectin bridge. *J. Cell Sci.* **107 (Pt 4**, 993–1005 (1994).

222. Wagner, C. *et al.* Differentiation of polymorphonuclear neutrophils in patients with systemic infections and chronic inflammatory diseases: evidence of prolonged life span and de novo synthesis of fibronectin. *J. Mol. Med.* **78**, 337–345 (2000).

223. Kraft, S. *et al.* Identification and characterization of a unique role for EDB fibronectin in phagocytosis. *J. Mol. Med.* **94**, 567–581 (2016).

224. Johansson, S., Rubin, K., Höök, M., Ahlgren, T. & Seljelid, R. In vitro biosynthesis of cold insoluble globulin (fibronectin) by mouse peritoneal macrophages. *FEBS Lett.* **105**, 313–316 (1979).

225. Wang, S. *et al.* Integrin α4β7 switches its ligand specificity via distinct conformer-specific activation. *J. Cell Biol.* **217**, 2799–2812 (2018).

226. Sun, H. *et al.* Distinct Chemokine Signaling Regulates Integrin Ligand Specificity to Dictate Tissue-Specific Lymphocyte Homing. *Dev. Cell* **30**, 61–70 (2014).

227. Altroff, H. *et al.* Interdomain Tilt Angle Determines Integrin-dependent Function of the Ninth and Tenth FIII Domains of Human Fibronectin. *J. Biol. Chem.* **279**, 55995–56003 (2004).

228. Benito-Jardón, M. *et al.* The fibronectin synergy site re-enforces cell adhesion and mediates a crosstalk between integrin classes. *Elife* **6**, 1–24 (2017).

229. García, A. J., Takagi, J. & Boettiger, D. Two-stage Activation for α 5 β 1 Integrin Binding to Surface-adsorbed Fibronectin. *J. Biol. Chem.* **273**, 34710–34715 (1998).

230. García, A. J., Schwarzbauer, J. E. & Boettiger, D. Distinct Activation States of α5β1 Integrin Show Differential Binding to RGD and Synergy Domains of Fibronectin †. *Biochemistry* **41**, 9063–9069 (2002).

231. Schwartz, M. A. & Ginsberg, M. H. Networks and crosstalk: Integrin signalling spreads. *Nat. Cell Biol.* **4**, 65–68 (2002).

232. Takada, Y., Takada, Y. K. & Fujita, M. Crosstalk between insulin-like growth factor (IGF) receptor and integrins through direct integrin binding to IGF1. *Cytokine Growth Factor Rev.* **34**, 67–72 (2017).

233. Simons, M., Gordon, E. & Claesson-Welsh, L. Mechanisms and regulation of endothelial VEGF receptor signalling. *Nat. Rev. Mol. Cell Biol.* **17**, 611–25 (2016).

234. Munger, J. S. & Sheppard, D. Cross talk among TGF-β signaling pathways, integrins, and the extracellular matrix. *Cold Spring Harb. Perspect. Biol.* **3**, a005017 (2011).

235. Xu, H. *et al.* Discoidin Domain Receptors Promote α1β1- and α2β1-Integrin Mediated Cell Adhesion to Collagen by Enhancing Integrin Activation. *PLoS One* **7**, e52209 (2012).

236. Porter, J. C. & Hogg, N. Integrin Cross Talk: Activation of Lymphocyte Function-associated Antigen-1 on Human T Cells Alters α4β1- and α5β1-mediated Function. *J. Cell Biol.* **138**, 1437–1447 (1997).

237. Chan, J. R., Hyduk, S. J. & Cybulsky, M. I. 4 1 Integrin/VCAM-1 Interaction Activates L 2 Integrin-Mediated Adhesion to ICAM-1 in Human T Cells. *J. Immunol.* **164**, 746–753 (2000).

238. Blystone, S. D., Graham, I. L., Lindberg, F. P. & Brown, E. J. Integrin alpha v beta 3 differentially regulates adhesive and phagocytic functions of the fibronectin receptor alpha 5 beta 1. *J. Cell Biol.* **127**, 1129–37 (1994).

239. Blystone, S. D. *et al.* Integrin beta 3 cytoplasmic tail is necessary and sufficient for regulation of alpha 5 beta 1 phagocytosis by alpha v beta 3 and integrin-associated protein. *J. Cell Biol.* **130**, 745–754 (1995).

240. Worth, D. C. *et al.* αvβ3 integrin spatially regulates VASP and RIAM to control adhesion dynamics and migration. *J. Cell Biol.* **189**, 369–383 (2010).

241. Tomatis, D. *et al.* The Muscle-Specific Laminin Receptor α7β1 Integrin Negatively Regulates α5β1 Fibronectin Receptor Function. *Exp. Cell Res.* **246**, 421–432 (1999).

242. Huhtala, P. *et al.* Cooperative signaling by alpha 5 beta 1 and alpha 4 beta 1 integrins regulates metalloproteinase gene expression in fibroblasts adhering to fibronectin. *J. Cell Biol.* **129**, 867–79 (1995).

243. Schiller, H. B. *et al.* β1- and αv-class integrins cooperate to regulate myosin II during rigidity sensing of fibronectin-based microenvironments. *Nat. Cell Biol.* **15**, 625–636 (2013).

244. Friedrichs, J., Helenius, J. & Müller, D. J. Stimulated single-cell force spectroscopy to quantify cell adhesion receptor crosstalk. *Proteomics* **10**, 1455–1462 (2010).

245. Destaing, O., Block, M. R., Planus, E. & Albiges-Rizo, C. Invadosome regulation by adhesion signaling. *Curr. Opin. Cell Biol.* **23**, 597–606 (2011).

246. Spuul, P. *et al.* Importance of RhoGTPases in formation, characteristics, and functions of invadosomes. *Small GTPases* **5**, e28195 (2014).

247. Bhuwania, R. *et al.* Supervillin couples myosin-dependent contractility to podosomes and enables their turnover. *J. Cell Sci.* **125**, 2300–2314 (2012).

248. Cervero, P., Wiesner, C., Bouissou, A., Poincloux, R. & Linder, S. Lymphocyte-specific protein 1 regulates mechanosensory oscillation of podosomes and actin isoform-based actomyosin symmetry breaking. *Nat. Commun.* **9**, 515 (2018).

249. Jerrell, R. J. & Parekh, A. Matrix rigidity differentially regulates invadopodia activity

through ROCK1 and ROCK2. *Biomaterials* **84**, 119–129 (2016).

250. Gulvady, A. C., Forsythe, I. J. & Turner, C. E. Hic-5 regulates Src-induced invadopodia rosette formation and organization. *Mol. Biol. Cell* **132**, mbc.E18-10-0629 (2019).

251. Zhang, Y. *et al.* Tail domains of myosin-1e regulate phosphatidylinositol signaling and F-actin polymerization at the ventral layer of podosomes. *Mol. Biol. Cell* **30**, 622–635 (2019).

252. Mersich, A. T., Miller, M. R., Chkourko, H. & Blystone, S. D. The formin FRL1 (FMNL1) is an essential component of macrophage podosomes. *Cytoskeleton* **67**, 573–585 (2010).

253. R. Miller, M. & Blystone, S. D. Human Macrophages Utilize the Podosome Formin FMNL1 for Adhesion and Migration. *CellBio* **04**, 1–11 (2015).

254. Deng, S., Bothe, I. & Baylies, M. K. The Formin Diaphanous Regulates Myoblast Fusion through Actin Polymerization and Arp2/3 Regulation. *PLOS Genet.* **11**, e1005381 (2015).

255. Chellaiah, M. A. *et al.* Rho-A Is Critical for Osteoclast Podosome Organization, Motility, and Bone Resorption. *J. Biol. Chem.* **275**, 11993–12002 (2000).

256. Zhang, D. *et al.* The small GTP-binding protein, rho p21, is involved in bone resorption by regulating cytoskeletal organization in osteoclasts. *J. Cell Sci.* **108 (Pt 6**, 2285–92 (1995).

257. Varon, C. *et al.* Transforming Growth Factor Induces Rosettes of Podosomes in Primary Aortic Endothelial Cells. *Mol. Cell. Biol.* **26**, 3582–3594 (2006).

258. Burns, S. *et al.* Configuration of human dendritic cell cytoskeleton by Rho GTPases, the WAS protein, and differentiation. *Blood* **98**, 1142–1149 (2001).

259. Kuroiwa, M., Oneyama, C., Nada, S. & Okada, M. The guanine nucleotide exchange factor Arhgef5 plays crucial roles in Src-induced podosome formation. *J. Cell Sci.* **124**, 1726–1738 (2011).

260. Yan, T. *et al.* Integrin αvβ3-associated DAAM1 is essential for collagen-induced invadopodia extension and cell haptotaxis in breast cancer cells. *J. Biol. Chem.* **293**, 10172–10185 (2018).

261. Chen, W., Ghobrial, R. M., Li, X. C. & Kloc, M. Inhibition of RhoA and mTORC2/Rictor by Fingolimod (FTY720) induces p21-activated kinase 1, PAK-1 and amplifies podosomes in mouse peritoneal macrophages. *Immunobiology* **223**, 634–647 (2018).

262. Destaing, O. *et al.* A novel Rho-mDia2-HDAC6 pathway controls podosome patterning through microtubule acetylation in osteoclasts. *J. Cell Sci.* **118**, 2901–2911 (2005).

263. Linder, S. & Aepfelbacher, M. Podosomes: adhesion hot-spots of invasive cells. *Trends Cell Biol.* **13**, 376–385 (2003).

264. Mehta, D., Rahman, A. & Malik, A. B. Protein Kinase C-α Signals Rho-Guanine Nucleotide Dissociation Inhibitor Phosphorylation and Rho Activation and Regulates the Endothelial Cell Barrier Function. *J. Biol. Chem.* **276**, 22614–22620 (2001).

265. Zhang, Y. E. Non-Smad pathways in TGF-β signaling. *Cell Res.* **19**, 128–139 (2009).

266. Danen, E. H. J. *et al.* Integrins control motile strategy through a Rho–cofilin pathway. *J. Cell Biol.* **169**, 515–526 (2005).

267. Lee, D. M. & Harris, T. J. C. An Arf-GEF Regulates Antagonism between Endocytosis and the Cytoskeleton for Drosophila Blastoderm Development. *Curr. Biol.* **23**, 2110–2120 (2013).

268. Lee, D. M., Wilk, R., Hu, J., Krause, H. M. & Harris, T. J. C. Germ Cell Segregation from the Drosophila Soma Is Controlled by an Inhibitory Threshold Set by the Arf-GEF Steppke. *Genetics* **200**, 863–872 (2015).

269. West, J. J. *et al.* An Actomyosin-Arf-GEF Negative Feedback Loop for Tissue Elongation under Stress. *Curr. Biol.* **27**, 2260-2270.e5 (2017).

270. Miura, K. *et al.* ARAP1: a point of convergence for Arf and Rho signaling. *Mol. Cell* **9**, 109–19 (2002).

271. Krugmann, S. *et al.* Identification of ARAP3, a Novel PI3K Effector Regulating Both Arf and Rho GTPases, by Selective Capture on Phosphoinositide Affinity Matrices. *Mol. Cell* **9**, 95–108 (2002).

272. Vinggaard, A. M., Provost, J. J., Exton, J. H. & Hansen, H. S. Arf and RhoA Regulate Both the Cytosolic and the Membrane-bound Phospholipase D from Human Placenta. *Cell. Signal.* **9**, 189–196 (1997).

273. Honda, A. *et al.* Phosphatidylinositol 4-Phosphate 5-Kinase α Is a Downstream Effector of the Small G Protein ARF6 in Membrane Ruffle Formation. *Cell* **99**, 521–532 (1999).

274. Chong, L. D., Traynor-Kaplan, A., Bokoch, G. M. & Schwartz, M. A. The small GTP-binding protein Rho regulates a phosphatidylinositol 4-phosphate 5-kinase in mammalian cells. *Cell* **79**, 507–513 (1994).

275. Boshans, R. L., Szanto, S., van Aelst, L. & D'Souza-Schorey, C. ADP-Ribosylation Factor 6 Regulates Actin Cytoskeleton Remodeling in Coordination with Rac1 and RhoA. *Mol. Cell. Biol.* **20**, 3685–3694 (2000).

276. Luo, R. *et al.* GTP-binding Protein-like Domain of AGAP1 Is Protein Binding Site That Allosterically Regulates ArfGAP Protein Catalytic Activity. *J. Biol. Chem.* **287**, 17176–17185 (2012).

277. Gawlak, G. *et al.* Paxillin mediates stretch-induced Rho signaling and endothelial permeability via assembly of paxillin-p42/44MAPK-GEF-H1 complex. *FASEB J.* **28**, 3249–3260 (2014).

278. Luong, P. *et al.* INAVA-ARNO complexes bridge mucosal barrier function with inflammatory signaling. *Elife* **7**, 203–213 (2018).

279. Arthur, W. T., Petch, L. A. & Burridge, K. Integrin engagement suppresses RhoA activity via a c-Src-dependent mechanism. *Curr. Biol.* **10**, 719–722 (2000).

280. Arthur, W. T. & Burridge, K. RhoA Inactivation by p190RhoGAP Regulates Cell Spreading and Migration by Promoting Membrane Protrusion and Polarity. *Mol. Biol. Cell* **12**, 2711–2720 (2001).

281. Bass, M. D. *et al.* p190RhoGAP is the convergence point of adhesion signals from α 5 β 1 integrin and syndecan-4. *J. Cell Biol.* **181**, 1013–1026 (2008).

282. Lim, Y. *et al.* PyK2 and FAK connections to p190Rho guanine nucleotide exchange factor

regulate RhoA activity, focal adhesion formation, and cell motility. *J. Cell Biol.* **180**, 187–203 (2008).

283. Dubash, A. D. *et al.* A novel role for Lsc/p115 RhoGEF and LARG in regulating RhoA activity downstream of adhesion to fibronectin. *J. Cell Sci.* **120**, 3989–3998 (2007).

284. Danen, E. H. J., Sonneveld, P., Brakebusch, C., Fässler, R. & Sonnenberg, A. The fibronectin-binding integrins α5β1 and αvβ3 differentially modulate RhoA–GTP loading, organization of cell matrix adhesions, and fibronectin fibrillogenesis. *J. Cell Biol.* **159**, 1071–1086 (2002).

285. Zhou, H. & Kramer, R. H. Integrin Engagement Differentially Modulates Epithelial Cell Motility by RhoA/ROCK and PAK1. *J. Biol. Chem.* **280**, 10624–10635 (2005).

286. Attanasio, F. *et al.* Novel invadopodia components revealed by differential proteomic analysis. *Eur. J. Cell Biol.* **90**, 115–127 (2011).

287. Cervero, P., Himmel, M., Krüger, M. & Linder, S. Proteomic analysis of podosome fractions from macrophages reveals similarities to spreading initiation centres. *Eur. J. Cell Biol.* **91**, 908–22 (2012).

288. Kuo, J.-C., Han, X., Hsiao, C.-T., Yates III, J. R. & Waterman, C. M. Analysis of the myosin-II-responsive focal adhesion proteome reveals a role for β-Pix in negative regulation of focal adhesion maturation. *Nat. Cell Biol.* **13**, 383–393 (2011).

289. Ajeian, J. N. *et al.* Proteomic analysis of integrin-associated complexes from mesenchymal stem cells. *PROTEOMICS - Clin. Appl.* **10**, 51–57 (2016).

290. Eich, C. *et al.* Proteome Based Construction of the Lymphocyte Function-Associated Antigen 1 (LFA-1) Interactome in Human Dendritic Cells. *PLoS One* **11**, e0149637 (2016).

291. Humphries, J. D. *et al.* Proteomic Analysis of Integrin-Associated Complexes Identifies RCC2 as a Dual Regulator of Rac1 and Arf6. *Sci. Signal.* **2**, ra51–ra51 (2009).

292. Dierks, H., Kolanus, J. & Kolanus, W. Actin Cytoskeletal Association of Cytohesin-1 Is Regulated by Specific Phosphorylation of Its Carboxyl-terminal Polybasic Domain. *J. Biol. Chem.* **276**, 37472–37481 (2001).

293. Geiger, C. *et al.* Cytohesin-1 regulates beta-2 integrin-mediated adhesion through both ARF-GEF function and interaction with LFA-1. *EMBO J.* **19**, 2525–36 (2000).

294. Hongu, T. *et al.* Arf6 regulates tumour angiogenesis and growth through HGF-induced endothelial β1 integrin recycling. *Nat. Commun.* **6**, 7925 (2015).

295. Clodi, M. *et al.* Effects of General Receptor for Phosphoinositides 1 on Insulin and Insulin-Like Growth Factor I-Induced Cytoskeletal Rearrangement, Glucose Transporter-4 Translocation, and Deoxyribonucleic Acid Synthesis**This work was supported by Grants J 01287-Med and. *Endocrinology* **139**, 4984–4990 (1998).

296. Boehm, T. *et al.* Attenuation of cell adhesion in lymphocytes is regulated by CYTIP, a protein which mediates signal complex sequestration. *EMBO J.* **22**, 1014–1024 (2003).

297. Cohen, L. A. *et al.* Active Arf6 Recruits ARNO/Cytohesin GEFs to the PM by Binding Their PH Domains. *Mol. Biol. Cell* **18**, 2244–2253 (2007).

298. Bourgoin, S. G. *et al.* ARNO but not cytohesin-1 translocation is phosphatidylinositol 3-

kinase-dependent in HL-60 cells. *J. Leukoc. Biol.* **71**, 718–28 (2002).

299. De Craene, J.-O., Bertazzi, D., Bär, S. & Friant, S. Phosphoinositides, Major Actors in Membrane Trafficking and Lipid Signaling Pathways. *Int. J. Mol. Sci.* **18**, 634 (2017).

300. Oikawa, T., Itoh, T. & Takenawa, T. Sequential signals toward podosome formation in NIH-src cells. *J. Cell Biol.* **182**, 157–169 (2008).

301. Yamaguchi, H. *et al.* Phosphatidylinositol 4,5-bisphosphate and PIP5-kinase Iα are required for invadopodia formation in human breast cancer cells. *Cancer Sci.* **101**, 1632–1638 (2010).

302. Hoshino, D. *et al.* Network Analysis of the Focal Adhesion to Invadopodia Transition Identifies a PI3K-PKC Invasive Signaling Axis. *Sci. Signal.* **5**, ra66–ra66 (2012).

303. Malek, M. *et al.* PTEN Regulates PI(3,4)P2 Signaling Downstream of Class I PI3K. *Mol. Cell* **68**, 566-580.e10 (2017).

304. Poon, J. S., Eves, R. & Mak, A. S. Both lipid- and protein-phosphatase activities of PTEN contribute to the p53-PTEN anti-invasion pathway. *Cell Cycle* **9**, 4450–4454 (2010).

305. Worbs, T., Hammerschmidt, S. I. & Förster, R. Dendritic cell migration in health and disease. *Nat. Rev. Immunol.* **17**, 30–48 (2017).

306. Abram, C. L., Roberge, G. L., Hu, Y. & Lowell, C. A. Comparative analysis of the efficiency and specificity of myeloid-Cre deleting strains using ROSA-EYFP reporter mice. *J. Immunol. Methods* **408**, 89–100 (2014).

307. Mouw, J. K., Ou, G. & Weaver, V. M. Extracellular matrix assembly: a multiscale deconstruction. *Nat. Rev. Mol. Cell Biol.* **15**, 771–785 (2014).

308. Egeblad, M., Rasch, M. G. & Weaver, V. M. Dynamic interplay between the collagen scaffold and tumor evolution. *Curr. Opin. Cell Biol.* **22**, 697–706 (2010).

309. Clark, R. A. F. *et al.* Fibronectin and fibrin provide a provisional matrix for epidermal cell migration during wound reepithelialization. *J. Invest. Dermatol.* **79**, 264–269 (1982).

310. Heidkamp, G. F. *et al.* Human lymphoid organ dendritic cell identity is predominantly dictated by ontogeny, not tissue microenvironment. *Sci. Immunol.* **1**, eaai7677–eaai7677 (2016).

311. Ginhoux, F. *et al.* The origin and development of nonlymphoid tissue CD103 + DCs. *J. Exp. Med.* **206**, 3115–3130 (2009).

312. Sousa, C. R. e *et al.* In Vivo Microbial Stimulation Induces Rapid CD40 Ligand–independent Production of Interleukin 12 by Dendritic Cells and their Redistribution to T Cell Areas. *J. Exp. Med.* **186**, 1819–1829 (1997).

313. Prinz, M. *et al.* Positioning of follicular dendritic cells within the spleen controls prion neuroinvasion. *Nature* **425**, 957–962 (2003).

314. Czeloth, N. *et al.* Sphingosine-1 Phosphate Signaling Regulates Positioning of Dendritic Cells within the Spleen. *J. Immunol.* **179**, 5855–5863 (2007).

315. Yi, T. & Cyster, J. G. EBI2-mediated bridging channel positioning supports splenic dendritic cell homeostasis and particulate antigen capture. *Elife* **2**, 203–213 (2013).

316. Nesbitt, S., Nesbit, A., Helfrich, M. & Horton, M. Biochemical characterization of human osteoclast integrins. Osteoclasts express alpha v beta 3, alpha 2 beta 1, and alpha v beta 1 integrins. *J. Biol. Chem.* **268**, 16737–45 (1993).

317. Helfrich, M. H. *et al.* β1 integrins and osteoclast function: Involvement in collagen recognition and bone resorption. *Bone* **19**, 317–328 (1996).

318. Rao, H. *et al.* α9β1: A Novel Osteoclast Integrin That Regulates Osteoclast Formation and Function. *J. Bone Miner. Res.* **21**, 1657–1665 (2006).

319. Häusler, G., Helmreich, M., Marlovits, S. & Egerbacher, M. Integrins and Extracellular Matrix Proteins in the Human Childhood and Adolescent Growth Plate. *Calcif. Tissue Int.* **71**, 212–218 (2002).

320. Hughes, D. E., Salter, D. M., Dedhar, S. & Simpson, R. Integrin expression in human bone. *J. Bone Miner. Res.* **8**, 527–533 (1993).

Acknowledgements

First of all, I would like to thank Prof. Dr. Waldemar Kolanus for his scientific support and guidance throughout my PhD project at the LIMES Institute.

Furthermore, many thanks to my thesis committee, PD Dr. Heike Weighardt as second reviewer, and Prof. Dr. Eva Kiermaier and Prof. Dr. Anton Bovier as members of the examination board.

Special thanks go to all collaborators who helped advancing this project. This includes Prof. Dr. Joachim Schultze and his group at the LIMES Institute, especially Nico Reusch, for the RNA transcriptome sequencing and data analysis, as well as Prof. Dr. Christoph Bourauel and his team at the Dental Clinics of Bonn University for the µCT scans. Dr. Andreas Schlitzer from the LIMES Institute helped with the analysis of myeloid cell populations in mice and Prof. Dr. Ambra Pozzi (Vanderbilt University, Nashville, USA), Prof. Dr. Triantafyllos Chavakis (University Hospital Dresden), and Prof. Dr. Karin Scharffetter-Kochanek (Ulm University) provided valuable integrin KO mice for this study. The elastomers used for this thesis project were made available by Dr. Bernd Hoffmann and Prof. Dr. Rudolph Merkel (Forschungszentrum Jülich).

I am very grateful to the whole Kolanus lab for their support during the past 5 years: Dr. Bettina Jux and Dr. Thomas Quast for their scientific advice and input. Lucía Torres Fernández for her company in the lab and her support, whenever our very different projects overlapped. Karolin Zölzer for her positive attitude throughout the most tedious lab days. Katrin Heße, Christa Mandel, Barbara Reichwein, Helga Ueing, and Susi Weese, as well as Gertrud Mierzwa and Katharina Fast, for their help and assistance in big and small everyday matters. Special thanks go to all students who joined me in the lab for their lab rotations or thesis work: Rubi Rabach, Santiago Valle Torres, See Lee Xian, Paola Guerrero Aruffo, Yonas Mehari, Tawfik Abou Assale, and Anil Akbar. Moreover, thanks to all present and former members of the Kolanus group, including Anastasia Solomatina, Yasmine Port, Carsten Küsters, Dr. Johanna Kolanus, Henriette John, Marie Kronmüller, Dr. Felix Tolksdorf, Dr. Michael Rieck, Dr. Felix Eppler, and Dr. Karin Schneider, for making my time at the LIMES such a great experience – both inside and outside the lab.

And finally, a big thank you to all friends and family who supported me during the past years.